INFORMATION TO USERS

This manuscript has been reproduced from the microfilm master. UMI films the text directly from the original or copy submitted. Thus, some thesis and dissertation copies are in typewriter face, while others may be from any type of computer printer.

The quality of this reproduction is dependent upon the quality of the copy submitted. Broken or indistinct print, colored or poor quality illustrations and photographs, print bleedthrough, substandard margins, and improper alignment can adversely affect reproduction.

In the unlikely event that the author did not send UMI a complete manuscript and there are missing pages, these will be noted. Also, if unauthorized copyright material had to be removed, a note will indicate the deletion.

Oversize materials (e.g., maps, drawings, charts) are reproduced by sectioning the original, beginning at the upper left-hand corner and continuing from left to right in equal sections with small overlaps.

Photographs included in the original manuscript have been reproduced xerographically in this copy. Higher quality 6" x 9" black and white photographic prints are available for any photographs or illustrations appearing in this copy for an additional charge. Contact UMI directly to order.

Bell & Howell Information and Learning
300 North Zeeb Road, Ann Arbor, MI 48106-1346 USA
800-521-0600

Université d'Ottawa · University of Ottawa

BLAST LOADING OF A CYLINDRICAL SHELL PANEL

Thesis Submitted to the School of Graduate Studies as Partial Fulfillment of the Requirements for the Degree of Master of Applied Science

© MOHAMMAD KETABI

Department of Mechanical Engineering

University of Ottawa

Ottawa, Ontario, December 1998

ABSTRACT

The present study is concerned with the dynamic behaviour of a shallow steel cylindrical shell subjected to an explosive blast. Although powerful numerical methods, such as the finite element method exist for the investigation of a multitude of problems in structural mechanics, a closed-form analytical method provides the researcher with a faster, cheaper, versatile and more practical tool of analysis.

An analytical solution based on the Galerkin-Vlasov variational principle applied to the Donnell-Mushtari equations of motion is developed, with trial functions taken as the products of beam functions. This work represents the first use of this approach to time response problems in shell analysis for a wide variety of boundary conditions. Independent confirmation of the analytical method is provided by the finite element program ADINA. The effects of curvatures upon the linear dynamic response of sixteen types of support conditions are determined.

A comparative study is carried out on the effect of removal of support conditions on the curved boundaries, in the linear and nonlinear domains, with numerical data provided by the ADINA program.

TABLE OF CONTENTS

NOTATIONS

D	$= Eh^3/12(1-\mu^2)$, Shell Flexural Rigidity
a	Shell Width
b	Shell Length
∇^2	$=(\partial^2/\partial x^2+\partial^2/\partial y^2)$ Laplace Operator
w(x,y,t)	Shell Lateral Displacement
E	Young's Modulus
h	Shell Thickness
R	Shell Radius
ρ	Shell Density
t	Time
x, y	Shell Planar Coordinates
u(x,y,t)	Shell Axial Membrane Displacement
v(x,y,t)	Shell Radial Membrane Displacement
μ	Poisson's Ratio
N_x, N_y, N_{xy}	Membrane Stress Resultants
M_x,M_y, M_{xy}	Bending Moment Resultants
Q_x, Q_y	Vertical Shear Resultants
l_{min}	Shortest Shell Edge
f	Shell's Highest Elevation
p(t)	Load Time Function
P_{max}	Peak Reflected Pressure
t_p	Positive Phase Duration
a_p	Constant
$\psi(x,y)$	Set of Independent Continuous Functions
A	Shell Surface Area
p(x,y,t)	Lateral Loading on the Shell Surface
$C_{mn}(t)$	Amplitude of the Shell Lateral Displacement
$P_{mn}(t)$	Amplitude of the Transverse Load
$X_m(x)$, $Y_n(y)$	Beam Function
m, n	Indices
$\bar{m}$	Mass per Unit Length
I	Beam Moment of Inertia
ξ	Beam Axial Coordinate

λ	Shape Parameter, Root of the Beam Characteristic Equation
ω	Beam Circular Frequency of Vibration
$w(\xi,t)$	Beam Lateral Displacement
A1, A2, A3, A4	Unknown Constants Determined from the Beam Boundary Conditions
$W(\xi)$	Beam Lateral Displacement Function
ω_{mn}	Shell Circular Frequency of Vibration
[M]	Mass Matrix
[K]	Stiffness Matrix
$\{U\}$	Vector of Nodal Displacements
$\{\dot{U}\}$	Vector of Nodal Velocities
$\{\ddot{U}\}$	Vector of Nodal Accelerations
{R}	Load Vector
FEM	Finite Element Method
CC	Clamped-clamped
CS	Clamped-hinged
FF	Free-free
CF	Clamped-free
SS	Hinged-hinged
CCCC	Shell CC on Straight Edges and CC on Curved Edges
CCCS	Shell CC on Straight Edges and CS on Curved Edges
CCCF	Shell CC on Straight Edges and CF on Curved Edges
CCSS	Shell CC on Straight Edges and SS on Curved Edges
CSCC	Shell CS on Straight Edges and CC on Curved Edges
CSCS	Shell CS on Straight Edges and CS on Curved Edges
CSCF	Shell CS on Straight Edges and Cf on Curved Edges
CSSS	Shell CS on Straight Edges and SS on Curved Edges
CFCC	Shell Cf on Straight Edges and CC on Curved Edges
CFCS	Shell Cf on Straight Edges and CS on Curved Edges
CFCF	Shell Cf on Straight Edges and Cf on Curved Edges
CFSS	Shell Cf on Straight Edges and SS on Curved Edges
SSCC	Shell SS on Straight Edges and CC on Curved Edges
SSCS	Shell SS on Straight Edges and CS on Curved Edges
SSCF	Shell SS on Straight Edges and Cf on Curved Edges
SSSS	Shell CC on Straight Edges and SS on Curved Edges
$'[K]$	Linear Strain Incremental Stiffness Matrix, Not Including Initial Displacement
$'_0[K_L]$, $'_i[K_L]$	Linear Strain Incremental Stiffness Matrices

${}^{t}_{0}[K_{NL}]$, ${}^{t}_{t}[K_{NL}]$	Nonlinear Strain Incremental Stiffness Matrix
${}^{t+\Delta t}\{R\}$	Vector of Externally Applied Nodal Points Load at T+δt
${}^{t}\{F\}$, ${}^{t}_{0}\{F\}$, ${}^{t}_{t}\{F\}$	Vectors of Nodal Point Forces
$\{U\}$	Vector of Increments in the Nodal Point Displacements
${}^{t}\{\ddot{U}\}$, ${}^{t+\Delta t}\{\ddot{U}\}$	Vector of Nodal Point Accelerations at Time T and T+δt

LIST OF FIGURES

LIST OF TABLES

CHAPTER 1
INTRODUCTION

1.1 General

Shells are common elements in many engineering applications. Their significant load carrying properties make them an ideal component in *turbomachinery, aircraft and ship* design, where light weight is essential. In other cases, the combined strength and enclosing properties of shells are utilized, for instance, in *pressure vessels, roofs and domes.*

1.2 Shell Geometries

Shells may be considered as three-dimensional bodies bounded by two closely spaced *curved surfaces*, the distance between surfaces being small compared with the other dimensions. The *middle surface* of the shell is defined as a surface which passes midway between the two faces.
The distance between the surfaces measured along the normal to the middle surface is called the *thickness.* The shell is geometrically fully described if one knows the shape of the middle surface and the thickness for every one of its points.

Shells have all characteristics of plates along with an additional one- curvatures. Thus, we have cylindrical (noncircular and circular), conical, spherical, ellipsoidal, toroidal and hyperbolic paraboidal as practical examples of various curvatures, Fig. 1.1. The plate, however, is a special limiting case of a shell having no curvature. Thus, the principal classifier of the field of shell analysis is the curvature. The next subdivision is boundary shape. Thus, for example, a conical shell can be open or closed, Fig. 1.2, have boundaries which are parallel to the principal

coordinates or have cut-outs or not.

There are two different classes of shells, *thick* shells and *thin* shells. A shell will be called thin, if the maximum value of the ratio of thickness over radii can be neglected in comparison to unity. Correspondingly shells will be called thick whenever such terms cannot be neglected.

Shells may be regarded as a generalization of a flat plate. There exist however a substantial difference in the behaviour of plates and shells under the action of an external loading. The equilibrium of a plate element under a lateral load is only possible by the action of bending and twisting moments, usually accompanied by shearing forces, while a shell element, in general is able to transmit the surface load by *membrane* stresses which act parallel to the tangential plane at a given point of the middle surface and are distributed over the thickness of the shell. This property of shells makes them as a rule, much more rigid and a more economical structure than a plate would be under similar conditions.

1.3 Shell Theories

If a shell is prevented from moving as a rigid body and upon application and removal of a load, it tends to return to its original shape then it is *elastic*. The thin shell theories form a part of the theory of elasticity concerned with the study of elastic bodies under the influence of a given load.

The behaviour of a thin elastic shell is said to be *linear* if under loading the deflection of any point of the shell is proportional to the magnitude of the applied load. The theory of small deflections of thin elastic shells is based upon the equations of the mathematical theory of linear elasticity. The particular geometry of shell, where one of its dimensions is much smaller than the other dimensions does not warrant in general, the consideration of the complete three-dimensional elasticity equations. In the development of thin shell theories, simplification is accomplished by reducing the shell problem to the study of the deformation of the middle surface of the shell. In all cases one, begins with the governing equations in the three-dimensional

theory of elasticity and attempts to reduce the system of equations, involving three independent space variables, to a new system involving only two space variables and in turn these two variables are usually taken as coordinates on the middle surface of the shell.

Shell theories of varying degrees of accuracy may be derived, depending upon the degree to which the elasticity equations are simplified. The approximations necessary for the development of an adequate theory of shells have been the subject of considerable controversy among investigators in the field. As a result, a large number of general and specialized thin shell theories exist, developed within the framework of linear elasticity.

The behaviour of an elastic shell is considered to be *nonlinear* if under loading the deflection of any point of the shell is *not* proportional to the magnitude of the applied load. Two sources of nonlinearity are often distinguished: *geometric* and *material*. One speaks of geometrically nonlinear shell theory if the strain-displacement relations are nonlinear but the stress strain relations linear. Most approaches on nonlinear shell theory make this latter assumption because traditional engineering material such as steel and aluminum remain elastic only if the principal strains are relatively small.

1.4 Thin Circular Cylindrical Shell

From the geometrical point of view, the cylindrical shell is generated by moving a straight line along a curve while maintaining it parallel to its original direction. It follows from this definition that through every point of the cylinder, one may pass a straight line which lies entirely on its surface. These lines are called the *generators*, Fig. 1.3. A surface element of the symmetric cylindrical shell is bounded by two generating lines and two cross-sections perpendicular, here to the x-axis. The position of an arbitrary point of the surface is defined in terms of the introduced coordinate system.

Cylindrical shells can be closed or open. An open circular cylindrical shell of length l

and angle α_0 is shown in Fig. 1.4. The shell boundaries shown in this figure are a special case where the lateral edges are generators of the shell and the ends are circle arcs which are the intersections of the shell surface with planes which are perpendicular to the shell axis. Thus if one were to view the shell from a view in its symmetry plane, $\theta = \alpha_0/2$, the boundaries would appear as a rectangle. Open shells can be classified as *deep* or *shallow*. A shallow shell may be regarded as a slightly curved plate. A deep shell is one whose smallest radius of curvature at every point is large compared with the greatest lengths measured along the middle surface of the shell.

There are three main types of support conditions on each boundary of a shell. They are continuous support, discontinuous or partial support, and point support.

1.5 Shell Solutions in Dynamic Analysis

Time-dependent vibratory motions are set up whenever a shell is disturbed from a position of stable equilibrium. If these motions occur in the absence of external loads, they are classified as *free* vibrations. If these motions are set up by time dependent external loads, they are referred to as *forced* vibrations.

The study of vibrational characteristics of thin elastic shell panels are of considerable technical interest in the context of modern industry and engineering. These characteristics are of immense interest to the designers for the in-service behaviour of such structures and their endurance. An in-depth knowledge of the resonant modes and natural frequencies of such structures is essential to ensure structural longevity and to avoid destructive resonant conditions. Knowledge of natural frequencies and modes is important from a design viewpoint and also forms the foundation for forced response study.

Generally the solutions for the vibration analysis can be grouped into two distinct categories:

- Exact
- Approximate

By exact solution it is meant that no other simplification is made beside the formulation of the differential equation of motion, and the solution satisfies both the governing differential equation of motion and the boundary conditions. Exact analytical solutions for shell panel are only feasible in the linear range and for a particular type of boundary condition, namely when two opposite sides are simply supported.

For a large variety of panel boundary conditions, exact solutions cannot be set up, so there is a need for approximate solutions. The approximate approaches can be divided into two categories. In the first category, a minimization of energy approach is used. The *Variational Integral* method, the *Galerkin* method, the *Rayleigh-Ritz* method, the *Extended Rayleigh-Ritz* method and the *Kantorovich* method are of this type. Special attention should be given to the type of dynamic analysis performed, because the three latter methods are more suitable for free vibrational analysis. In the second category we find the Finite Element, Finite Difference and Finite Strip methods. A considerable amount of research on the dynamic analysis of shells has been carried out using the above methods. The finite element method was found to be the most powerful and versatile for the solution of a wide scope of engineering problems. It enables one to convert a problem with an infinite number of degrees of freedom to one with a finite number leading to a simplification in the solution process. Although it yields an approximate solution based upon assumed displacement fields, it is sometimes the only recourse for shell problems with irregular geometries or complex boundary conditions.

1.6 Outline of Present Investigation

The literature dealing with dynamic analysis of thin elastic cylindrical shells is voluminous, the majority of which deals with closed shells. Much less information is available for open circular cylindrical shells, i.e., panels. For this class of shell geometry, analytical solutions exist mainly for the small amplitude free vibration, much fewer exist for forced vibrations in linear and/or nonlinear ranges. The reason stems from the difficulty of solving the non-homogenous partial differential equations subjected to some boundary constraints for cases other than simply-supported, and also the advent of high speed digital computers combined with powerful numerical algorithm such as the finite element or finite difference.

The application of explosive energy in various fields of the economy confronts researchers with new problems in the study of the behaviour of thin-walled structures under intense dynamic loads. The present study concerns itself with the dynamic analysis of a steel cylindrical shell panel subjected to an external free-field air-blast loading.

An analytical approach based on the Galerkin variational principle is used for the linear small deflection shell behaviour. The modal solution is taken as the product of beam functions. Validation is provided by comparison with a numerical solution based on the finite element method. The latter method is extended to cover also the case of large displacements.

CHAPTER 2

LITERATURE SURVEY

2.1 Historical Background and Early Developments

Shell dynamics had its early origins in the study of the vibrations of bells. The oldest work on the subject is due to Euler, who in 1776 approached this problem by imagining the bell subdivided into thin annuli behaving as curved bars. In 1789, Jakob Bernoulli proposed a model consisting of a double sheet of curved bars, placed at right angles, along parallels and meridians.

The first treatment of the general dynamic theory of thin elastic shells, where the effects of both flexural and extensional deformations are included is due to Love [1], whose work resulted in the classical bending theory of thin elastic shells known as Love's first approximation.

Early work on the vibration of curved panels was done by Palmer [2] and Reissner [3]. Palmer used Rayleigh's method to evaluate the natural frequencies of simply supported and fixed panels. Reissner simplified the shallow shell theory by Marguerre [4], omitting the longitudinal inertia terms for classes of dynamic problems in which the principal vibrations take place in the transverse direction. In the following sections we will survey exact and approximate solutions in the field of shell vibration.

2.2 Previous Work on Exact Analytical Solutions

The simply supported circular cylindrical shell has received the most attention in the literature, due to the fact that one simple form of the solution for the eight order partial

differential equations of motion is capable of satisfying the simple support boundary exactly. There exist a multitude of frequency equations for each shell theory. A comprehensive study of this particular boundary condition was made by Forsberg [5], using the Donnell and Flügge theory.

The primary contribution to the exact analysis for the determination of modal characteristics for linear free vibration of closed circular cylindrical shells for different boundary support was outlined by Flügge [6]. This method required the numerical evaluation of an eight order determinant to find its value for any set of end conditions. Forsberg [7] examined all sixteen sets of homogenous boundary conditions at each end of the shell. The equations of motion developed by Flügge for thin circular cylindrical shell were used. Contrary to the usual approach of determining the natural frequencies of a shell of a given length, Forsberg's strategy required the initial assumption of a natural frequency and then the length of the cylinder with the prescribed end condition is derived after a number of iterations. Results were given for 10 cases and the influence of boundary conditions was investigated. Warburton [8] used Forsberg approach with Flügge's equations of motion and presented results for the edge free case.

The Donnell-Mushtari (D-M) or shallow shell theory is most frequently used to analyze circular cylindrical shell panels. Sewall [9] using the D-M theory and neglecting the tangential inertias obtained numerical results for a cylindrical shell panel simply supported on all edges. The effect of curvature upon small amplitude vibration frequencies for shallow shell panels was investigated by Leissa [10] using the Donnell type equations of motion. The frequency is given for a simply supported shell. For simply supported lateral support and curved edges arbitrarily supported (Webster [11]), the methods used by Forsberg and Warburton for complete cylindrical shells can be used. Recently Al-Khayat [12] gave an explicit frequency equation for a circular cylindrical panel subjected to arbitrary conditions along the curved edges and the straight edges simply supported. The modal forms are assumed to have a linear axial dependence in the Fourier series instead of the commonly used exponential axial dependence. Sander's equations of motion are used to formulate the eigenvalue problem, and the boundary conditions which are not

satisfied directly by the assumed series are enforced. The accuracy was tested against some available theoretical, numerical and experimental results. The influence of shell geometries upon the natural frequencies was also investigated.

Ballentine [13], using the Euler-Lagrange variational principle in conjunction with the total energy, derived the differential equations of motion for the study of the structural response of a simply supported cylindrical curved panel subjected to an arbitrary acoustical excitation. Redekop and Azar [14], using the Donnell-Mushtari theory, developed a closed form solution of a shallow cylindrical shell panel, simply supported on all sides and subjected to a uniform exponential blast load having a time variation given by the Friedlander decay law. The effects of curvature upon the shell response was examined and the results were compared with a finite element solution.

2.3 Previous Work on Approximate Solutions

For the majority of possible shell configurations in dynamics, where an exact analytical solution is difficult or impossible to set up, *approximate* solutions are warranted. There are two major classes of approximate methods, the energy and the numerical method.

2.3.1 Energy Method in Shell Dynamics

Applying the Lagrange equation to derive expressions of strain and kinetic energy and taking beam functions for modal displacement forms, Arnold and Warburton [15] derived theoretical expressions for the natural frequencies for the simply supported and clamped thin circular cylinder. The results were validated with experimental values. Gontkevich [16] used the Rayleigh-Ritz method with beam functions to obtain characteristic equations for the six problems having clamped, shear diaphragm or free supports at either or both ends of a circular cylindrical shell. The argument on the use of beam functions is that the behaviour of an axial strip of the

shell should be similar to that of a beam of the same type of boundary conditions.

Analytical frequencies were presented for the cantilever cylindrical shell by Sharma [17] using Flügge's thin shell theory. The Rayleigh-Ritz procedure was used together with beam functions for the assumed displacement mode shapes. Formulas for the natural frequencies of circular cylindrical shells for modes in which transverse deflections dominate are given by Soedel [18]. His approach was to solve a Donnell-Mushtari type of equation by the Galerkin method using general beam functions. The results were compared with some experimental results obtained by various authors and good agreement was obtained.

Sewall [9] calculated the natural frequencies of curved panels with simply supported or clamped edges, by employing the Rayleigh-Ritz procedure. The trial functions were the products of beam functions used in modal forms in the calculations and these were then compared with some experimental results. For the completely clamped shallow cylindrical shell, Webster [11] using Flügge's shell equations and a variational approach obtained theoretical results for the natural frequencies. The procedure consisted of applying Hamilton's principle subject to the constraints supplied by the geometric boundary conditions, which were enforced by means of Lagrange multipliers in the variational problem. The displacement functions are taken in the form of polynomials.

Petyt [19] made a collection of theoretical and computational predictions such as the Rayleigh-Ritz, Kantorovich, and the finite element method for the problem of a fully clamped cylindrical shell panel and compared these with experiments. Leissa [20] presented accurate non-dimensional frequency parameters for a cantilevered shallow cylindrical shells of a rectangular planforms for wide ranges of geometric parameters. The analysis was based on the shallow shell theory. Numerical results were obtained by using the Ritz method with algebraic polynomial as trial functions for the displacements. The same method by the same author was extended in the analysis of a completely free shallow shell [21] and in the analysis of edge constraints upon shallow shell frequencies [22].

Lim and Liew [23] presented a free flexural vibration analysis of shallow cylindrical shells of rectangular planform with arbitrary combination of free, simply supported and clamped boundaries. The Ritz approach with the pb-2 shape functions is used to formulate the problem. The shape functions consist of the product of a complete set of two-dimensional orthogonally generated polynomial functions and a basic function formed from the product of the equations of the boundaries each raised to an appropriate power is used to formulate the problem. Again extensive numerical results for a multitude of geometric parameters are given and comparison is made with the well established results from the literature.

For the case of shallow shell on rectangular planform, Leissa [10] assessed the curvature effects upon the vibration frequencies for the linear small deflection as well as nonlinear large deflection regime again for a shell supported by shear diaphragm. The large amplitude vibration and response of a cylindrical shell panel subjected to a step or a harmonic load function was investigated by Cummings [24]. Two different models were presented for the solution of a freely supported panel. The first model satisfies the stress condition at the boundaries exactly, but it satisfies the compatibility only on the average. The second model satisfies compatibility exactly, but satisfies the stresses on the boundaries only on the average.

Kanazawa [25] studied the effects of Gaussian curvatures and the boundary conditions on the nonlinear flexural vibrations of thin shallow shells. The nonlinear differential equations are derived by applying the Galerkin method to the Vlasov type equations of shallow shells. Both the free vibration and forced response (for a sinusoidal load) are analyzed. Several boundary conditions such as clamped and simply supported and different curvatures are examined.

The nonlinear large deformation dynamic response of a rectangular shell panel subjected to a free-field air blast was covered by Redekop and Azar [26]. Both a theoretical and a numerical approach using the finite element is given for the case of a hinged and immovable boundary conditions. Again results are given for several panel rises and conclusions are drawn.

Jiang [27] proposed a numerical model for large deflection, elasto-plastic analysis of cylindrical shell structures under blast loading. The model is based on a transversely-curved finite strip formulation. The problem of dynamic response in the linear and nonlinear range was investigated for a simply supported conditions.

2.3.2 Numerical Methods in Shell Dynamics

The advent of high speed digital computers made possible the application of powerful numerical methods such as the finite element and the finite difference methods in many practical engineering applications. Both methods result in multi-degree-of-freedom matrix equations. The finite difference approach is a purely mathematical technique. The equations of motion must be known for the structure under investigation. By contrast, the finite element approach does not require the differential equations of motion once the element stiffness and mass matrices are defined. The finite element method is particulary very well suited to problems where an analytical method is difficult or impossible due to the complexity of the geometry or the boundary condition for the structure under investigation.

Attempts to develop a finite element method for general shell structures have taken two different approaches. In the first approach, the shell is replaced by an assemblage of flat plate elements which are either triangular or quadrilateral in shape, Hrennikoff [28]. In the second approach, the shell is replaced by curved shell elements that permit exact geometrical representation of the structure.

The earlier attempts to develop a general shell element were made by, among others, Gallagher [29]. He presented a quadrilateral shell element with two constant principal radii of curvature. Connor and Brebbia [30] introduced a rectangular element based on shallow shell theory. Both elements used only linear distributions for membrane displacements and consequently did not include all rigid body mode. The resulting elements were too stiff and not efficient enough.

The degenerated shell element is another popular type of shell elements. This element is degenerated from a three-dimensional elasticity element. The additional consideration is one which incorporates, the Kirchhoff hypothesis. Ahmad [31] *et al.* first presented the degenerated shell element. Ahmad degenerated a three dimensional brick element into a general curved shell element which has nodes only at the midsurface. This type of element performs reasonably well for moderately thick shell situations. However, for thin shells when full integration is used to evaluate the stiffness matrix, overstiff solutions are often produced due to shear or membrane locking.

An extensive survey of the finite element modelling of structural vibration has been given by Reddy [32]. This survey concentrates on the basic structural elements, such as plates and shells and beams from 1967 to 1979. Numerical studies of uniform and tapered steel fan blades under various boundary conditions were carried out by Olson and Lindberg [33, 34]. The cylindrical shell elements of rectangular planform and doubly curved triangular elements were used. Walker [35] investigated cantilevered shells using a doubly curved helicoidal shell element. Yang [36] et al. carried a survey of the advances in the formulations for thin shell finite elements. The survey is illustrated with some extensions and applications to cases such as static and dynamic responses, and, in all, case studies of the effects of geometric and material nonlinearities are discussed. The bibliography by Mackerle [37] provides a list of references on finite element and boundary element analysis of shells. The main topics include element library for thin and thick shell element, free and forced vibration and wave propagation in shells, linear and nonlinear static and dynamic analysis of thin and thick shells (material and geometric nonlinearities).

CHAPTER 3
THEORETICAL BACKGROUND FOR THE ANALYTICAL SOLUTION

3.1 Introduction

The basic equations which describe the behaviour of thin elastic shells were originally derived by Love. He formulated the precondition under which simplified two-dimensional equations of shell deformation could be derived. Love's precondition is also termed Love's first approximation. Love's first approximation to the theory of thin elastic shells is based upon the following premises:

1. The shell thickness is very small in comparison with the other shell dimensions.
2. Shell deformations are sufficiently small to allow the second and higher power of these deformations to be neglected with respect to the first powers.
3. The transverse normal stress is small compared to the other normal stresses in the shell, and thus it can be neglected.
4. The normals of the undeformed middle surface remain normal to it and undergo no change in length during deformation.

The assumption of thinness sets the stage for the entire theory. The assumption that the deflections of the shell are small permits us to refer all derivations and calculations to the original configuration of the shell and, together with Hooke's law, assures us that the resulting theory will be a linear elastic one. The third and fourth assumptions transform the original three-

dimensional problem of the mathematical theory of elasticity into a two-dimensional one.

3.2 Donnell-Mushtari's (D-M) Equations of Motion

The theory behind the development of the D-M governing equations of motions is quite lengthy and has been stated by many authors, ref. [38,39]. This approach ignores damping and is the one used most widely in linear shell vibration. It neglects neither bending nor membrane effects. It applies well to shallow shells that are loaded normal to their surface and concentrates on transverse deflection behaviour.

The governing equations in terms of displacements u, v, w are

$$D\nabla^8 w(x,y,t) + \frac{Eh}{R^2}\frac{\partial^4 w(x,y,t)}{\partial y^4} + \rho h \nabla^4 \frac{\partial^2 w(x,y,t)}{\partial t^2} = \nabla^4 p(x,y,t) \tag{3.1a}$$

$$\nabla^4 u(x,y,t) = \frac{\mu}{R}\frac{\partial^3 w(x,y,t)}{\partial x^3} - \frac{1}{R}\frac{\partial^3 w(x,y,t)}{\partial x \partial^2 y} \tag{3.1b}$$

$$\nabla^4 v(x,y,t) = -\frac{(2+\mu)}{R}\frac{\partial^3 w(x,y,t)}{\partial x^2 \partial y} + \frac{1}{R}\frac{\partial^3 w(x,y,t)}{\partial^3 y} \tag{3.1c}$$

Eq. (3.1) has enjoyed wide usage because of the fact that the displacements are decoupled. The equations are more amenable to analytical solutions, and must be solved for prescribed boundary conditions. It is seen that the problem is reduced to the solution of a single equation (3.1a) for a single unknown, w. All symbols are defined in the notations, p. viii.

3.3 Boundary Conditions

The classical boundary conditions were derived by considering that the boundaries of the shell are localized precisely along the cylindrical coordinates axes, and that the work done by the reactions at the boundaries is zero. Leissa [39] presented the conditions for the edge x=const. as

$$
\begin{aligned}
N_x &= 0 \quad or \quad u = 0 \\
N_{xy} + \frac{M_{xy}}{R} &= 0 \quad or \quad v = 0 \\
Q_x - \frac{\partial M_{xy}}{\partial y} &= 0 \quad or, \quad w = 0 \\
M_x &= 0 \quad or \quad \frac{\partial w}{\partial x} = 0
\end{aligned}
\tag{3.2}
$$

The following boundary conditions on the straight sides (x=const) are considered in this work

a) Clamped-clamped

$$
w = \frac{\partial w}{\partial x} = u = v = 0 \qquad at\ x = 0, a \tag{3.3}
$$

b) Clamped-simply supported

$$
\begin{aligned}
w = \frac{\partial w}{\partial x} = u = v = 0 \qquad & at\ x = 0 \\
w = M_x = N_x = v = 0 \qquad & at\ x = a
\end{aligned}
\tag{3.4}
$$

c) Clamped-free

$$
\begin{aligned}
w = \frac{\partial w}{\partial x} = u = v = 0 \qquad & at\ x = 0 \\
Q_x - \frac{\partial M_{xy}}{\partial y} = M_x = N_x = N_{xy} + \frac{M_{xy}}{R} = 0 \qquad & at\ x = a
\end{aligned}
\tag{3.5}
$$

d) Simply supported-simply supported

$$w = M_x = N_x = v = 0 \qquad at\ x = 0, a \tag{3.6}$$

Similar expressions will be used at the curved edges, providing sixteen types of boundary conditions for the shell panel.

The displacements, and force and moment resultants in the preceding expressions are shown in Fig. 3.1. Their mathematical expression in terms of mid-surface displacements are as follow, ref.[39]

$$\begin{aligned}
N_x &= \frac{Eh}{1-\mu^2}\left(\frac{\partial u}{\partial x} + \mu\left(\frac{\partial v}{\partial y}\right) - \frac{w}{R}\right) \\
N_y &= \frac{Eh}{1-\mu^2}\left(\frac{\partial v}{\partial y} + \mu\left(\frac{\partial u}{\partial x} - \frac{w}{R}\right)\right) \\
N_{xy} &= \frac{Eh}{2(1+\mu)}\left(\frac{\partial u}{\partial y} + \frac{\partial v}{\partial x}\right) \\
M_x &= -D\left(\frac{\partial^2 w}{\partial x^2} + \mu\frac{\partial^2 w}{\partial y^2}\right) \\
M_y &= -D\left(\frac{\partial^2 w}{\partial y^2} + \mu\frac{\partial^2 w}{\partial x^2}\right) \\
M_{xy} &= (1-\mu)D\frac{\partial^2 w}{\partial x \partial y} \\
Q_x &= -D\left(\frac{\partial^3 w}{\partial x^3} + \frac{\partial^3 w}{\partial x \partial y^2}\right) \\
Q_y &= -D\left(\frac{\partial^3 w}{\partial y^3} + \frac{\partial^3 w}{\partial y \partial x^2}\right)
\end{aligned} \tag{3.7}$$

3.4 Geometry and loading

The cylindrical shell panel under investigation is given in Fig. 3.2. Values a, b, R and h indicate, respectively, the width, length, radius and thickness. Any point on the mid-surface is described by the Cartesian coordinates x and y.

According to the definition of Rekach [40], a thin shallow shell should satisfy the conditions

$$\frac{l_{\min}}{f} \geq 5, \qquad \frac{R_{\min}}{h} \geq 20, \qquad \frac{l_{\min}}{h} \geq 20 \tag{3.8}$$

where l_{min} is the shortest edge, f is the highest elevation of the mid-surface of the shell above the projected base plane, R_{min} is the smallest radius of curvature and h as before is the thickness of the shell. In our case, $a=l_{min}$, $R=R_{min}$ and f is given by the following expression

$$f = R - \left(R^2 - \left(\frac{a}{2} \right)^2 \right)^{\frac{1}{2}} \tag{3.9}$$

The loading is assumed to consist of a normal pressure p that is uniform over the shell surface and has a time variation given by the Friedlander decay law as

$$p(t) = \begin{cases} P_{\max}\left(1 - \frac{t}{t_p} \right) \exp\left(-a_p \frac{t}{t_p} \right) & 0 \leq t \leq t_p \\ 0 & t > t_p \end{cases} \tag{3.10}$$

where P_{max} is the peak reflected pressure, t_p is the positive phase duration, a_p is a constant and t is the time.

3.5 Galerkin's Method Applied to D-M Shell Equations

The variational principle was reformulated into a general form by Galerkin [41, 42]. The resulting Galerkin method can be applied successfully to such diverse types of problems as small and large deflection theories, linear and nonlinear vibration and stability problems of plates and shells, provided that the differential equations of the problem under investigation have already been determined.

The mathematical development of the method is quite complex and a detailed description is beyond the scope of this work. Briefly, it is necessary to assume a mode shape (trial function) satisfying at least the geometrical boundary conditions. The differential equations are multiplied with the same trial function used as a weighing function and integrated over the shell surface. Denoting $\psi(x,y)$ as the mode shape, the mathematical expression of the Galerkin's method in terms of the shell equation of motion can be written as:

$$\int_A \left(D\nabla^8 w + \frac{Eh}{R^2}\frac{\partial^4 w}{\partial y^4} + \rho h \nabla^4 \frac{\partial^2 w}{\partial t^2} \right) \psi(x,y)\, dA = \int_A \left(\nabla^4 p\right) \psi(x,y)\, dA \tag{3.11}$$

The lateral deflections and the load are expanded into infinite series respectively as:

$$\begin{aligned} w(x,y,t) &= \sum_m \sum_n C_{mn}(t)\, \psi_{mn}(x,y) \\ p(x,y,t) &= \sum_m \sum_n p_{mn}(t)\, \psi_{mn}(x,y) \end{aligned} \tag{3.12}$$

where ψ_{mn} is the product of two functions, each depending on a single argument. Thus

$$\psi_{mn}(x,y) = X_m(x)\,Y_n(y) \tag{3.13}$$

Separation of variables reduces the variational problem to the selection of two linearly independent sets of functions $X_m(x)$ and $Y_n(y)$ satisfying the boundary conditions. An appropriate set of functions (first proposed by Vlasov [43]) is the set of eigenfunctions of vibrating beams, provided that the boundary conditions of the beam and the shell are similar. A justification for the use of beam functions is that, for example, the behaviour of an axial strip of a cylindrical shell should be similar to that of a beam of the same boundaries.

The free vibration of a beam of a uniform cross section is described by the differential equation

$$\frac{\partial^4 w(\xi,t)}{\partial \xi^4} + \frac{\bar{m}}{EI}\frac{\partial^2 w(\xi,t)}{\partial t^2} = 0 \tag{3.14}$$

where $w(\xi,t)$ is the time dependent lateral deflection and $\bar{m}$ is the mass per unit length. It is possible to begin development of mode shape expressions for each particular set of boundary condition by adopting a solution in the form

$$w(\xi,t) = W(\xi)\sin(\omega t) \tag{3.15}$$

where ω is free vibration natural frequency. Substitution of Eq. (3.11) in (3.10) gives

$$W^{IV}(\xi) - \frac{\lambda^4}{l^4} W(\xi) = 0 \tag{3.16}$$

where

$$\frac{\lambda^4}{l^4} = \frac{\bar{m}\omega^2}{EI} \tag{3.17}$$

The solution of this well known fourth order ordinary differential equation is taken as

$$W(\xi) = A_1 \sin\left(\lambda \frac{\xi}{l}\right) + A_2 \cos\left(\lambda \frac{\xi}{l}\right) + A_3 \sinh\left(\lambda \frac{\xi}{l}\right) + A_4 \cosh\left(\lambda \frac{\xi}{l}\right) \tag{3.18}$$

The constants A_1, A_2, A_3 and A_4 are determined from the boundary conditions, while λ is a root of the characteristic equation. This equation is derived by equating the determinants of the homogenous boundary equation to zero. Eigenfunctions $W_m(\xi)$ of the beam vibration are given in Table 3.1 for a variety of boundary conditions.

The lateral deflection and the load are now expressed in terms of eigenfunctions as:

$$\begin{aligned} w(x,y,t) &= \sum_m \sum_n C_{mn}(t)\psi_{mn}(x,y) = \sum_m \sum_n C_{mn}(t) X_m(x) Y_n(y) \\ p(x,y,t) &= \sum_m \sum_n p_{mn}(t)\psi_{mn}(x,y) = \sum_m \sum_n p_{mn}(t) X_m(x) Y_n(y) \end{aligned} \tag{3.19}$$

Substituting the expressions (3.15) into (3.7) gives

$$\sum_m \sum_n \int_A \Big(DC_{mn}(t)\Big(X_m^{viii} X_i Y_n Y_j + X_m X_i Y_n^{viii} Y_j + 6 X_m^{iv} X_i Y_n^{iv} Y_j + \Big(X_m^{vi} X_i Y_n^{ii} Y_j + X_m^{ii} X_i Y_n^{vi} Y_j\Big)\Big)$$
$$+ C_{mn}(t)\frac{Eh}{R^2} X_m X_i Y_n^{iv} Y_j + \rho h \ddot{C}_{mn}(t)\Big(X_m^{iv} X_i Y_n Y_j + 2X_m^{ii} X_i Y_n^{ii} Y_j + X_m X_i Y_n^{iv} Y_j\Big)\Big) dA \qquad (3.20)$$
$$= \sum_m \sum_n \int_A p_{mn}(t)\Big(X_m^{iv} X_i Y_n Y_j + 2X_m^{ii} X_i Y_n^{ii} Y_j + X_m X_i Y_n^{iv} Y_j\Big) dA$$

The eigenfunctions and their derivatives satisfy important mathematical relations. They are *orthogonal,* i.e the integral of the product of two eigenfunctions of the vibrating beam, corresponding to different modes, is zero. Thus

$$\int_0^a X_i X_j \, dx = 0$$
$$\int_0^a X_i'' X_j'' \, dx = 0 \qquad (3.21)$$

The same property holds for the 4th, 6th, 8th order derivatives as well. A numerical investigation pertaining to the following product

$$\int_0^a X_i'' X_j \, dx \qquad (3.22)$$

shows that the orthogonality condition is slightly violated. This holds true also for the other non-equal derivative products such as

$$\int_0^a X_i^{iv} X_j'' \, dx \qquad (3.23)$$

However, the magnitudes of the expressions (3.18) and (3.19) are negligible and, for all intents the eigenfunctions, can be considered as being orthogonal. Since the eigenfunctions are orthogonal, it is possible to expand the load functions $p(x,y,t)$ in terms of the eigenfunctions. The constants p_{mn} in (3.15) can be expressed in terms of eigenfunctions $X_m(x)$ and $Y_n(y)$ by means of

$$p_{mn}(t) = p(t)\frac{\int_0^a\int_0^b X_m(x)\,Yn(y)\,dy\,dx}{\int_0^a\int_0^b X_m^2(x)\,Y_n^2(y)\,dy\,dx} \tag{3.24}$$

By neglecting the terms with nonidentical subscripts mi and jk, we introduce the following notations

$$\begin{aligned}
I_1 &= \int_0^a X_m X_m\,dx \quad , \quad I_2 = \int_0^a X_m^{II} X_m\,dx \\
I_3 &= \int_0^a X_m^{IV} X_m\,dx \quad , \quad I_4 = \int_0^a X_m^{VI} X_m\,dx \\
I_5 &= \int_0^a X_m^{VIII} X_m\,dx \quad , \quad I_6 = \int_0^a X_m\,dx \\
I_7 &= \int_0^b Y_n Y_n\,dy \quad , \quad I_8 = \int_0^b Y_n^{II} Y_n\,dy \\
I_9 &= \int_0^b Y_n^{IV} Y_n\,dy \quad , \quad I_{10} = \int_0^b Y_n^{VI} Y_n\,dy \\
I_{11} &= \int_0^b Y_n^{VIII} Y_n\,dy \quad , \quad I_{12} = \int_0^b Y_n\,dy
\end{aligned} \tag{3.25}$$

then Eq. 3.14 can be written as

$$D\left(I_5 I_6 + I_1 I_{10} + 6 I_3 I_8 + 4\left(I_4 I_7 + I_2 I_9\right) + \frac{Eh}{R^2} I_1 I_8 \right) C_{mn}(t) + \rho h \left(I_3 I_6 + 2 I_2 I_7 + I_1 I_8\right) \ddot{C}_{mn}(t) = p_{mn}(t)\left(I_3 I_6 + 2 I_2 I_7 + I_1 I_8\right) \tag{3.26}$$

with

$$\omega_{mn}^2 = \frac{D\left(I_5 I_6 + I_1 I_{10} + 6 I_3 I_8 + 4\left(I_4 I_7 + I_2 I_9\right) + \frac{Eh}{R^2} I_1 I_8 \right)}{\rho h \left(I_3 I_6 + 2 I_2 I_7 + I_1 I_8\right)} \tag{3.27}$$

as the square of the natural frequency of vibration, and

$$P^{\cdot} = \frac{P_{\max} I_6 I_{12}}{\rho h I_1 I_7} \tag{3.28}$$

Substitution of (3.23) and (3.24) in (3.22) and considering a specific set of *m* and *n*, the variational shell equation can be reduced to the solution of the following second order differential equation

$$\ddot{C}_{mn}(t) + \omega_{mn}^2 C_{mn}(t) = P^{\cdot}\left(1 - \frac{t}{t_p} \right) \exp\left(-\frac{a_p t}{t_p} \right) \tag{3.29}$$

Eq. (3.25) admits a solution of the form

$$C_{mn}(t) = A_{mn} \sin(\omega_{mn} t) + B_{mn} \cos(\omega_{mn} t) + (Q_{mn} - R_{mn} t) \exp\left(-\frac{a_p t}{t_p} \right) \tag{3.30}$$

Substituting Eq. (3.26) into Eq. (3.25) and matching terms give

$$Q_{mn} = \frac{P \cdot \left(\left(\frac{a_p}{t_p} \right)^2 + \omega_{mn}^2 \right) - 2P \cdot \frac{a_p}{t_p^2}}{\left(\left(\frac{a_p}{t_p} \right)^2 + \omega_{mn}^2 \right)^2} \quad , \quad R_{mn} = \frac{P \cdot}{t_p \left(\left(\frac{a_p}{t_p} \right)^2 + \omega_{mn}^2 \right)} \tag{3.31}$$

Imposing the initial conditions of zero displacement and velocity the unknown constants are determined as

$$A_{mn} = \frac{\left(R_{mn} + \left(\frac{a_p}{t_p} \right) Q_{mn} \right)}{\omega_{mn}} \quad , \quad B_{mn} = -Q_{mn} \tag{3.32}$$

The solution for the dynamic loading of a cylindrical shell panel then consists of the following superposition of the mode shapes

$$w(x,y,t) = \sum_{m=1,2,3,\ldots} \sum_{n=1,2,3,\ldots} C_{mn}(t) X_m(x) Y_n(y) \tag{3.33}$$

Stress resultants may then be determined using (3.3).

3.6 Special Consideration on the Free Boundaries

The clamped-free beam functions do not satisfy exactly the *free* boundary condition at a given shell edge. To illustrate the point consider the case when $x=a$ represents an edge. The

boundary conditions at a free edge are given by

$$N_x = N_{xy} + \frac{M_{xy}}{R} = M_x = Q_x - \frac{\partial M_{xy}}{\partial y} = 0 \tag{3.34}$$

The last two conditions are of particular interest. In terms of displacements they are written as

$$\begin{aligned} M_x &= -D\left(\frac{\partial^2 w}{\partial x^2} + \mu\frac{\partial^2 w}{\partial y^2}\right) = 0 \\ Q_x - \frac{\partial M_{xy}}{\partial y} &= -D\left(\frac{\partial^3 w}{\partial x^3} + (2-\mu)\frac{\partial^3 w}{\partial x \partial y^2}\right) = 0 \end{aligned} \tag{3.35}$$

It is extremely difficult to construct coordinate functions which satisfies these conditions. But it is possible to construct functions satisfying, ref. [44]

$$\begin{aligned} \frac{\partial^2 w}{\partial x^2} &= 0 \\ \frac{\partial^3 w}{\partial x^3} &= 0 \end{aligned} \tag{3.36}$$

Beam functions are part of these possible array of expressions for a free edge examination. However convergence is slower for panels with free sides, since more eigenfunctions are required to achieve a reasonable degree of accuracy. Comparison later on will confirm that the effect of this approximation is negligible.

CHAPTER 4

NUMERICAL SOLUTION BY THE FEM

4.1 General

Most problems in structural analysis have a geometry too complex to be solved by classical analytical methods. The advent of high speed computers together with the finite element procedures make possible the solution of problems which were previously intractable. In general, the finite element method models a structure as an assemblage of small parts (elements). Each element is of simple geometry and is therefore much easier to analyze than the complete structure. In essence a continuous system has been discretized. Hence a set of differential equations is transformed into a set of algebraic equations, and is solved to give the solution of a given problem.

4.2 Finite Element Formulation

4.2.1 Introduction

There exist several types of formulations for the finite element method. The most important formulation, which is widely used for the solution of many practical problems, is the *displacement-based* finite element. This is because of its simplicity, generality and special adaptability to computer techniques. Practically all major general-purpose analysis programs have been written using this type of formulation.

4.2.2 The Displacement-Based Finite Element Method

The basic steps in the analysis of a given structure using the displacement-based finite element methods are

1. Idealize the actual physical problem into an assemblage of discrete elements which are interconnected at the structural nodal points.
2. Identify the unknown nodal points displacements that completely define the displacement response of the structural idealization.
3. Establish force balance equations corresponding to the unknown joint displacement and solve these equations.
4. Calculate the internal stress distribution with the nodal-displacements known.
5. Interpret the displacement and stresses predicted by the solution of the structure idealization when considering the assumptions used and correct interpretation of the results.

In actual analysis, the most important steps are the proper idealization and the interpretation of the results. In the next two sections the basic equations of equilibrium governing the linear and nonlinear response of a system of finite elements are presented.

4.3 Finite Element Formulation in Linear Analysis

The derivation of the FEM equilibrium equations is well known standard and has been discussed in numerous publications. The finite element equations of motion are given, Bathe [45] as:

$$[M]\{\ddot{U}\} + [C]\{\dot{U}\} + [K]\{U\} = \{R\} \tag{4.1}$$

where *[M], [C] and [K]* are mass, damping and stiffness matrix of the structure, and *{Ü},*

$\{\dot{U}\}$ and $\{U\}$ are vectors of nodal point acceleration, velocity and displacement. Vector $\{R\}$ is the load vector which includes the effects of body forces, surface forces, initial stress forces, concentrated loads, initial strain forces and thermal loads. It should be noted that in linear analysis the mass, damping and stiffness matrices are independent of time.

In a dynamic analysis, the stiffness $[K]$ and the mass matrix $[M]$ and the load vector $\{R\}$ should be calculated and the equations of motion are solved for the structural response $\{U\}$, $\{\dot{U}\}$ and $\{\ddot{U}\}$. If necessary, the stresses may be evaluated from displacements.

4.4 Finite Element Formulation in Nonlinear Analysis

The finite element formulation of section 4.3 is possible under the following assumptions

- Infinitesimal small displacements
- The constitutive matrix is considered constant and independent of the stress state

The use of infinitesimal displacements permits the evaluation of the $[K]$ matrix and $\{R\}$ vector over the original volume of the finite element. Furthermore the strain displacement matrix can be assumed to be constant and independent of the element displacements.

Table 4.1, ref. [45], gives a classification of nonlinear analyses that considers separately material nonlinear effects and kinematic nonlinear effects. The major task of researchers or designers is to decide whether the problem falls into one or the other category of analysis. Based on the requirements, the proper formulation can be selected to describe the actual physical situation.

In nonlinear analysis where the configuration of the body is load dependent, the solution must be carried out incrementally and iteratively until the desired accuracy is obtained.
For the derivation of the governing finite element equations, the principle of virtual work is used, including both the possibility that the body considered undergoes large displacements, rotations

and large strains, and that the stress-strain relationship is nonlinear.

A direct solution to the equations arising from the virtual work principle is not feasible in the case of severe nonlinearities. However an approximate solution can be devised by referring all variables to a previously calculated known equilibrium configuration. Therefore two types of approximations have been developed, namely the *total Lagrangian (TL)* and the *updated Lagrangian (UL)* formulations. The solution scheme for the *TL* formulation is one where all variables are referred to the initial configuration at time 0. In *UL* all variables are referred to the previously calculated configuration. The choice of the use of either of these methods depends on which has the greater numerical efficiency. Details of the derivations of the *TL* and *UL* are given in ref. [45].

4.4.1 General Matrix Equations for the Nonlinear Displacement-Based Finite Element

The basic steps to derive the governing finite element equations are the same as in the linear analysis. In the case of dynamic nonlinear analysis the governing equations neglecting damping are given as, ref. [45]

Using TL formulation

Implicit time integration

$$[M]\,{}^{t+\Delta t}\{\ddot{U}\} + ({}_{t}^{t}[K_L] + {}_{t}^{t}[K_{NL}])\{U\} = {}^{t+\Delta t}\{R\} + {}_{t}^{t}\{F\} \tag{4.2}$$

Explicit time integration

$$[M]\,{}^{t}\{\ddot{U}\} = {}^{t}\{R\} - {}_{0}^{t}\{F\} \tag{4.3}$$

Using UL formulation

Implicit time integration

$$[M]^{t+\Delta t}\{\ddot{U}\} + ({}^{t}_{0}[K_L] + {}^{t}_{0}[K_{NL}])\{U\} = {}^{t+\Delta t}\{R\} + {}^{t}_{0}\{F\} \tag{4.4}$$

explicit time integration

$$[M]^{t}\{\ddot{U}\} = {}^{t}\{R\} - {}^{t}_{t}\{F\} \tag{4.5}$$

where

[M]	Mass matrix
[K]	Stiffness matrix
${}^{t}[K]$	Linear strain incremental stiffness matrix, not including initial displacement
${}^{t}_{0}[K_L]$, ${}^{t}_{t}[K_L]$	Linear strain incremental stiffness matrices
${}^{t}_{0}[K_{NL}]$, ${}^{t}_{t}[K_{NL}]$	Nonlinear strain incremental stiffness matrix
${}^{t+\Delta t}\{R\}$	Vector of externally applied nodal points load at t+Δt
${}^{t}\{F\}$, ${}^{t}_{0}\{F\}$, ${}^{t}_{t}\{F\}$	Vectors of nodal point forces
$\{U\}$	Vector of increments in the nodal point displacements
${}^{t}\{\ddot{U}\}$, ${}^{t+\Delta t}\{\ddot{U}\}$	Vector of nodal point accelerations at time t and t+Δt

4.5 Finite Element Modelling for Thin Shells

The geometric discretization of shells using finite elements has been attempted using four types of elements. These are as follows

1. Flat plate elements with the shapes of rectangles, quadrilaterals and triangles together with the use of coordinate transformation.
2. Axisymmetric shell elements with straight or curved edges along the meridian.
3. Curved elements with the shapes of rectangles, quadrilaterals and triangles based on classical shell theories.
4. Elements derived or 'degenerated' from axisymmetric or three dimensional solid elements

The choice of the finite element depends on many factors, such as, the geometry of the structure, type of analysis etc.

4.6 The ADINA Finite Element Computer Code

The commercial FEM code ADINA (Automatic Dynamic Incremental Nonlinear Analysis) was used for the numerical analysis. The computer code was originally developed by K. J. Bathe in 1986 and has since become one of the most versatile tools in the finite element domain.

The computer program can be employed effectively for linear and nonlinear, static and dynamic general three-dimensional analysis. Its vast array of elemental, and material library makes it particularly well suited for such diverse domains of analysis as stress analysis, heat transfer and fluid flow.

The ADINA system consists of three solution modules bound together by the ADINA user interface

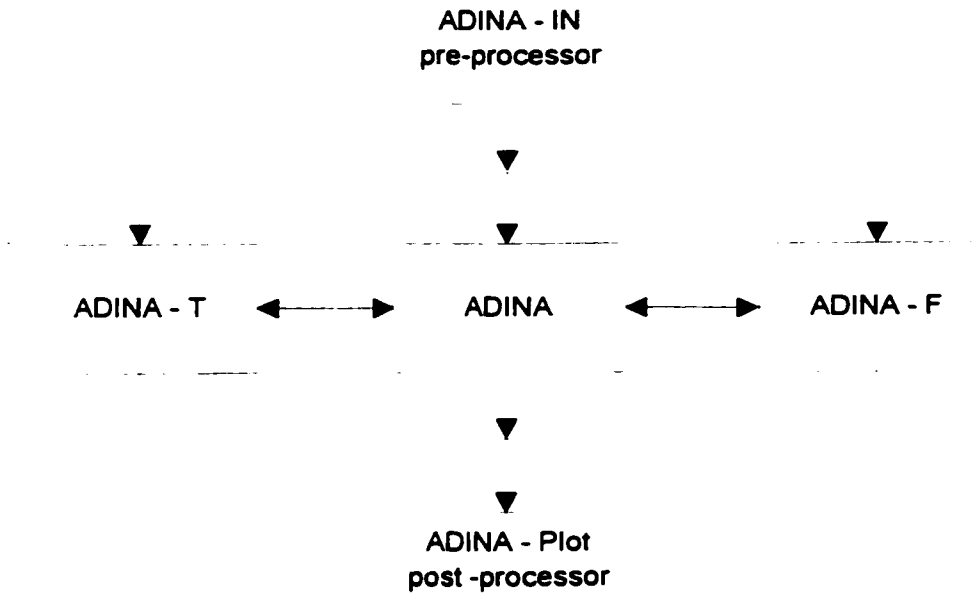

ADINA-T is for analysis of heat transfer in solids, ADINA is for displacement and stress analysis, ADINA-F is for fluid flow and heat transfer. Furthermore, each solution module comes with the same pre- and post-processing program, ADINA-IN is for preparation and display of input data and ADINA-PLOT is for display of the calculated results.

ADINA can be supported by a wide range of hardware platforms in the industry, from super-computers to workstations to low cost personal computers which run under Windows 95/NT.

4.6.1 Program Organization

The complete solution process in ADINA program is divided into four distinct phases:

1) Finite Element Mesh and Element Data Input

The control information and the nodal point input are read and generated by the program. The equation numbers for the active degrees of freedom at each nodal point are established. The initial conditions are read. The element data are read and generated, the element connection array is calculated and all element information is stored.

2) Assemblage of Structure Matrices

Various matrices such as mass, stiffness and damping are assembled and stored.

3) Load Vector Calculations

The externally applied load vectors for each time step are calculated and stored

4) Step-by Step Solution

During this phase, the solution of the finite element equations is obtained at all time points. In addition to the nodal displacements, velocities and accelerations, the element stresses are calculated.

4.6.2 ADINA-IN Input File Preparation

The input data required by ADINA is prepared using the commands and parameters of the ADINA-IN pre-processor program. Unlike other programs, ADINA-IN does not require any particular order of command, and the names of the commands were chosen for easy recognition of the corresponding function. The key names of parameters, which can be used optionally to allow parameter input in any order, has been similarly been chosen to easily recognize the functions of the parameters.

There are about twelve command groupings used for the creation of the ADINA-IN input file for the problem at hand, and they are

- **MASTER**

The MASTER command defines the master control information for the entire model. In dynamic analysis, the number of solution steps, time step increment and the time at solution start is also specified.

- **ANALYSIS**

The command ANALYSIS selects the analysis to be either static or dynamic, specifies the mass matrix type and other analysis parameters. For dynamic analysis, the time integration method and parameters are also specified.

- **KINEMATICS**

The command KINEMATICS defines the kinematic formulation to be used for all element groups.

- **SYSTEM**

The command SYSTEM is used to define local coordinate systems

- **COORDINATES**

The command COORDINATES defines nodes coordinates for the current structure. The coordinates are given in global system or in a local system as specified by the last preceding SYSTEM command,

- **MATERIAL**

The command MATERIAL defines the type of material used in the structure.

- **EGROUP**

The command EGROUP defines the current element group to consist of shell elements, giving its identifying number and control parameters.

- **THICKNESS**

The command THICKNESS inputs the thicknesses of four corner nodes of a surface containing shell elements.

- **LINE ARC**

The command LINE ARC generates a curved line of up to maximum 1000 nodes. New nodes are immediately generated in the global coordinate systems.

- **GSURFACE**

The command GSURFACE generates the surface of SHELL elements. The generation is performed in the global coordinate systems

- **BOUNDARIES**

The command BOUNDARIES specifies the six displacement boundary conditions, fixed or free, applicable to nodes of the main structure or any substructure.

- **TIMEFUNCTION**

The command TIMEFUNCTION defines the time dependence of all the loads applied to the structure.

- **LOADS ELEMENT**

The command LOADS ELEMENT defines pressure loading acting on elements of the current element group when it consists of SHELL elements.

The control of the printed output is done using the following three commands, *PRINTOUT, PRINTNODES* and *PRINTSTEPS*. Also to view or check the generated mesh, the commands *FRAME* AND *MESH* are used.

For a more detailed account of the ADINA, and ADINA-IN commands the reader is referred to [46].

CHAPTER 5

RESULTS

This chapter is divided into three main sections. First, validation for the Galerkin-Vlasov scheme is obtained. Then, analytical results for different curvature ratios are presented. Finally, the finite element solutions for some particular cases are given.

5.1 Validation

Analytical and numerical results for forced vibration were determined for the following material, loading and geometric properties

E=206.8 GPa	P_{max}=6.89 MPa	a=0.381 m
ρ=7770 kg/m^3	a_p=1.98	b=1.016 m
μ=0.3	t_p=0.004	h=0.0125 m

Panel curvatures are represented by the following rise ratios: f/a=0.0, 0.02, 0.033, 0.05 and 0.1. These values are similar to those of Gupta et al. [47] for rolled homogeneous armour tests and enable direct comparison with available plate and shell results(Redekop and Azar [14,26]).

Throughout the discussion, the symbols *C*, *F* and *SS* respectively denote clamped, free and simply-supported edges. A four letter character describes the support condition of the shell, for example *SSCC* represents a shell having its straight edges simply-supported while its curved edges clamped. Fig. 5.1, summarizes the 16 different support conditions under investigation.

A FORTRAN computer program operating on a *PC* was written to determine the analytical results for panel response and is given in Appendix A. Fig. 5.2 depicts the load intensity versus time. Results are determined for the point of maximum deformation in the shell panel. For symmetric boundary conditions, such as *SS* and *CC*, the point selection is the mid-point. For the *CS* boundary condition, the maximum deformation is found by solving the appropriate beam function in Table 3.1, and it is found to be 0.5817ξ, where ξ is the beam span. For the cantilever, *CF* support condition, the maximum deformation occurs at the end of the panel.

Since the solution formulated is in the form of an infinite series, it is necessary to truncate the series. Truncation was made when the deviation of two successive solutions was less than 0.5%.

Validation of the analytical model was made possible by the use of the ADINA finite element program. Due to the simplified geometry of the problem at hand, the shell panel under study can be modelled easily as an assembly of 2-D isoparametric shell elements with a single layer in the transverse direction. In ADINA, the isoparametric shell element has four options;

four, eight, nine and sixteen midsurface nodes. Each node has six degrees of freedom, three translational and three rotational (although in actual analysis the twist in z-direction is prevented), Figs. 5.3 to 5.7.

The structure's kinematics should be defined as well, the choice lies between a linear or nonlinear range of analysis. Also the solution method for the equilibrium equations should be selected beforehand. The Mode Superposition and the Direct Integration Method are the most widely used, and are available in ADINA.

The positive phase duration, t_p of the exponential load in this case dictates the solution method. The direct integration scheme is selected over the mode superposition method due to the fact that the response, for a relatively 'short' duration is required. The unconditionally stable scheme proposed by Newmark is selected. This type of direct integration scheme is stable regardless of the time step selected. However an appropriate time step should be chosen for a desired accuracy.

The accuracy of the finite element solution depends on three factors

1. Shell element selection
2. Mesh selection
3. Time step selection

However solution accuracy should be balanced with computation cost. In order to come up with an input file where upon program execution, the results are accurate enough and where the

computation cost is not excessive, trial runs where found to be necessary. The trials were taken in the linear range for the *CCCC*, *SSFF* and *CFCF* support conditions, with the fifth rise ratio. In addition to the shell elements selection, three different meshes were used, *2 x 5, 4 x 10* and *8 x 20,* Figs. 5.8 to 5.10. The time-steps were taken as *1, 0.1, 0.01 ms* respectively. A total number of 108 input files were generated. After successive runs and taking into account the solution accuracy versus computational time, a *4 x 10* mesh of nine noded isoparametric shell elements, Fig 5.11 with a *0.1 ms* time step is selected. A sample ADINA-IN input file is provided in Appendix A.

The basis of comparison between the Galerkin-Vlasov and the finite element based model is for the *f=0.1* rise case. Figs. 5.12 to 5.27 depict the plot of the analytical model versus the numerical one for the sixteen cases presented by the Galerkin-Vlasov approach. There appears to be good agreement between the two approaches. In most cases of structural dynamics, the finite element provides an upper bound solution, hence it is called a *stiff* solution. However the analytical solution provided a '*stiffer*' solution compared to the finite element. The reason may stem from the fact that, the beam functions already have higher mode shapes built in them, and that is why for some of the boundaries, such as *CCCC*, a one term solution , $m=n=1$ is about 5% from the desired accuracy. This holds true for all but the *SSSS* boundary condition. Here the analytical solution is more *'relaxed'* than that of the finite element solution. That is because of the fact that for this type of support, the mode shape not only satisfies the boundary conditions exactly but also the differential equation of motion. Hence the *SSSS* solution is considered an exact solution.

The discrepancies between the two methods ranges from about 8 to 16%, noting that for the exact solution, in *SSSS* the 'error' is of the order of 8.4%.

5.2 Analytical Results

Successive runs of the *FORTRAN* computer program enables us to plot the maximum shell panel deflection for all sixteen boundary condition types considered, Figs. 5.28 to 5.43. Results for the *SSSS* case are further validated with respect to work done in ref. [14], [26] and [47].

5.3 Special Cases

Cylindrical panels with curved free edges, *SSFF* are of technical interest due to their greater economy in fabrication relative to fully supported ones. Examining Table 3.1, we observe that the first mode of the *FF* beam functions is a translational one, meaning that upon substitution in Eq. 3.15, the effect of membrane stretching disappears, and so in effect the shell problem is downgraded to the solution of a plate problem. The ADINA finite element is used for the dynamic analysis of this type of support condition. Fig. 5.44 depicts the mid-point lateral shell deformation, for all rise cases for this particular boundary condition.

The linear analysis can easily be extended to the nonlinear range in ADINA. First the *KINEMATICS* command in ADINA-IN is redefined to obtain the option with large displacement

and small strain. Since the nonlinear solution is an incremental procedure, the command *ITERATION* is introduced. For the iterative method, the Full Newton method is adopted. To achieve convergence, the command *AUTOMATIC- ATS* is used. This command subdivides the time-step if no convergence is achieved.

Results are provided for all curvatures for *SSFF* as well as *SSSS* support conditions, Figs. 5.45 and 5.46. Sample ADINA-IN input file for the linear and nonlinear analysis of *SSFF* shell panel is provided in Appendix A.

CHAPTER 6

DISCUSSION

6.1 Introduction

Boundary symmetry or non-symmetry are the main criterion for the convergence of the analytical solution. The sixteen support conditions under investigation, can be classified as being, *fully, partially, or non -symmetric.*

6.2 Fully Symmetric Boundary Conditions

Shells with *CCCC*, *CCSS*, *SSCC* and *SSSS* support conditions are of this kind. For these types of boundaries, only modes that are symmetric with respect to $x=a/2$ *and* $y=b/2$ are taken. The net result in the mode superposition involves the removal of non-symmetric modes, hence a faster convergence rates. Also the fact that the boundary conditions for all of the above support conditions are satisfied helps to speed up the convergence rate, unlike when one edge is free. The actual shell response in dynamic analysis is a function of load, material properties, boundary conditions, and geometry. In this work, only the geometric effects, specifically the curvature for a given shell support type are investigated. The point of maximum deformation for symmetric boundaries is the midpoint of the shell. Fig. 5.28 depicts the time response at the panel centre for the *CCCC* support condition. As expected, curvature has a marked effect upon the lateral

displacements. The rise ratio increase is accompanied with the stiffening of the structure. The effects of the structure stiffening is a decrease in the lateral displacement and the vibration period as seen. The same effects with varying degrees are observed for *CCSS*, *SSCC* and *SSSS* support, in Figs. 5.31, 5.40 and 5.43. For example deformations have nearly tripled in the case of *SSSS* as opposed to *CCCC*. Also, the clamping of the straight edges, *CCSS* have almost the same effect on displacements as of a fully clamped shell, *CCCC*. A summary of the results is given in Table 6.1.

6.3 Partially Symmetric Boundary Conditions

These types of support conditions can be grouped into two categories, boundaries symmetric with respect to $x=a/2$ and boundaries symmetric with respect to $y=b/2$. Shells with *CCCS, CCCF, SSCS* and *SSCF* are of the former kind, and shells with *CSCC, CFCC, CSSS* and *CFSS* are of the latter kind. Since the modes of the first kind have an axis of symmetry at $x=a/2$, only modes with $m=1,3,5...$ subscripts are taken. However because of a lack of symmetry in the y-direction modes with $n=1,2,3...$ subscripts must be taken during response evaluation. We can see already an increase in the amount of calculation compared to the fully symmetric support condition. The same arguments hols true for modes that have an axis of symmetry at $y=b/2$. Furthermore, free edge supports slow the convergence for shells with *CCCF, SSCF, CFCC and CFSS* support conditions.

The lateral displacement for shells with, *CCCS, CSCC, CSSS, CFCC, CFSS and SSCS, Figs.* 5.29, 5.32, 5.35, 5.36, 5.39 and 5.41, shows similar behaviour with respect to the rise case

variation as was obtained for symmetric boundaries. However, except for the *CCCS* case, the influence of curvature is more pronounced. For shells with *CF* support condition in the y-direction, the point of maximum deformation is situated on the curved boundary. Shells with *CCCF* and *SSCF* are of this kind. The expected increase in stiffening due to the increasing rise ratio does not bring a smaller displacement in *CCCF* and *SSCF* cases as expected, but the contrary happens as seen in their Figs. 5.30 and 5.42. Again, a summary of the results pertaining to the maximum lateral displacement is given for all of the cases in Table 6.1.

6.4 Non-Symmetric Boundary Conditions

Shells with *CSCS*, *CSCF*, *CFCS* and *CFCF*, Figs. 5.33, 5.34, 5.37 and 5.38, because of lack of symmetry, have a comparatively slow convergence rate. For the cases of *CSCF* and CFCF not only all the modes, $m=1,2,3..$ and $n=1,2,3..$ must be taken. Also the computation toward a desired degree of accuracy is hampered because of the free edge at their respective boundaries. For *CSCS*, *CSCF* and *CFCF*, the response of their respective maximum deformation versus time, with the curvatures variation is as expected, i.e., similar to the ones encountered in the symmetric boundary conditions. Again, for the case of *CSCF* the response is similar to the kind encountered in *CCCF* and *SSCF*. A summary of the results pertaining to these types of support is given in Table 6.1.

6.5 Special Cases and Nonlinear Analysis

In chapter 5 another support case that was not covered by the analytical method, namely *SSFF* was introduced. In the linear range, by plotting the lateral displacement of its midpoint for

all rise cases, Fig 5.44, we notice a behaviour similar to that observed before. There is a decrease in the shell vibration amplitude with an increase in the rise ratio. The removal of the support on the curved edges, as expected is followed with an increase in vibration amplitude compared to the *SSSS* case, for a given curvature. Fig. 6.1 demonstrates this fact for the 5th rise case. In general the relaxing of a given boundary, will lower the fundamental frequency, accompanied by an increase in the magnitude of the amplitude of the dynamic response. Table 6.3 demonstrates the increase of the lateral displacement compared to the simply supported panel for all rise cases.

The finite element analysis was extended to cover the case of nonlinear large deformation for *SSFF* and *SSSS* support conditions. For both types of support conditions, an increase in the rise ratio, is followed by an increase in the displacement, Figs. 5.45 and 5.46. A comparison in the nonlinear range of *SSSS* and *SSFF* confirms the relaxing of the response, Fig. 6.2. Table 6.4 provides the maximum deformation for all rise cases for the two boundaries under investigation.

CHAPTER 7

FURTHER RESEARCH POSSIBILITIES AND CONCLUSIONS

An analytical solution based on the Galerkin-Vlasov variational principle, was developed for the investigation of the dynamics of shallow shell panels subjected to an explosive load, with validation of the approach provided by the finite element program ADINA. The analytical solution developed in this work showed good agreement with the finite element approach but required substantially less computer time. Geometric effects, namely the curvature and support conditions upon shell response were investigated for a total of five rise ratios and sixteen types of boundary conditions. It was found that the convergence rate in the analytical solution is a strong function of the boundary symmetry or non-symmetry. For most support conditions, as expected, an increase in rise ratio was followed by the shell stiffening. Exceptions were for shells with the following boundaries *CCCF*, *CSCF* and *SSCF* where, contrary to expectation, the dynamic response increased.

Particular attention was paid to shells with free support on the curved edges and simple support on straight sides. The response of this particular shell was compared to one simply-

supported on all sides, in linear and nonlinear domains by the ADINA finite element program. It was found again that the removal of the support on the curved edges increases the amplitude of the dynamic response in both the linear and nonlinear domains.

The use of flat beam functions as trial functions provides a good approximation for the forced vibration analysis. A logical extension would be for the use of curved beam functions, Leissa [39], for shells which need not be shallow. This coupled with the use of a more accurate shell theory such as Sanders's, could improve the accuracy of the analytical results.

Another possible extension of the Galerkin-Vlasov approach would be for materials that need not be isotropic.

All deformations seen in this work are quite "large" (for the given load and shell geometry), contrary to the small deflection linear shell theory. Consequently, we need to extend the use of beam trial functions to the nonlinear large displacement domain. This approach would start from the coupled nonlinear differential equations of motion, and with the appropriate selection of functions satisfying the lateral displacement, an expression satisfying the stress state could be found.

REFERENCES

1- Love, A.E.H., "Mathematical Theory of Elasticity," Cambridge University Press, 4th edition, 1927.

2- Palmer, P. J., "The Natural Frequency of Vibration of Curved Rectangular Plate," *Aeoronaut.* Q. 5, pp. 101-110, 1954.

3- Reissner, E., "On Transverse Vibration of Thin, Shallow Elastic Shells," *Quarterly of Applied Mathematics*, Vol. 13, pp. 169-176, 1955.

4- Marguerre, V. K., "Die Mittragende Breite der Gedrückten Platte," *Luftfahrtforschung*, Vol. 14, No. 3, pp. 121-128, 1937.

5- Forsberg, K., "A Review of Analytical Method Used to Determine Modal Characteristics of Cylindrical Shells," NASA CR-613, 1964.

6- Flügge, W., "Stresses in Shells," Springer Verlag, Berlin, 1964.

7- Forsberg, K., "Influence of Boundary Conditions on the Modal Characteristics of Thin

Cylindrical Shell," *AIAA Journal*, Vol. 2, pp. 2150-2157, 1964.

8- Warburton, G. B., "Vibration of Thin Cylindrical Shells," *J. Mech. Eng. Sci.*, Vol. 7, pp. 309-407, 1965.

9- Sewall, J. L., "Vibration Analysis of Cylindrical Curved Panels with Simply-Supported or Clamped-Edges, and Comparisons with Some Experiments," *NASA TND3791*, 1967.

10- Leissa, A. W., and Sadi, A. S., "Curvature Effects on Shallow Shell Vibrations," *Journal of Sound and Vibrations*, Vol 12, No 2, pp. 173-187, 1971.

11- Webster, J. J., "Free Vibration of Rectangular Curved Panels," *Int. J. Mech. Sci.*, Vol. 10, pp. 571-582, 1968.

12- Al-Khayat, Isa A., and Sharma, C. B., "Free Vibration Characteristics of a Cylindrical Panel," *Math. Eng. Ind.*, Vol. 3, No 1, pp. 59-73, 1990.

13- Ballentine, John R., Plumblee, H. E., and Schneider, C. W., "Sonic Fatigue in Combined Environment," *Lockheed-Georgia Company Technical Report*, AFFDL-TR-66-7, 1966.

14- Redekop, D., and Azar P., "Dynamics of a Cylindrical Shell Panel under Explosive Loading," *Proc. of Ninth Symposium on Engineering Mechanics*, W. H. Elmaraghy and S. M.

Dickinsons, eds., London, Ontario, pp. 50-57, 1988.

15- Arnold, R. N. and Warburton, G. B., "The Flexural Vibrations of Thin Cylinders," *Inst. of Mech. Engr. Proc.*, vol. 167, pp 55-76, 1974.

16- Gontkevich, V. S., "Natural Vibrations of Plates and Shells," Kiev: Nank Dumka, 1964. (English translation by Lockheed Missiles and Space Co.)

17- Sharma, C. B., "Calculation of Natural Frequencies of Fixed-Free Circular Cylindrical Shells," *Journal of Sound and Vibrations*, Vol. 35, No 1, pp. 55-76, 1974.

18- Soedel, W., "New Frequency Formula for Closed Circular Cylindrical Shells for a Large Variety of Boundary Conditions," *Journal of Sound and Vibrations*, Vol. 70, No 3, pp. 309-317, 1980.

19- Petyt, M., "Vibration of Curved Plates, *Journal of Sound and Vibrations*," Vol. 15, No 3, pp. 381-395, 1971.

20- Leissa, A. W., Lee, J. K., and Wong, A. J., "Vibrations of Cantilevered Shallow Cylindrical Shells of Rectangular Planform," *Journal of Sound and Vibrations*, Vol. 78, no 3, pp. 311-328, 1981.

21- Leissa, A. W., and Narita, Y., "Vibrations of Completely Free Shallow Shells of rectangular Planform," *Journal of Sound and Vibrations*, vol. 96, No 2, pp. 207-218, 1984.

22- Leissa, A. W., and Qatu, M. S, "Effects of Edge Constraints Upon Shallow Shell Frequencies," *Thin Walled Structures*, Vol. 14, pp. 347-379, 1992.

23- Lim, C. W., and Liew, K. M., "A pb-2 Ritz formulation for Flexural Vibration of Shallow Cylindrical Shells of Rectangular Planform," *Journal of Sound and Vibrations*, Vol. 173, No 3, pp. 343-375, 1994.

24- Cummings, B. E., "Large -Amplitude Vibrations and Response of Curved Panels," *AIAA Journal,* Vol. 2, pp. 709-716, 1964.

25- Kanazawa, K., and Hangai, Y., "Nonlinear Flexural Vibrations of Thin Shallow Shells," *Theoretical and Applied Mechanics*, University of Tokyo, Vol. 25, pp. 75-87, 1975.

26- Redekop, D., and Azar, P., "Dynamic Response of Cylindrical Shell Panel to Explosive Loading," *Journal of Vibration and Acoustics*, Vol. 113, pp. 273-281, 1991.

27- Jiang, J., and Olson, M. D., "Nonlinear Dynamic Analysis of Blast Loaded Cylindrical Shell," *Computers and Structures*, Vol. 41, No 1, pp. 41-52, 1991.

28- Hrennikoff, A., and Tezcan, S. S., "Analysis of Cylindrical Shells by the Finite Element Method," *Symposium on Problems of Design and Construction of Large Span Shells for Industrial and Civic Building,* Leningrad, U.S.S.R., Sept. 6-9, 1966.

29- Gallagher, R. H., "The Development and Evaluation of Matrix Methods for Thin Shell Structural Analysis," Ph. D. Thesis, State University of New York at Buffalo, NY, 1966.

30- Connor, J. J., and Brebbia, C. A., "A Stiffness Matrix for a Shallow Rectangular Shell Element," *Journal of Engng. Mech.*, ASCE, Vol 93, No5, pp. 43-65, 1967.

31- Ahmad, S., Irons, B. M., and Zienkiewicz, O. C., "Analysis of Thick and Thin Shell Structures by Curved Elements," *International Journal for Numerical Methods in Engineering,* Vol. 2, pp. 419-451, 1970.

32- Reddy, J. N, "Finite Element Modelling of Structural Vibrations: A Review of Recent Advances," *The Shock and Vibration Digest*, Vol. 11, No 1, pp. 25-39, 1979.

33- Olson, M. D., and Lindberg, G. M., "Vibration Analysis of Cantilevered Curved Plates using a New Cylindrical Shell Finite Element," *Proceedings of the Second Conference on Matrix Methods in Structural Mechanics*, Wright Patterson Air Force Base, Dayton Ohio, AFFDL-TR-68-150, 1969.

34- Olson, M. D., and Lindberg, G. M., "Dynamic Analysis of Shallow Shells with Doubly Curved Triangular Finite Element," *Journal of Sound and Vibrations*, Vol. 19, No 3, pp. 299-318, 1971.

35- Walker, K. P., "Vibrations of Helicoidal Fan Blades," *Journal of Sound and Vibrations,* Vol. 59, No. 1, pp. 35-57, 1978.

36- Yang, H. T. Y., Saigal, S., and Liew, D. G., "Advances of thin Shell Finite Element and Some Applications, Version I," *Computers and Structures*, Vol. 35, No 4, pp. 481-504, 1990.

37- Mackerle, J. "Finite and Boundary Element Analysis of Shells - A Bibliography (1990-1992)," *Finite Element in Analysis and Design*, Vol. 14, pp. 73-83, 1993.

38- Soedel, W., "Vibrations of Shells and Plates," Marcel Decker, New York, 1995.

39- Leissa, A. W., " Vibration of Shells," *NASA SP-282*, Washington DC, pp. 165-175, 1973.

40- Rekach, V. G., " Static Theory of Thin Walled Structures," *Moscow: Mir*, pp. 13-146, 1978.

41- Galerkin, B. G., " Series-Solution of Some Cases of Equilibrium of Elastic Beams and Plates," Vestnik. Insh., pp- 879-903, 1915.

42- Galerkin, B. G., " Thin Elastic Plates, " *Gostrojizdat*, Leningrad, 1933.

43- Vlasov, V. Z., " Some New Problems on Shell and Thin Structures," *Nat. Adv. Comn. Aero.*, NACA Tech. Memo, No. 1204, 1949.

44- Grossi, R. O., "On the Role of Natural Boundary Conditions in the Ritz Method," *International Journal of Mechanical Engineering Education*, Vol. 16, No. 3, pp. 207-210, 1987.

45- Bathe, K. J., "Finite Element Procedures in Engineering Analysis," Prentice-Hall, Englewood Cliffs, New Jersey, 1995.

46- ADINA-User's Manual, ARD-87-1, ADINA Engineering, Watertown, Mass., 1995.

47- Gupta, A. D., Gregory, F. H., Bittting, R. L. and Bhattacharya, S., "Dynamic Analysis of an Explosively Loaded Hinged Rectangular Plate," *Computers and Structures*, Vol. 26, No. 1, pp. 339-344, 1987.

48- Szilard, R., "Theory and Analysis of Plates: Classical and Numerical Methods," Prentice-Hall, Englewood Cliffs, New Jersey, 1973.

FIGURES

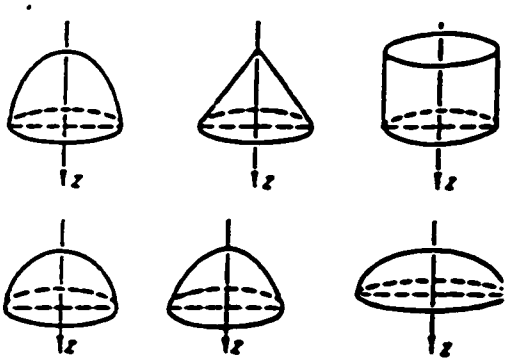

Figure 1.1 Various Shell Geometries

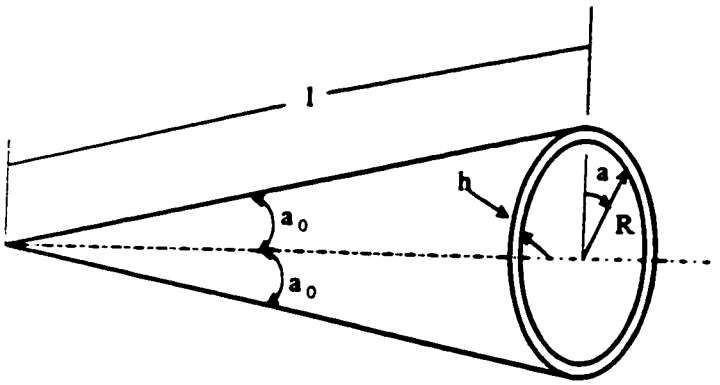

Figure 1.2 Boundary Shapes for Conical Shell

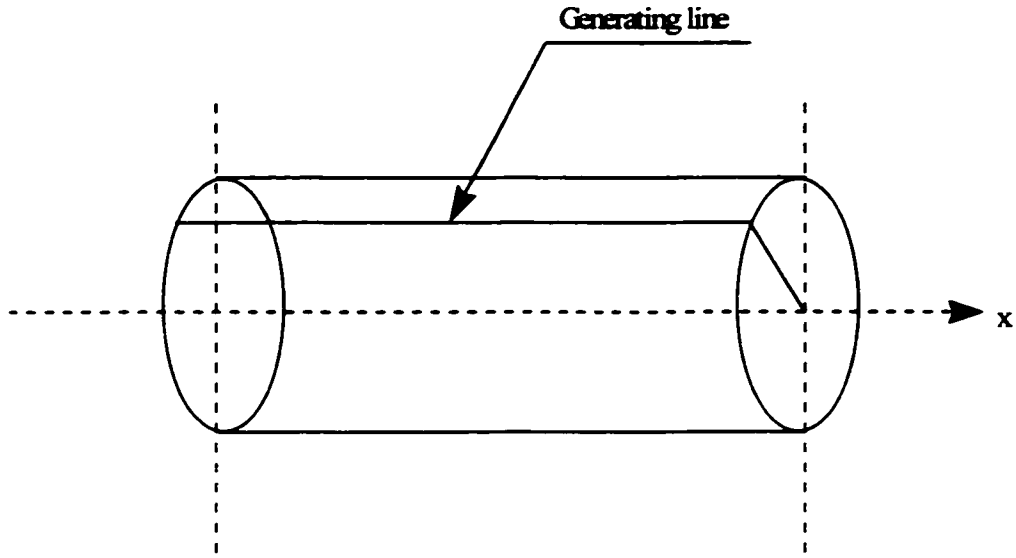

Figure 1.3 Cylindrical Shell Generation

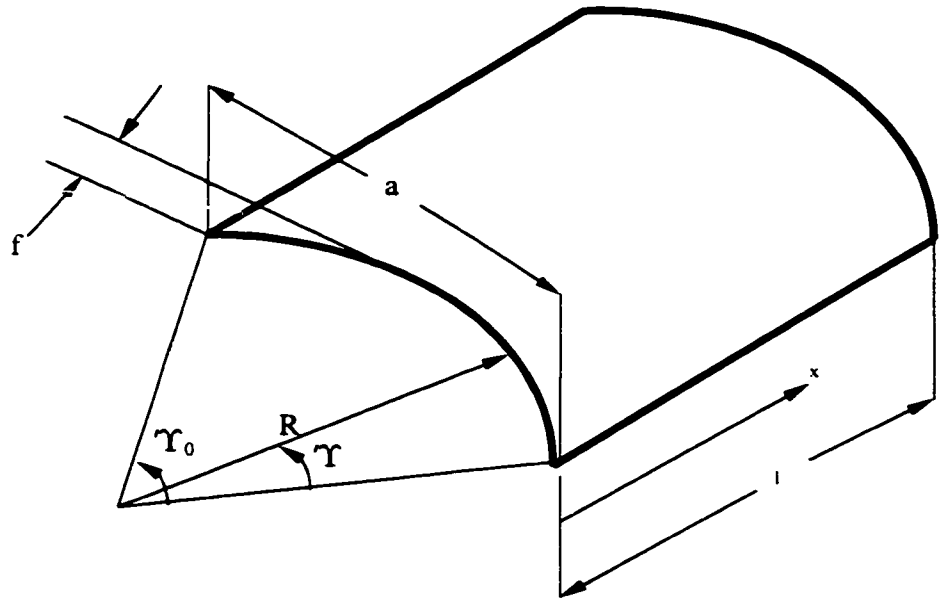

Figure 1.4 An Open Cylindrical Shell Panel

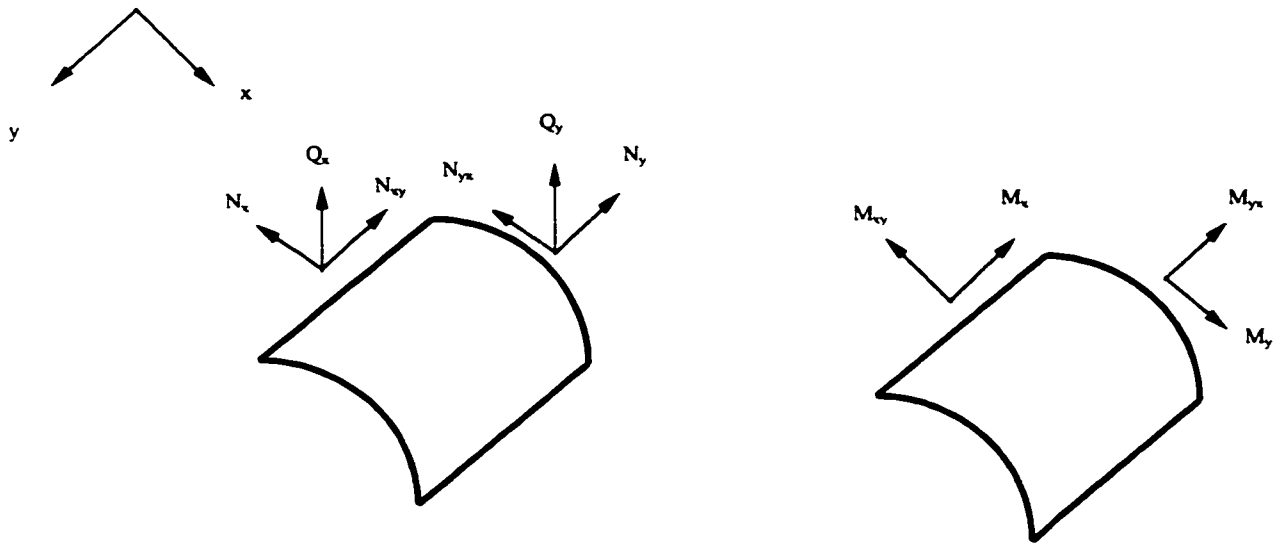

Figure 3.1 Shell Stress Resultants

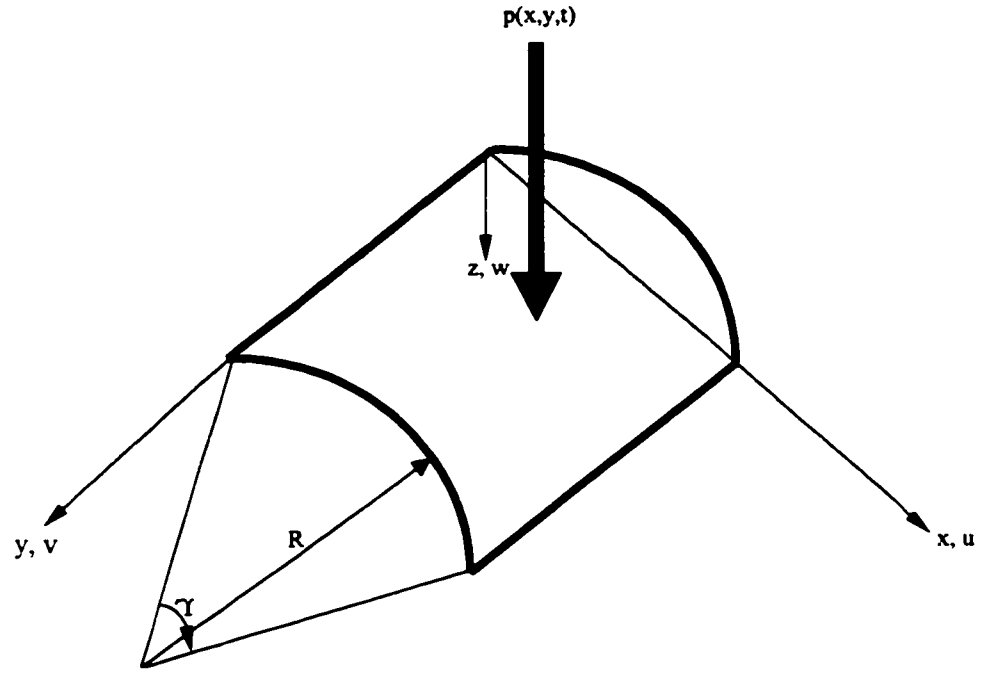

Figure 3.2 Geometry of the Shell Panel under Investigation

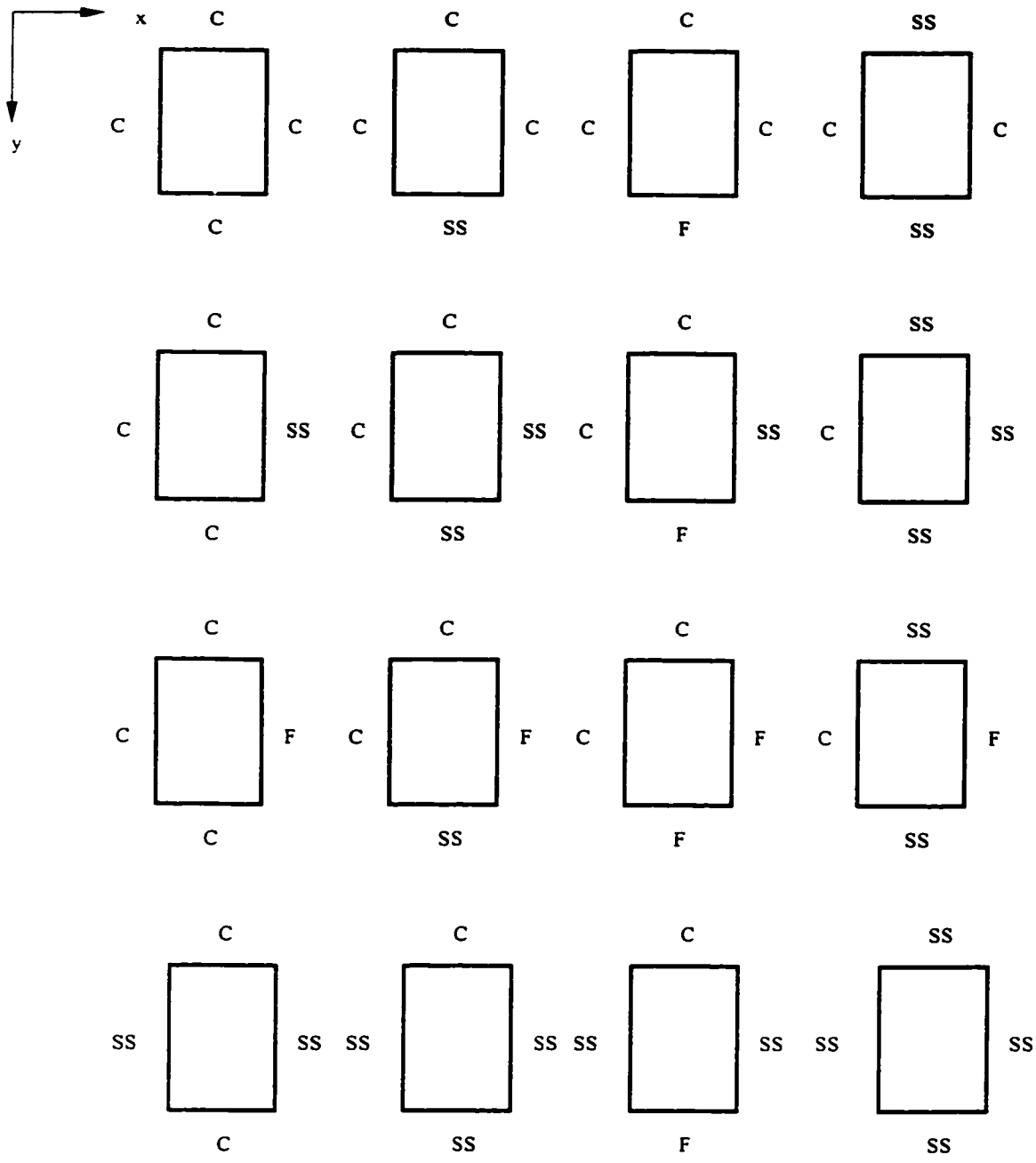

Figure 5.1 **Boundary Condition Types under Investigation**

PRESSURE LOAD FUNCTION

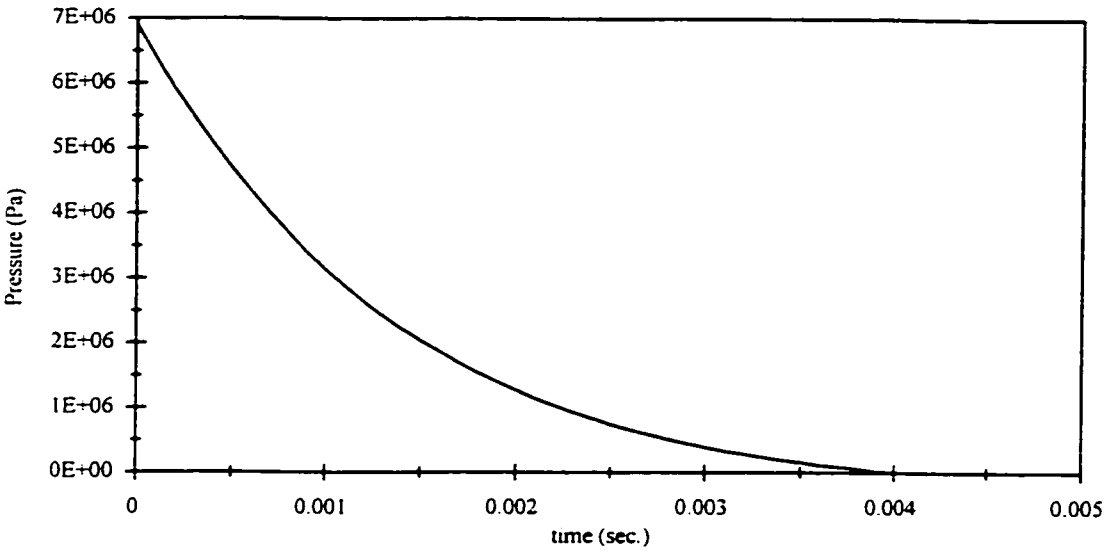

Figure 5.2 Load Function *p(t)* for the Shell Panel

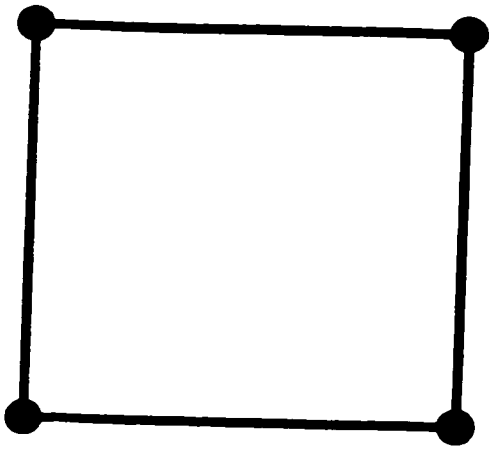

Figure 5.3 4-noded Shell Element

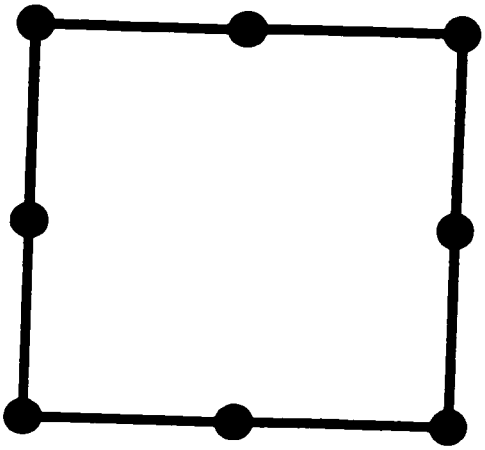

Figure 5.4 8-noded Shell Element

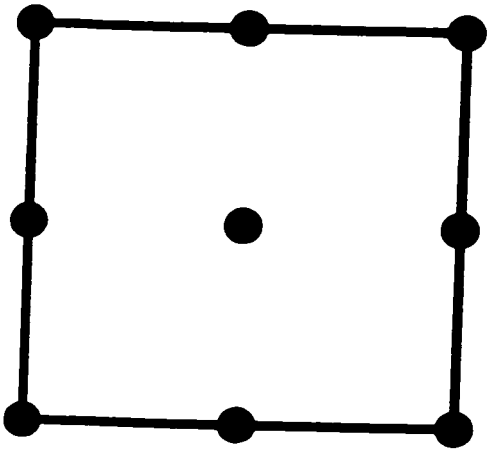

Figure 5.5 9-noded Shell Element

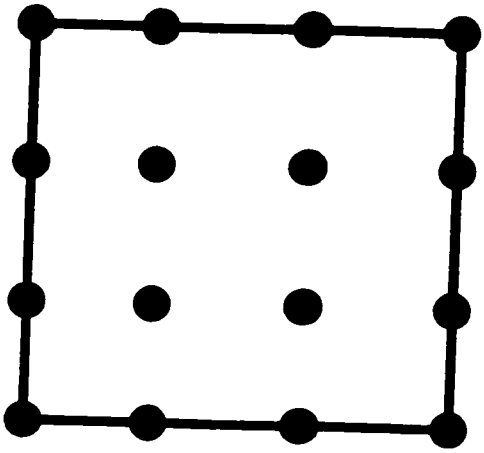

Figure 5.6 16-noded Shell Element

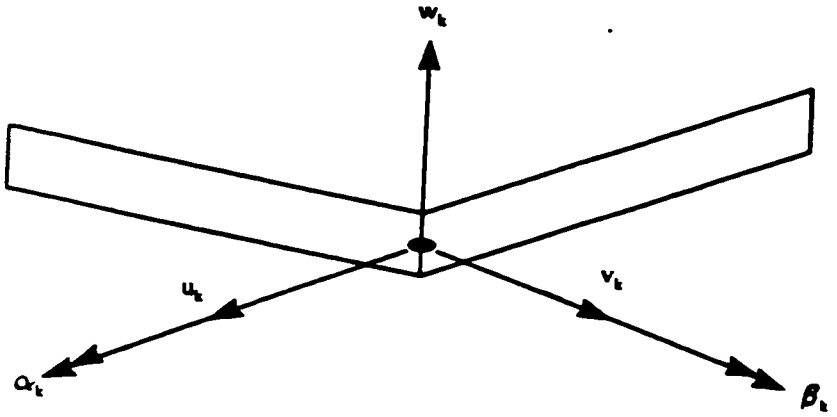

Figure 5.7 D.O.F of a Given Node

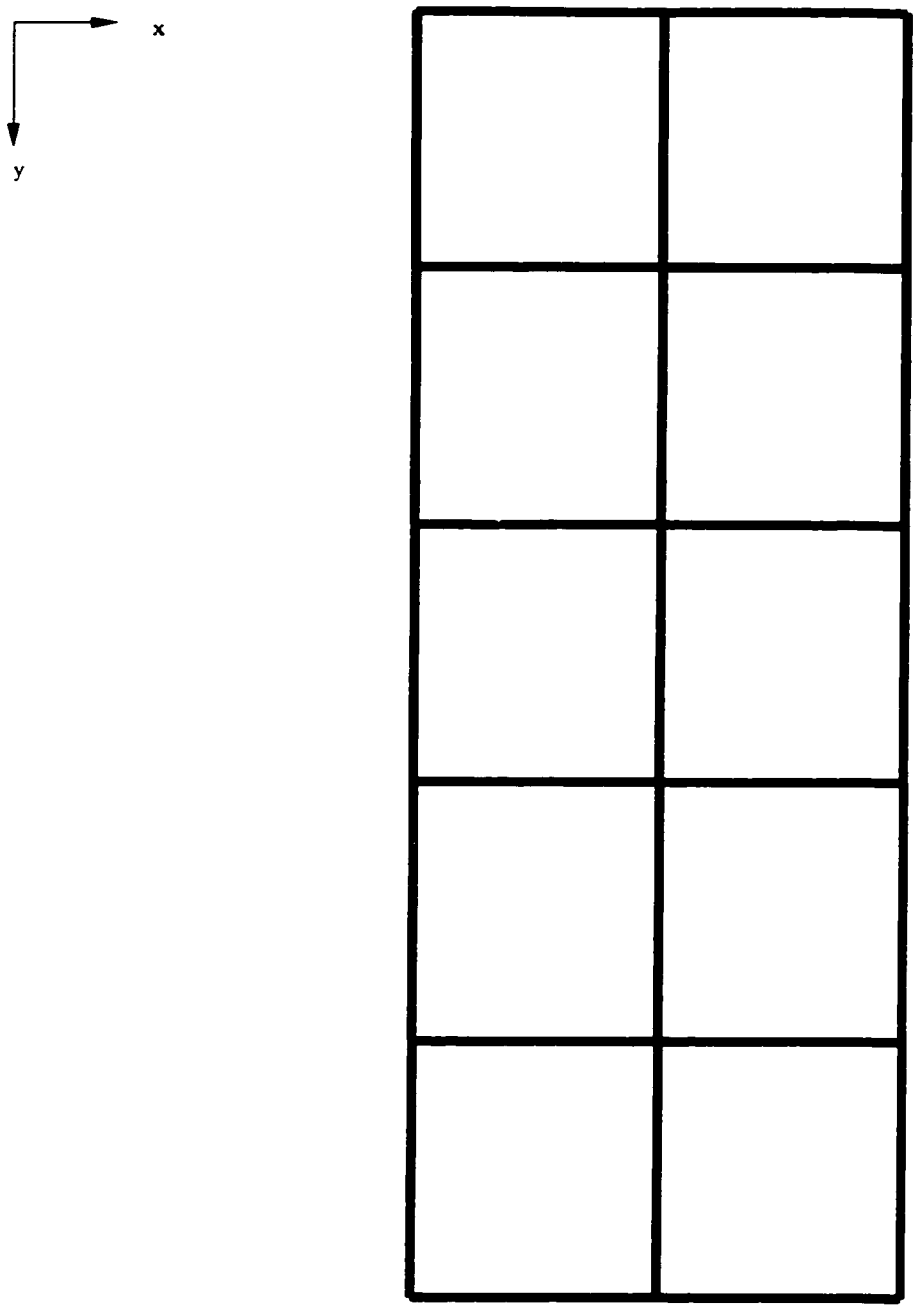

Figure 5.8 2 x 5 **Mesh**

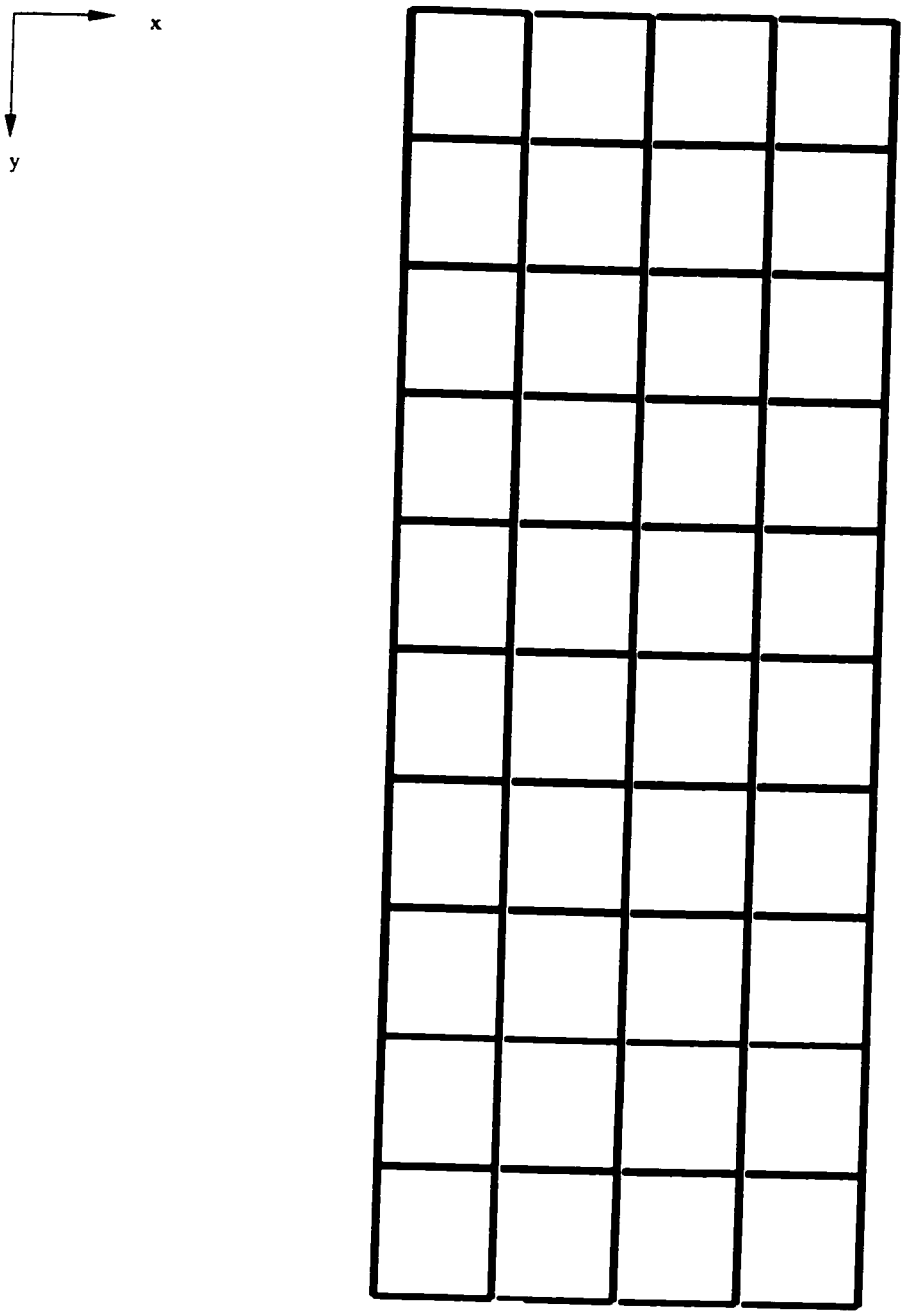

Figure 5.9 4 x 10 Mesh

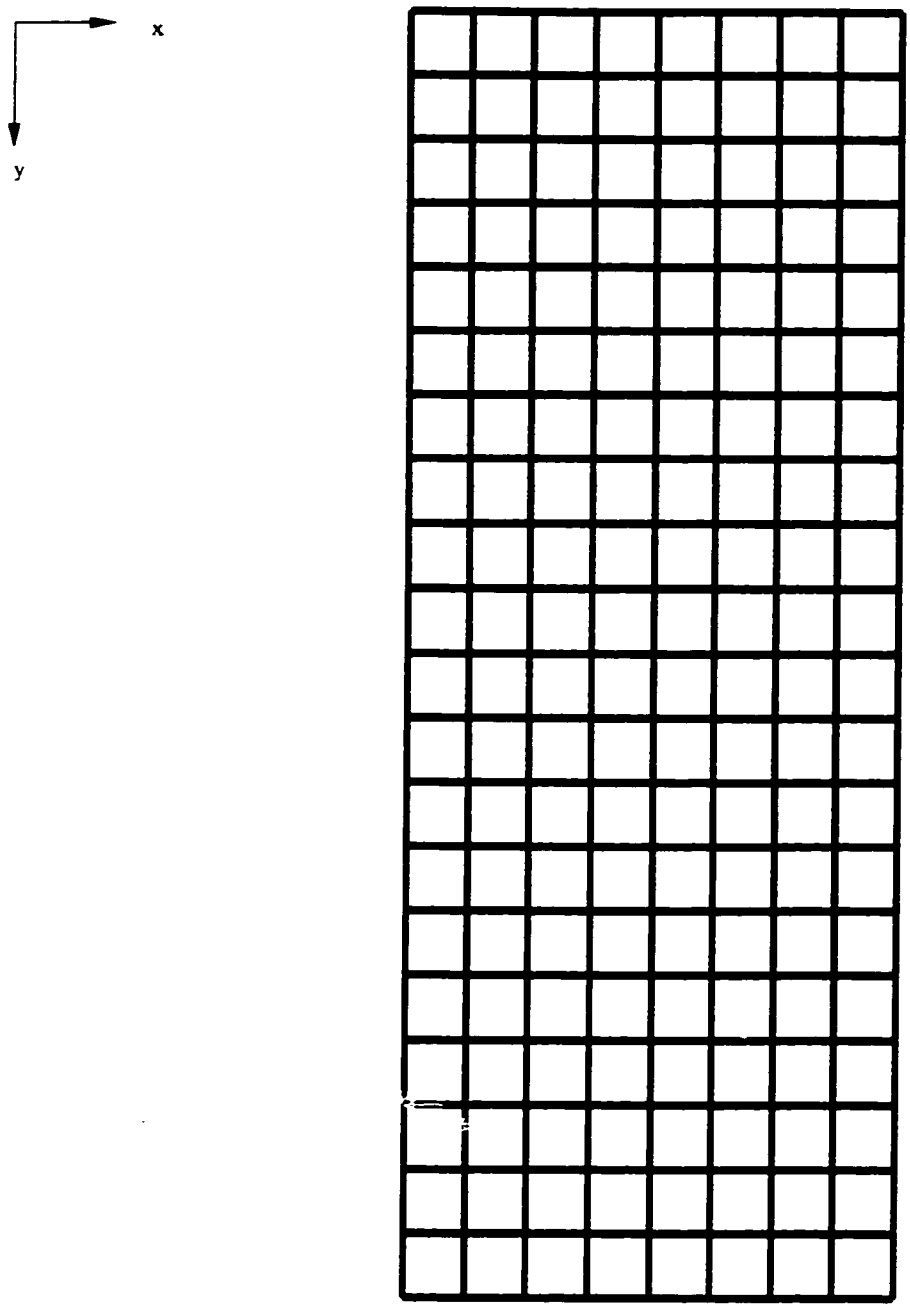

Figure 5.10 8 x 20 Mesh

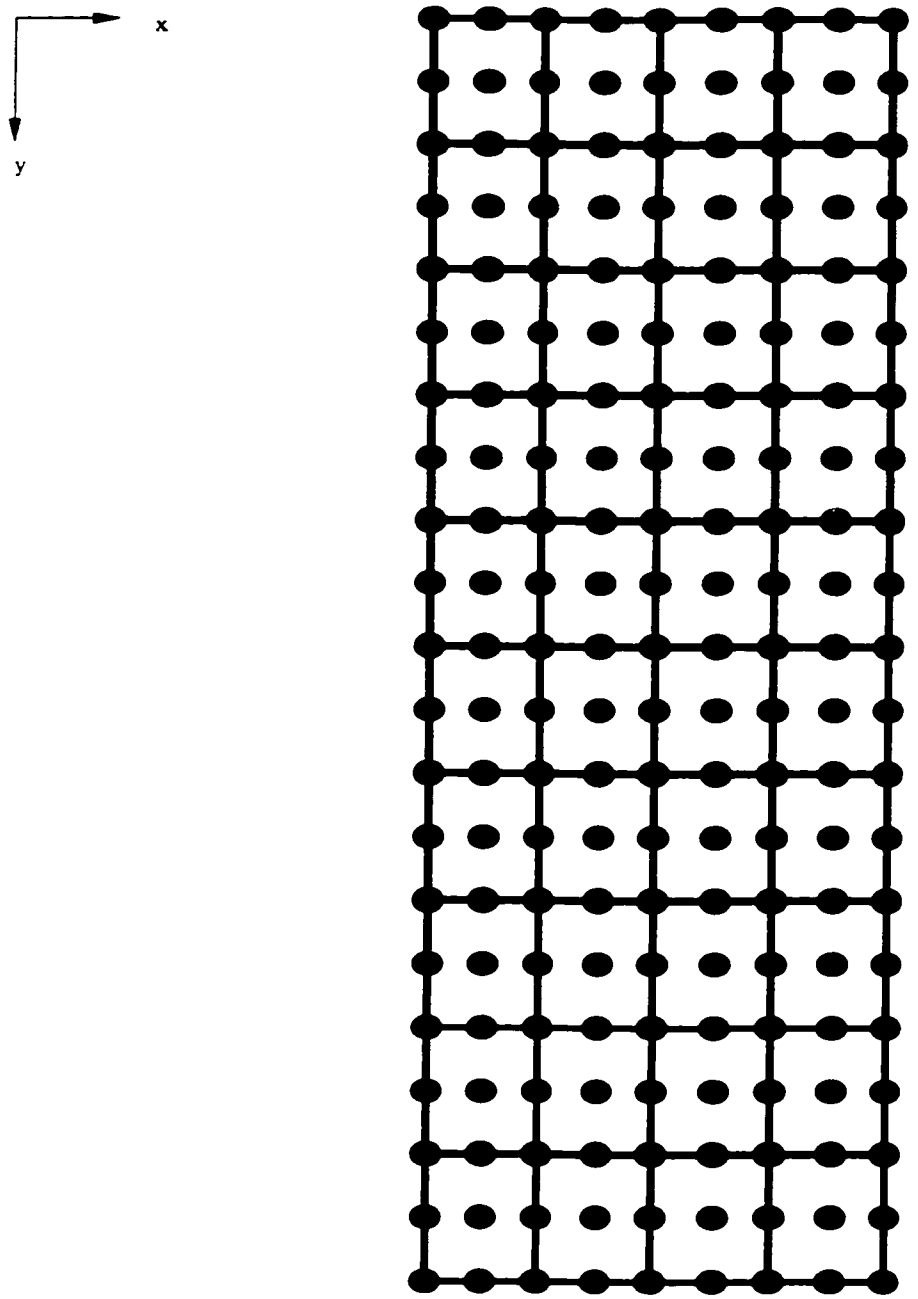

Figure 5.11 4 x 10, 9-noded Mesh

COMPARISON OF THE ANALYTICAL SOLUTION VS FEM FOR f=0.1RISE CASE

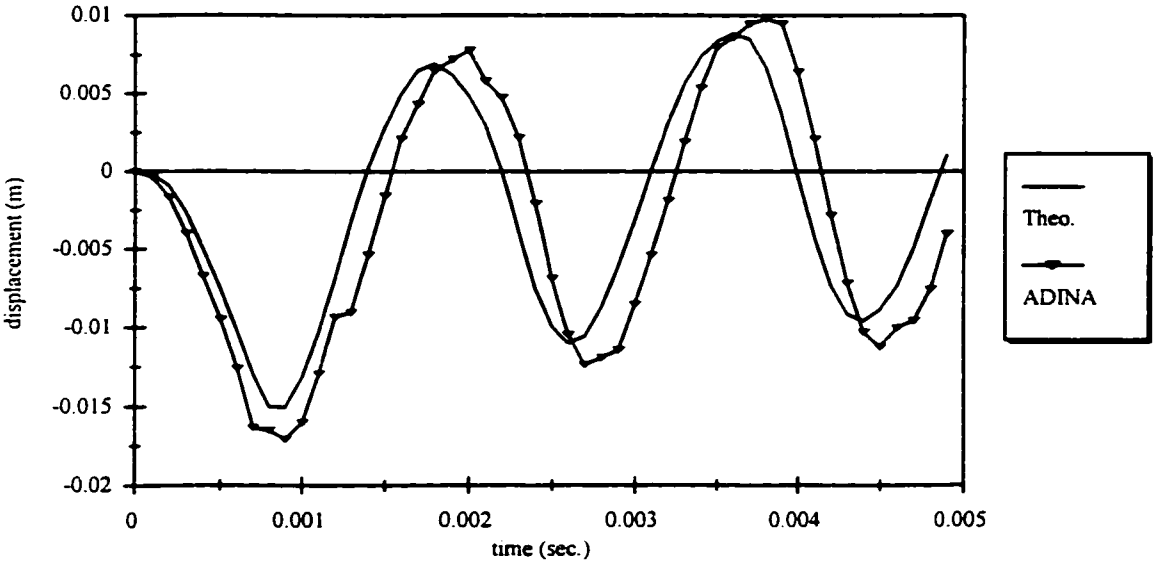

Figure 5.12 Comparison of Shell Theory and FEM for CCCC

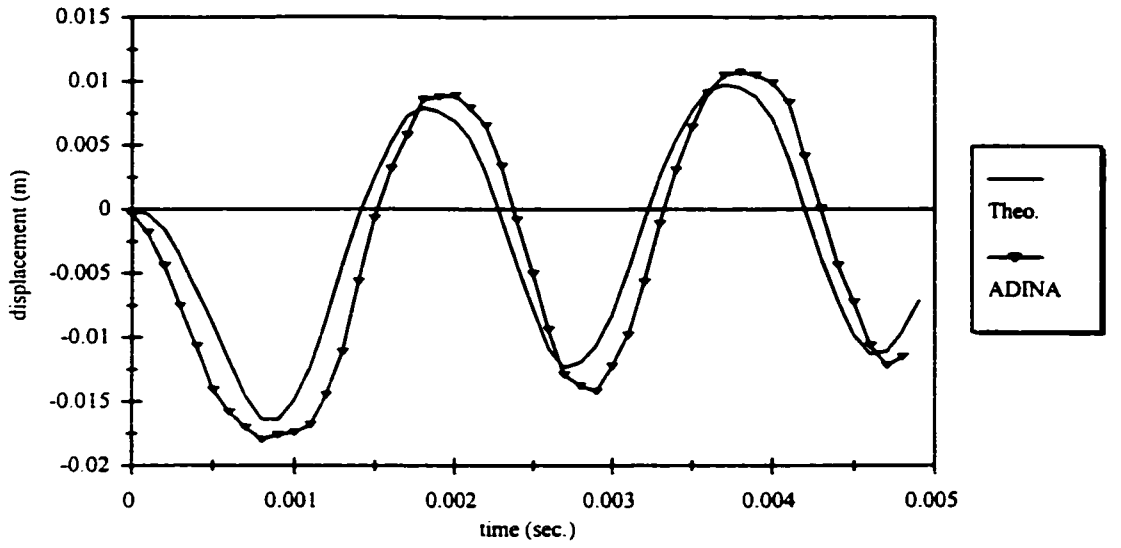

Figure 5.13 Comparison of Shell Theory and FEM for CCCS

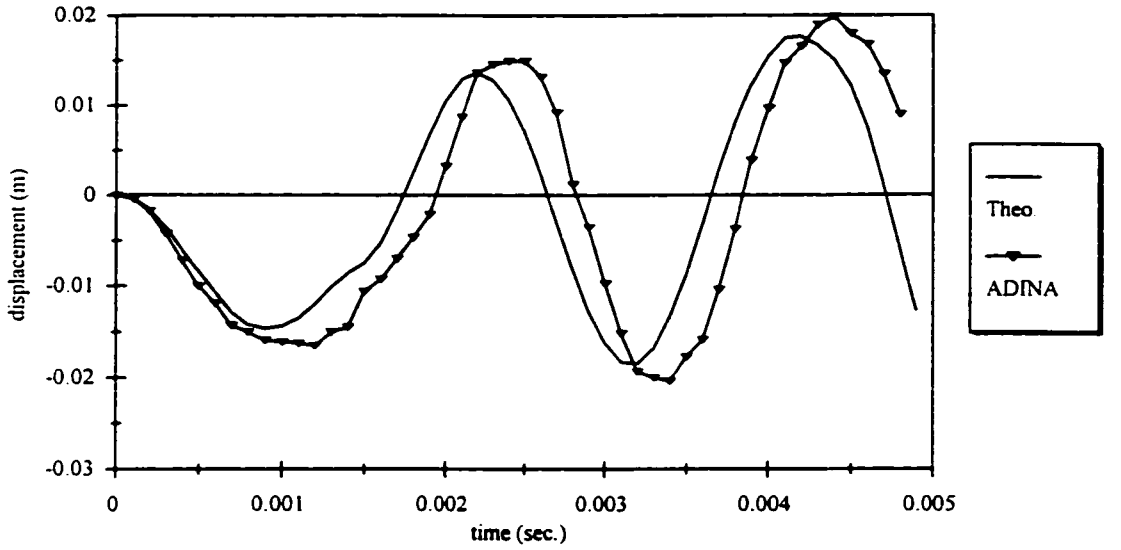

Figure 5.14 Comparison of Shell Theory and FEM for CCCF

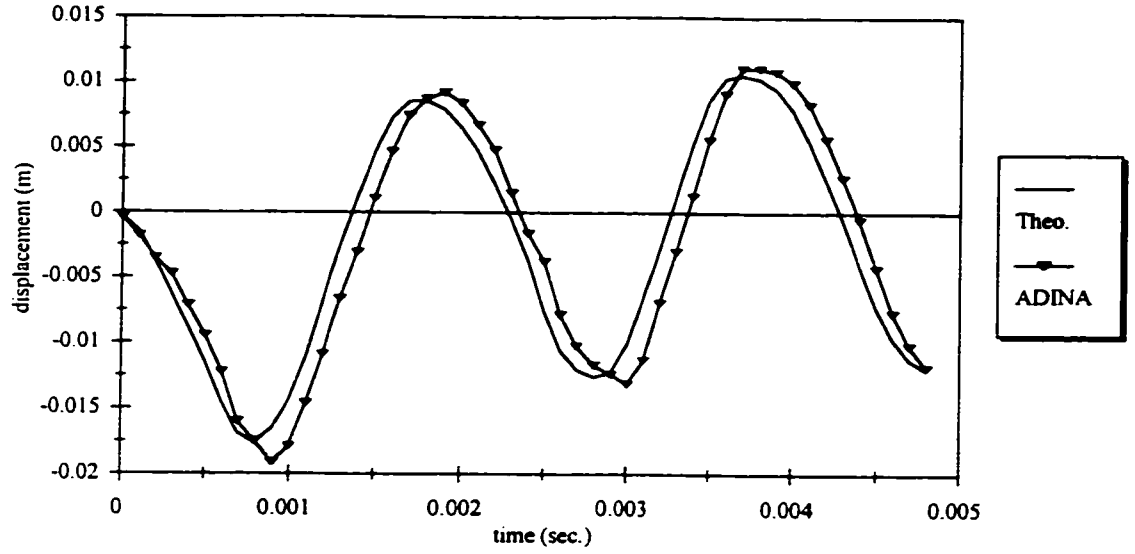

Figure 5.15 Comparison of Shell Theory and FEM for CCSS

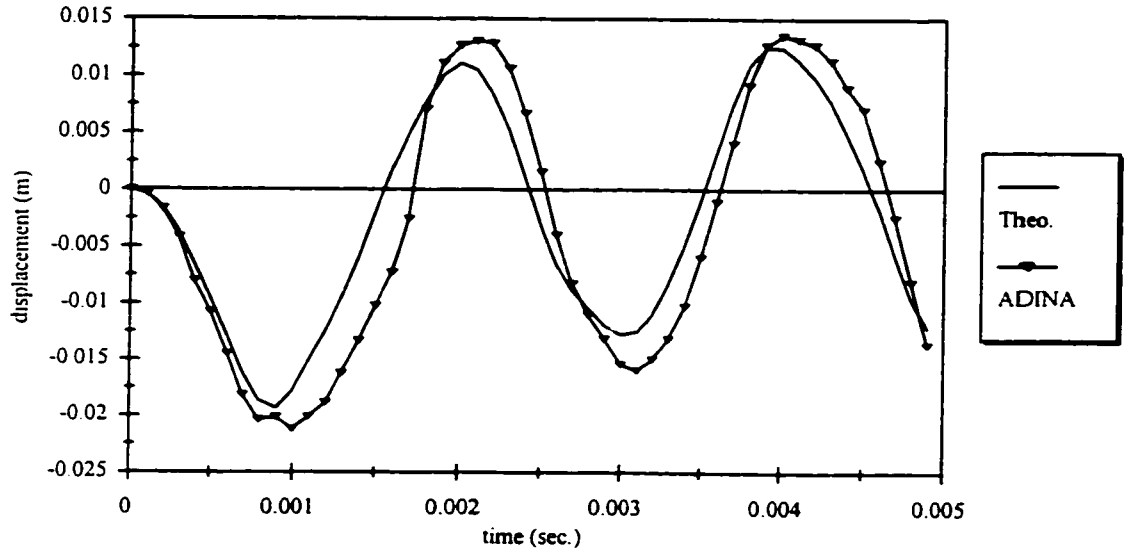

Figure 5.16 Comparison of Shell Theory and FEM for CSCC

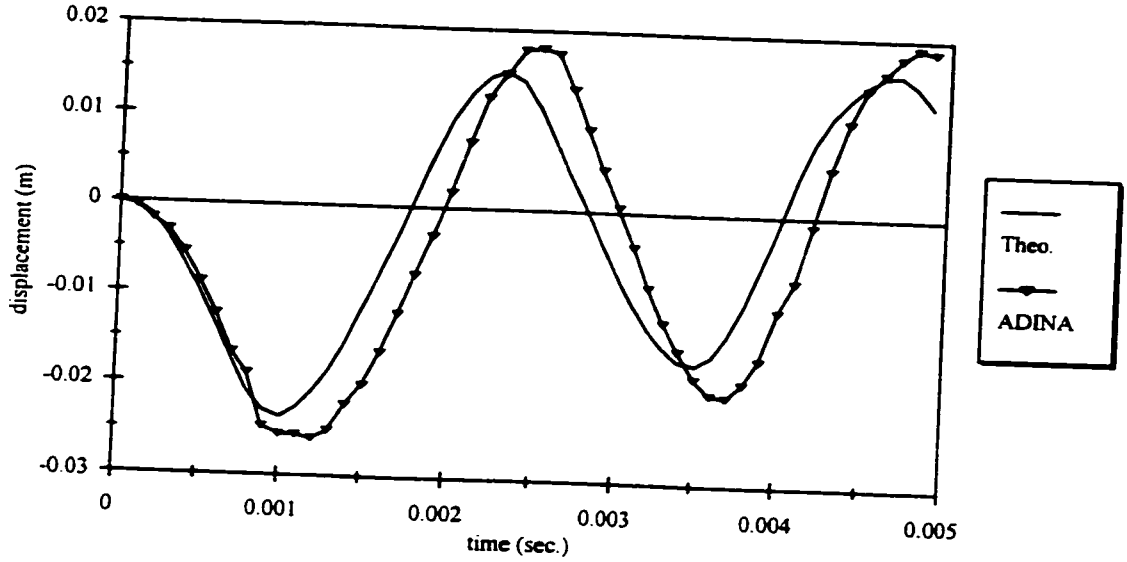

Figure 5.17 Comparison of Shell Theory and FEM for CSCS

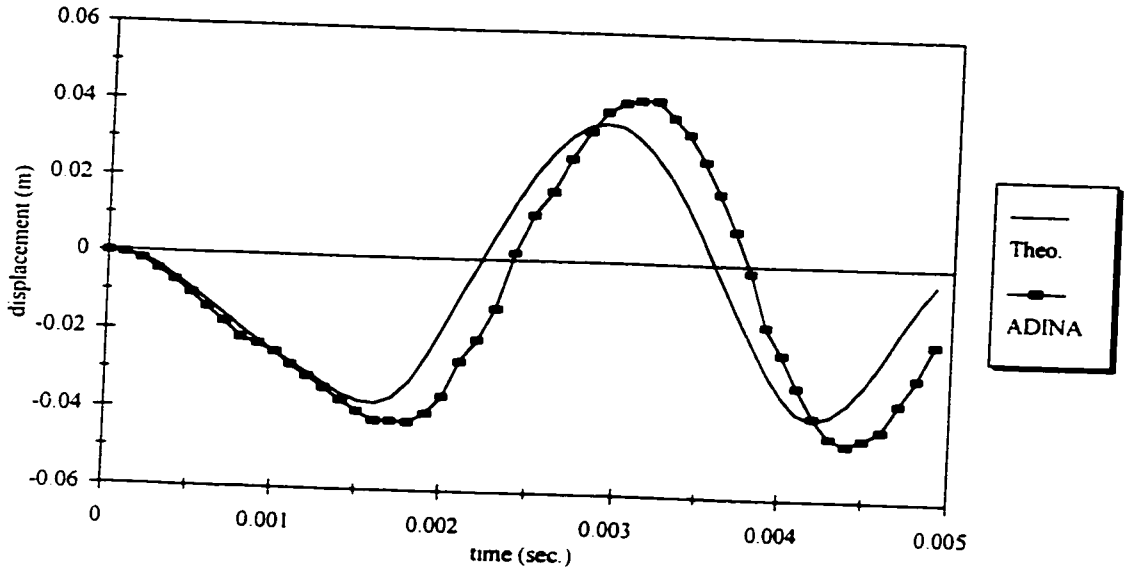

Figure 5.18 Comparison of Shell Theory and FEM for CSCF

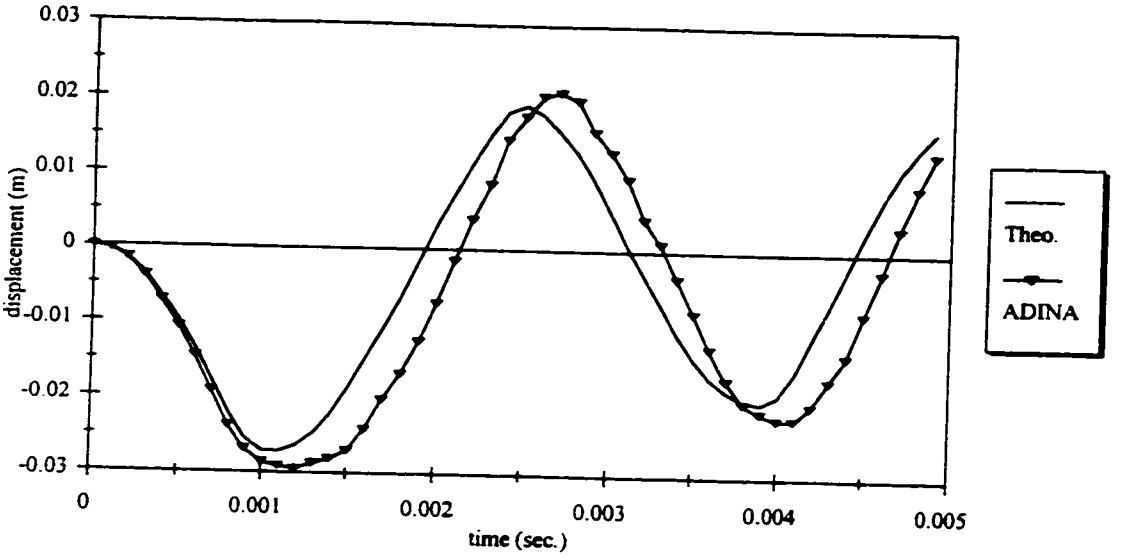

Figure 5.19 Comparison of Shell Theory and FEM for CSSS

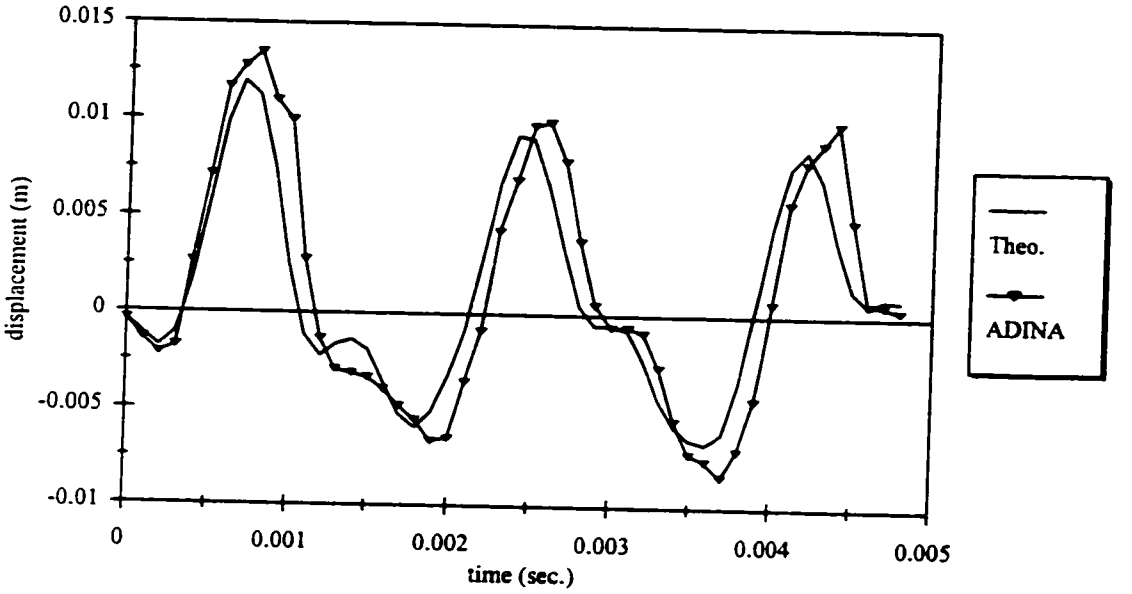

Figure 5.20 Comparison of Shell Theory and FEM for CFCC

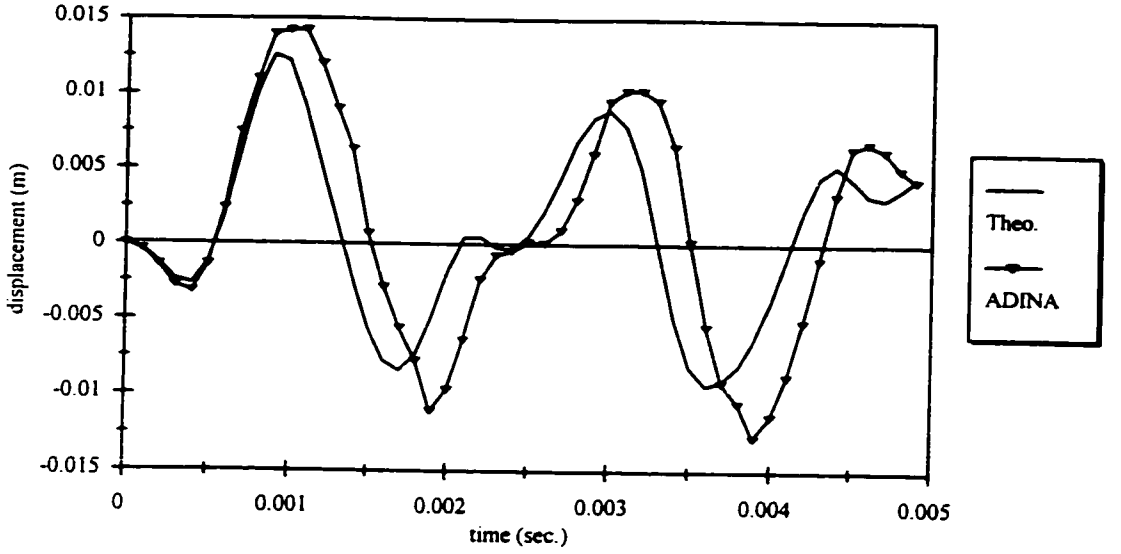

Figure 5.21 Comparison of Shell Theory and FEM for CFCS

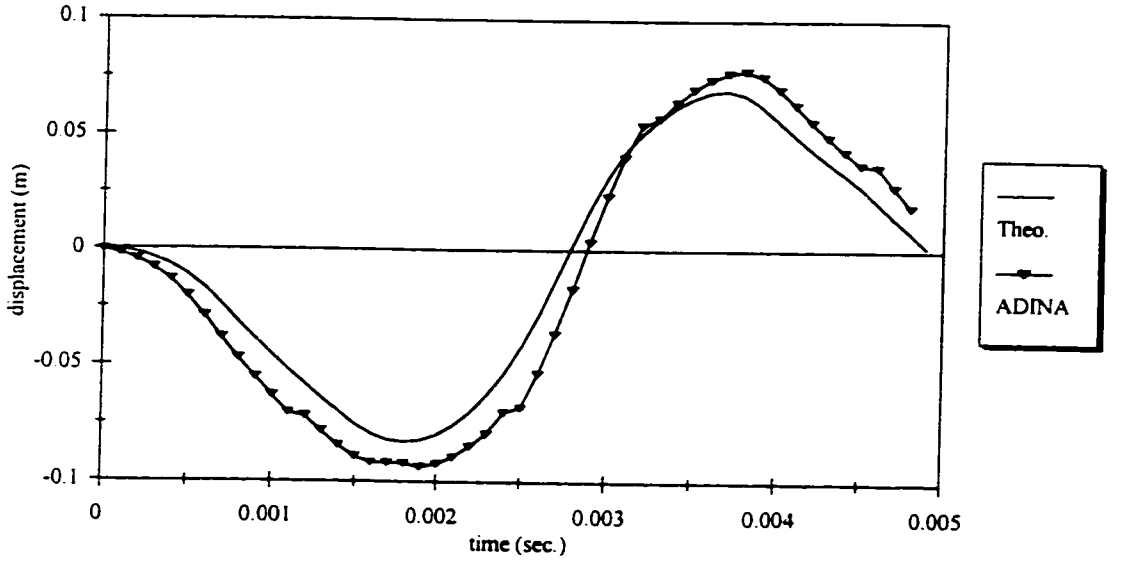

Figure 5.22 Comparison of Shell Theory and FEM for CFCF

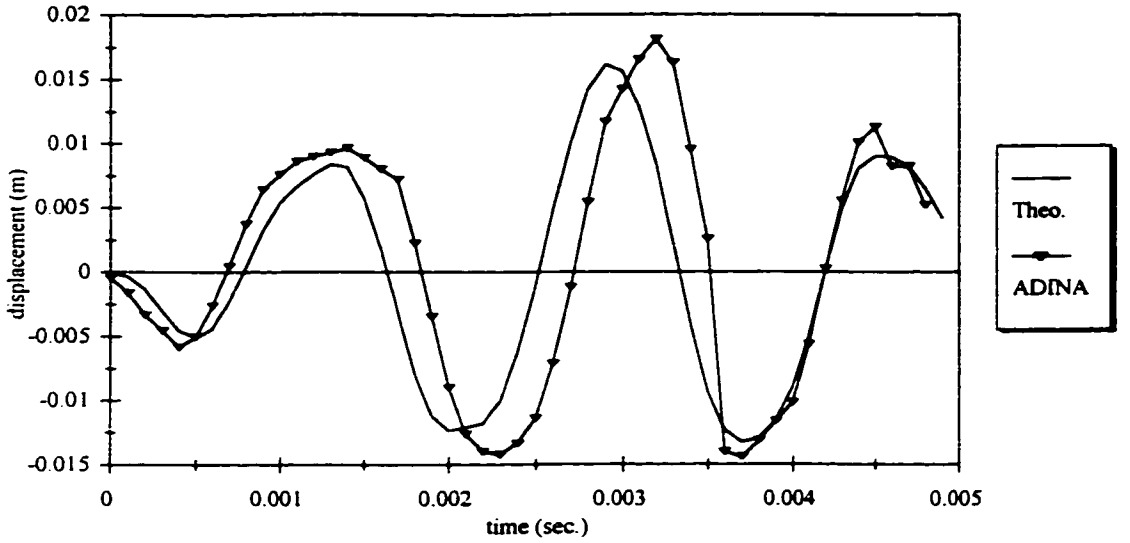

Figure 5.23 Comparison of Shell Theory and FEM for CFSS

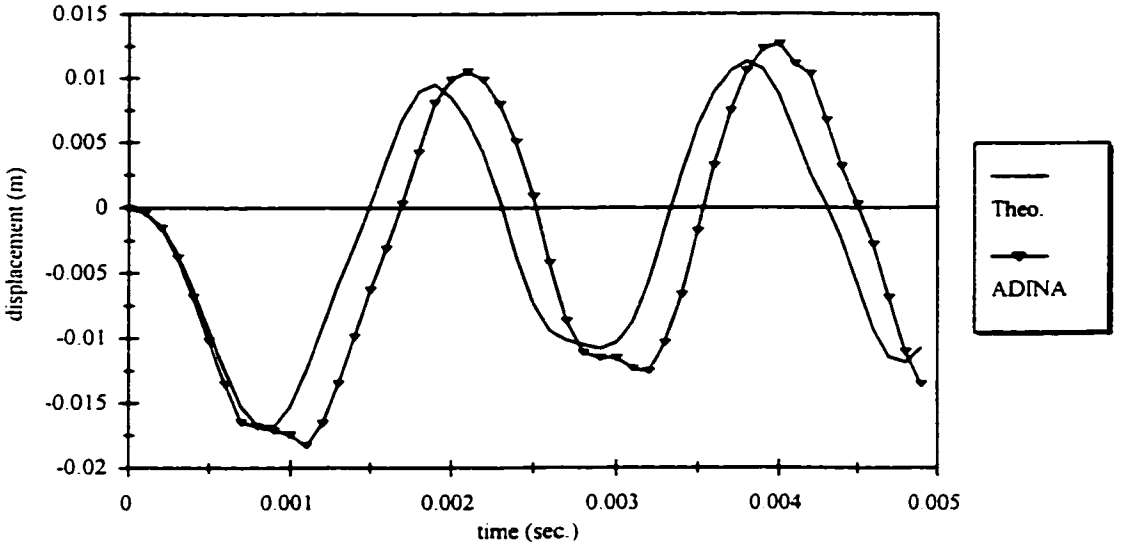

Figure 5.24 Comparison of Shell Theory and FEM for SSCC

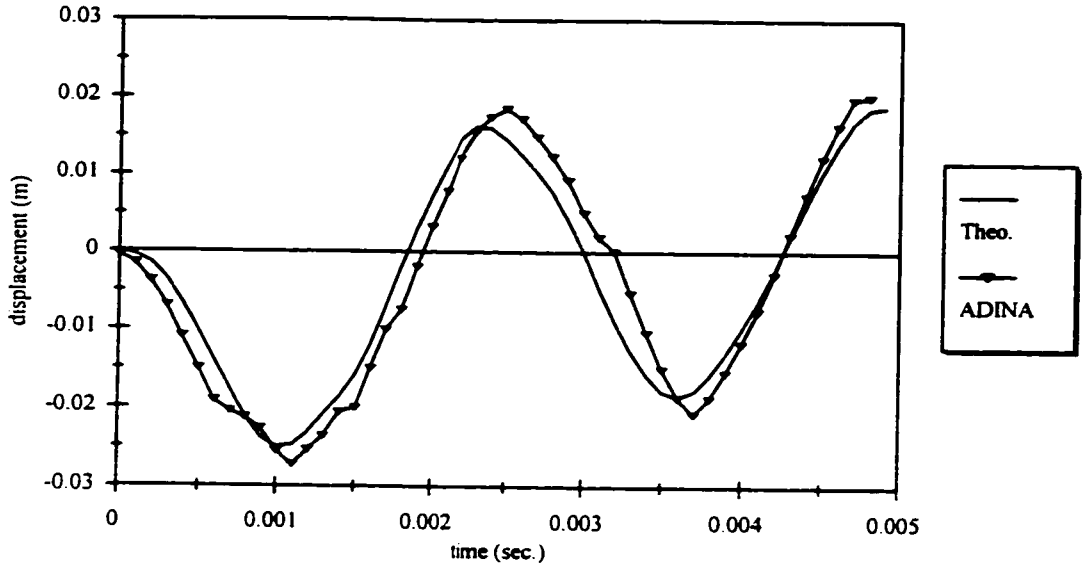

Figure 5.25 Comparison of Shell Theory and FEM for SSCS

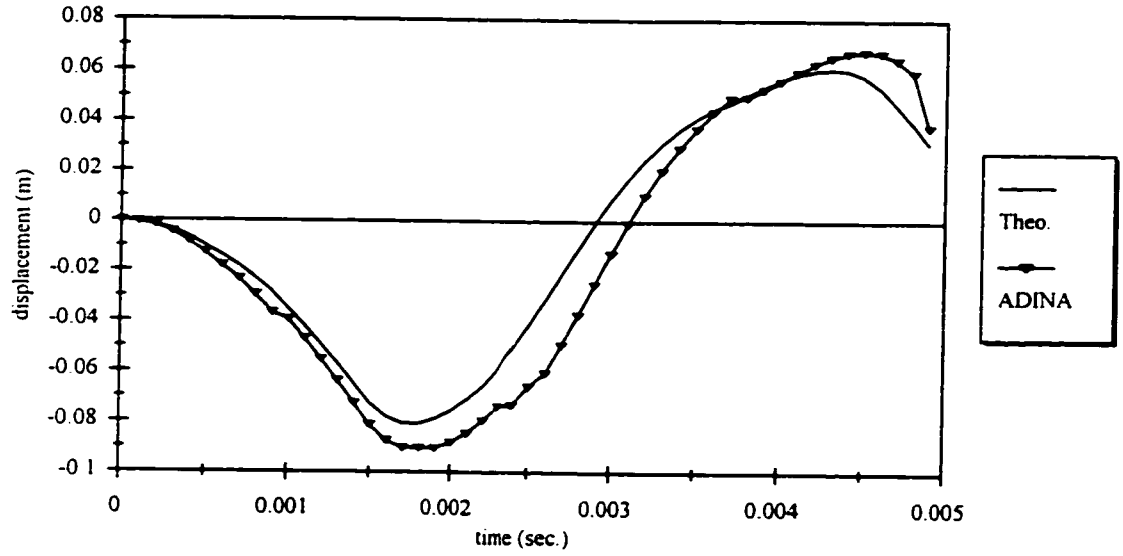

Figure 5.26 Comparison of Shell Theory and FEM for SSCF

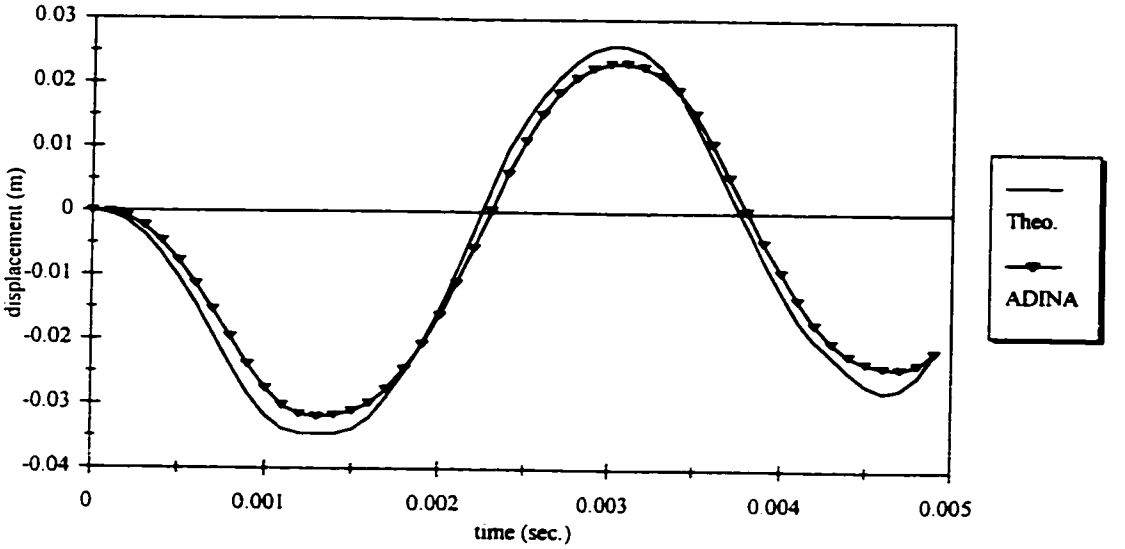

Figure 5.27 **Comparison of Shell Theory and FEM for SSSS**

PREDICTION FROM THE ANALYTICAL METHOD

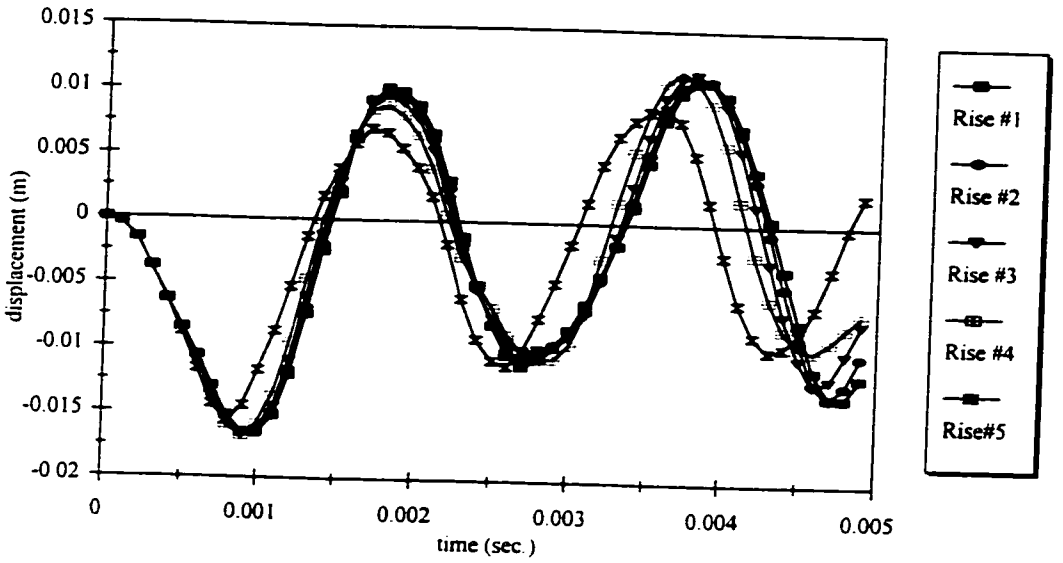

Figure 5.28 Time Response of Panel at $x=a/2$, $y=b/2$ for CCCC

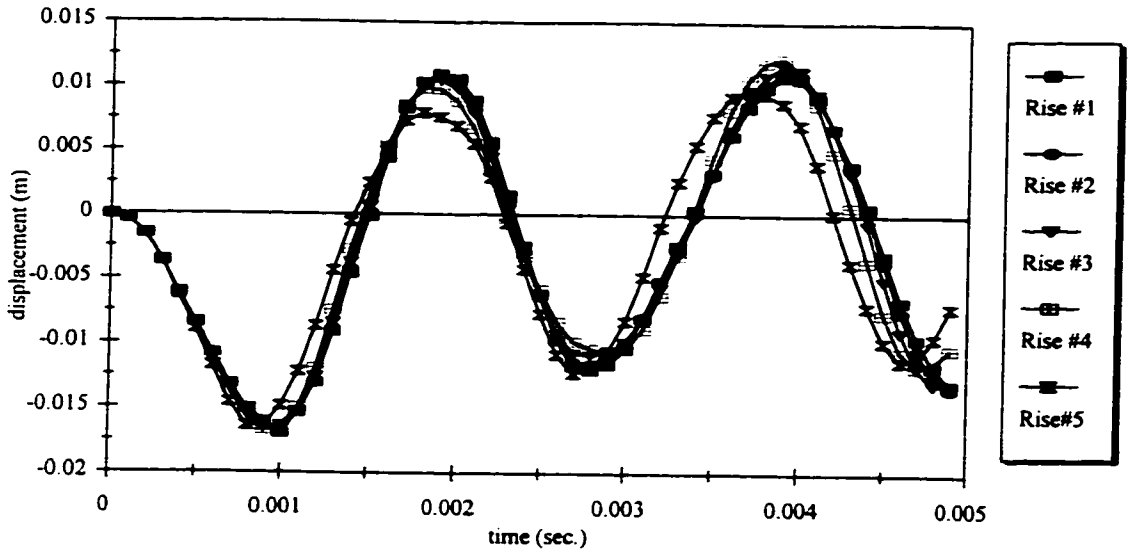

Figure 5.29 Time Response of Panel at $x=a/2$, $y=0.5817$ for CCCS

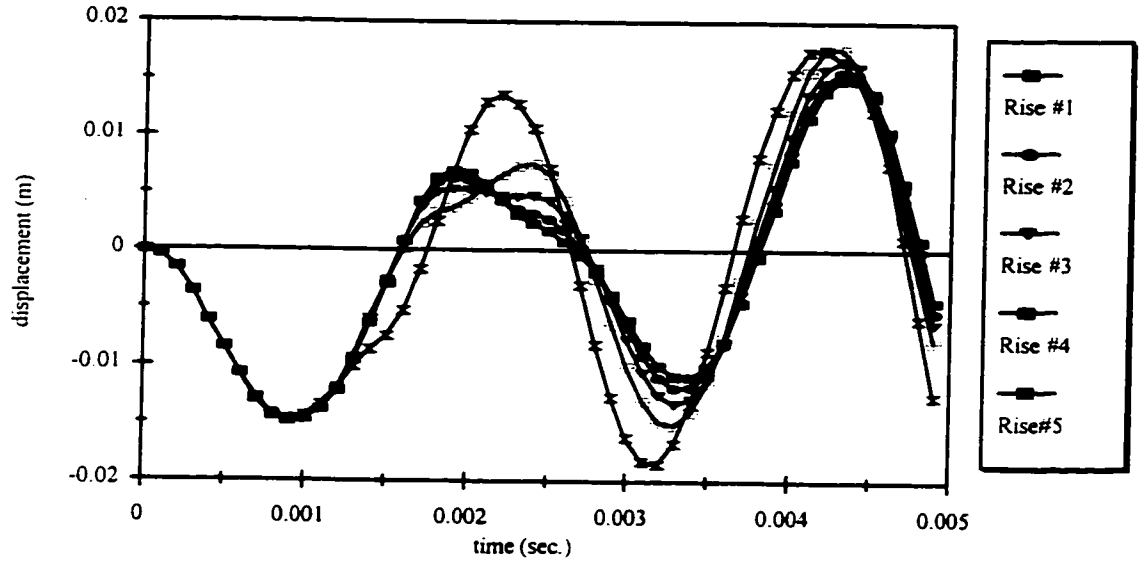

Figure 5.30 Time Response of Panel at $x=a/2$, $y=b$ for CCCF

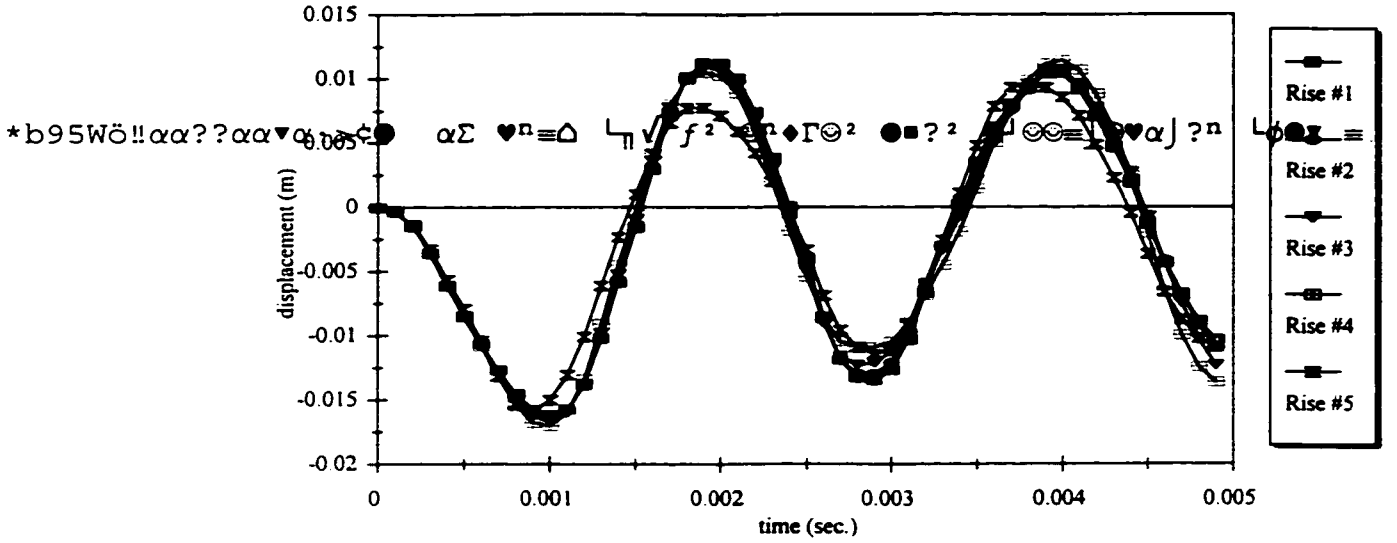

Figure 5.31 Time Response of Panel at $x=a/2$, $y=b/2$ for CCSS

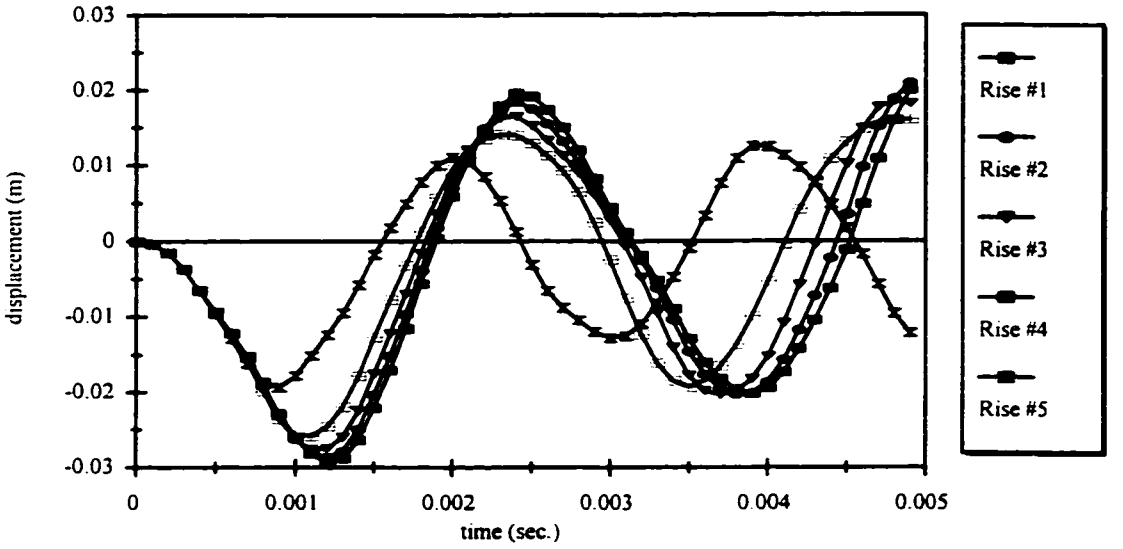

Figure 5.32 Time Response of Panel at $x=0.5817a$, $y=b/2$ for CSCC

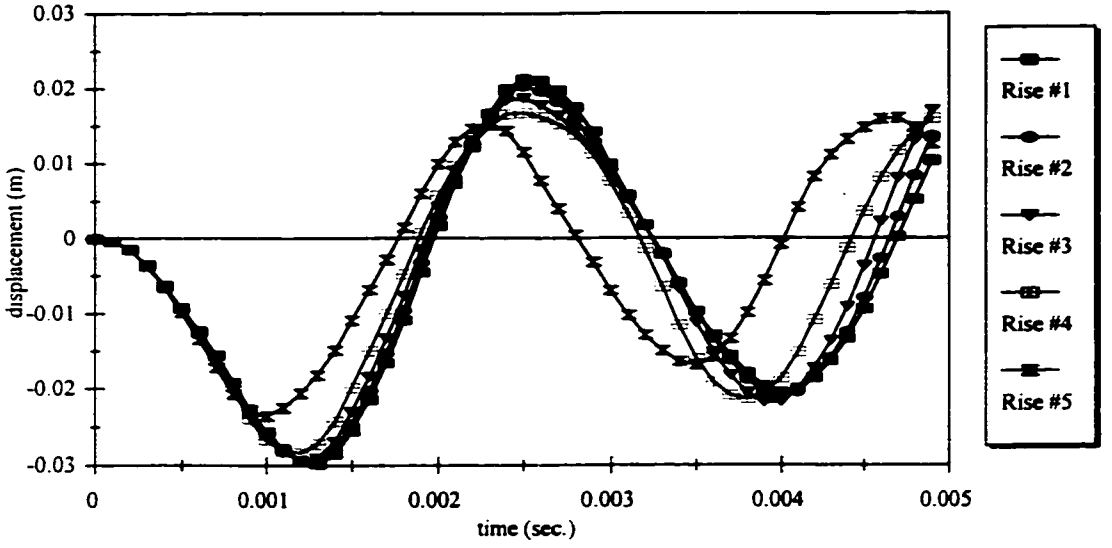

Figure 5.33 Time Response of Panel at $x=0.5817a$, $y=0.5817b$ for CSCS

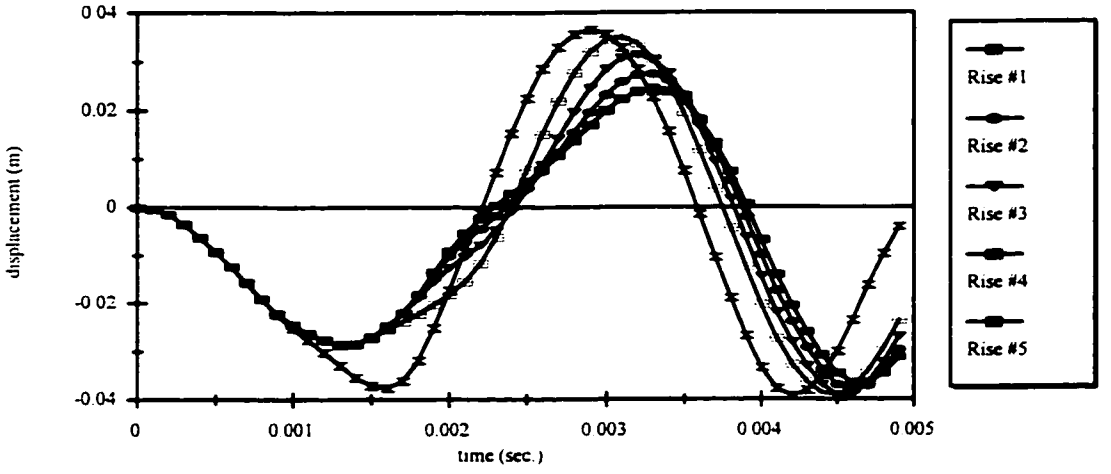

Figure 5.34 Time Response of Panel at $x=a$, $y=b$ for CSCF

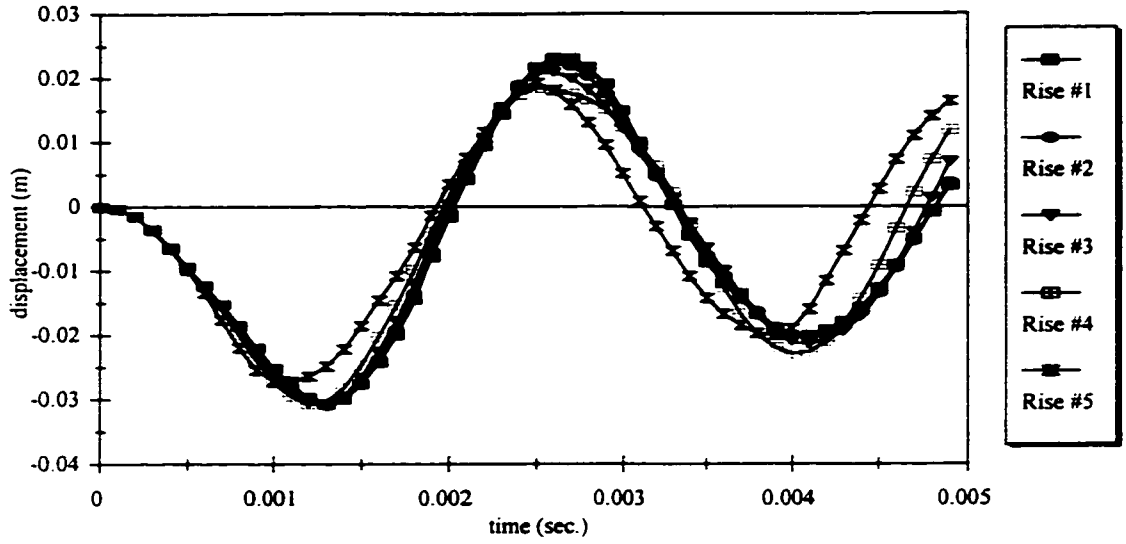

Figure 5.35 Time Response of Panel at $x=0.5817a$, $y=b/2$ for CSSS

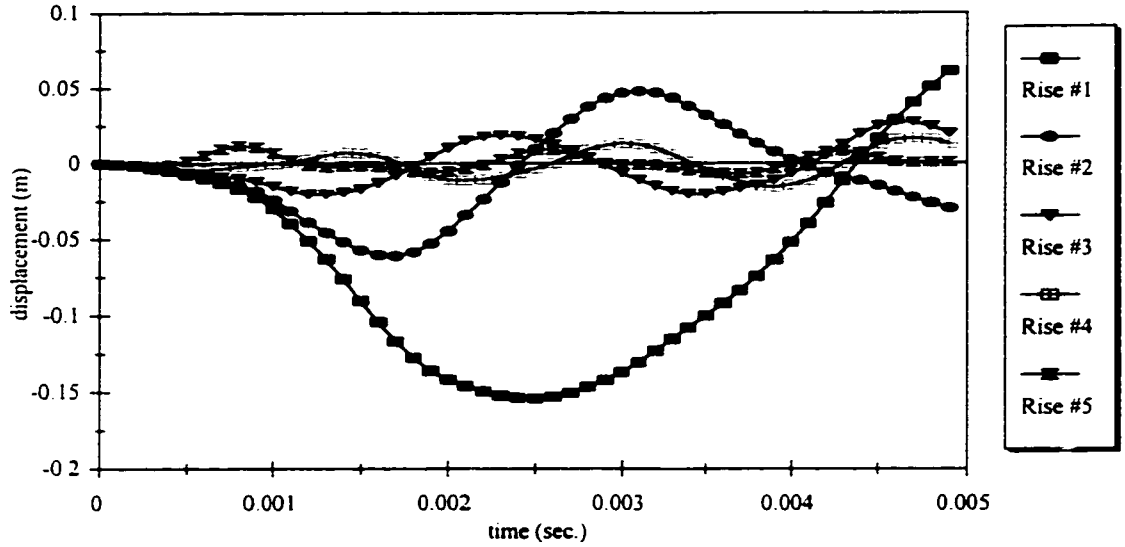

Figure 5.36 Time Response of Panel at $x=a$, $y=b/2$ for CFCC

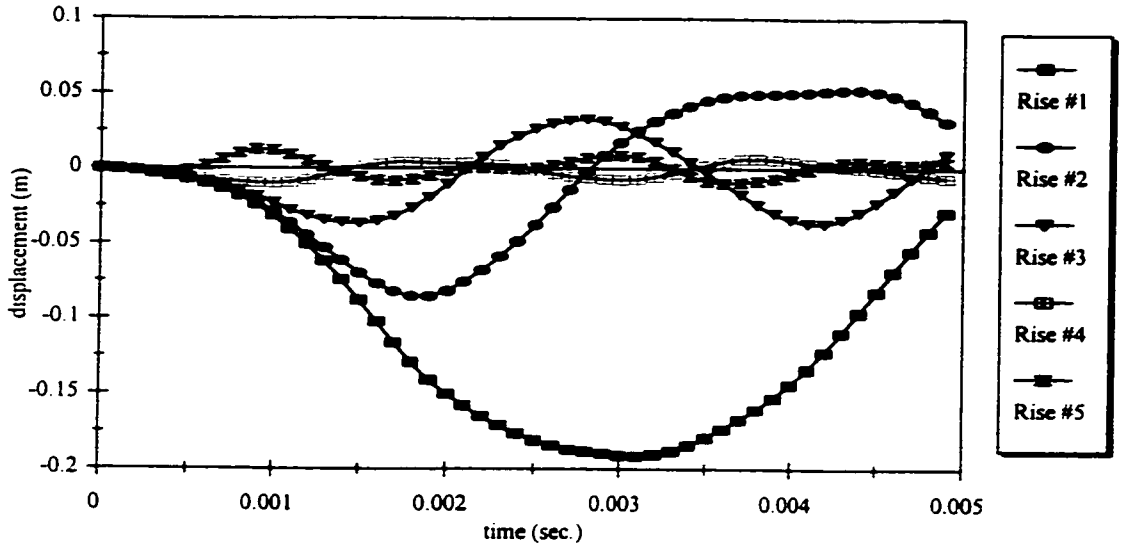

Figure 5.37 Time Response of Panel at $x=a$, $y=0.5817b$ for CFCS

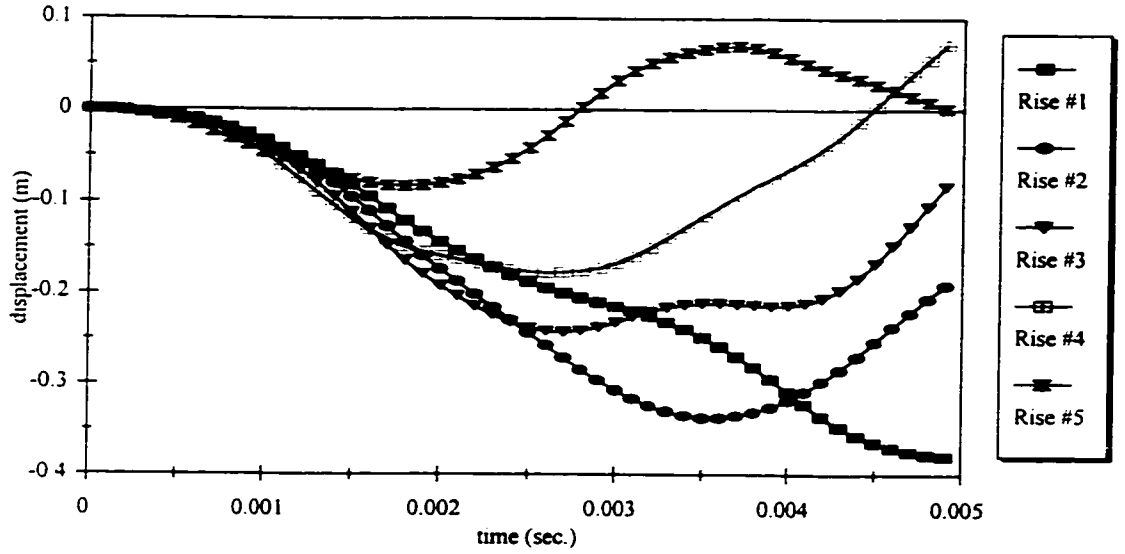

Figure 5.38 Time Response of Panel at $x=a$, $y=b$ for CFCF

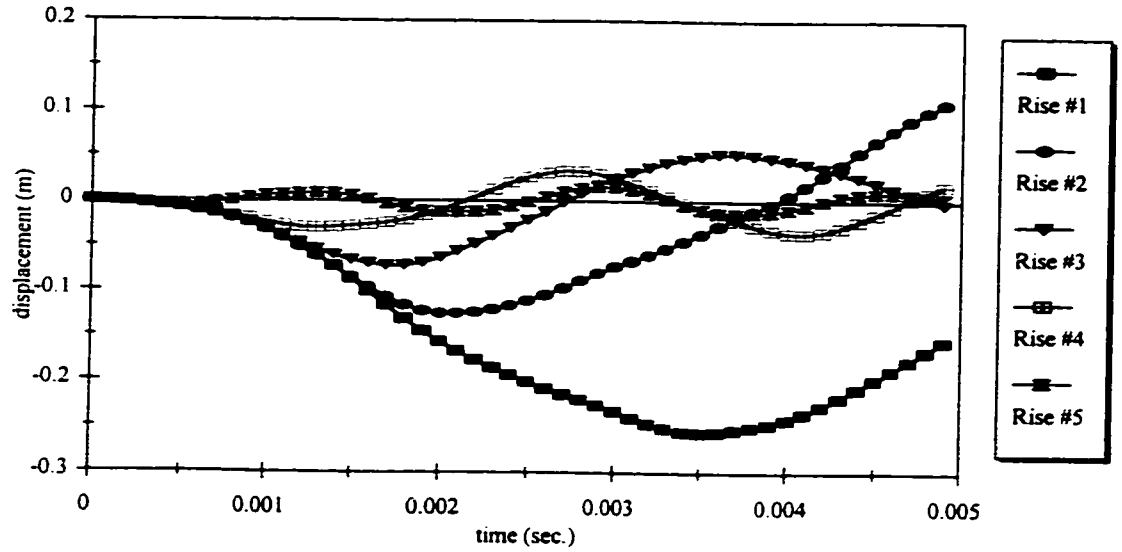

Figure 5.39 Time Response of Panel at $x=a$, $y=b/2$ for CFSS

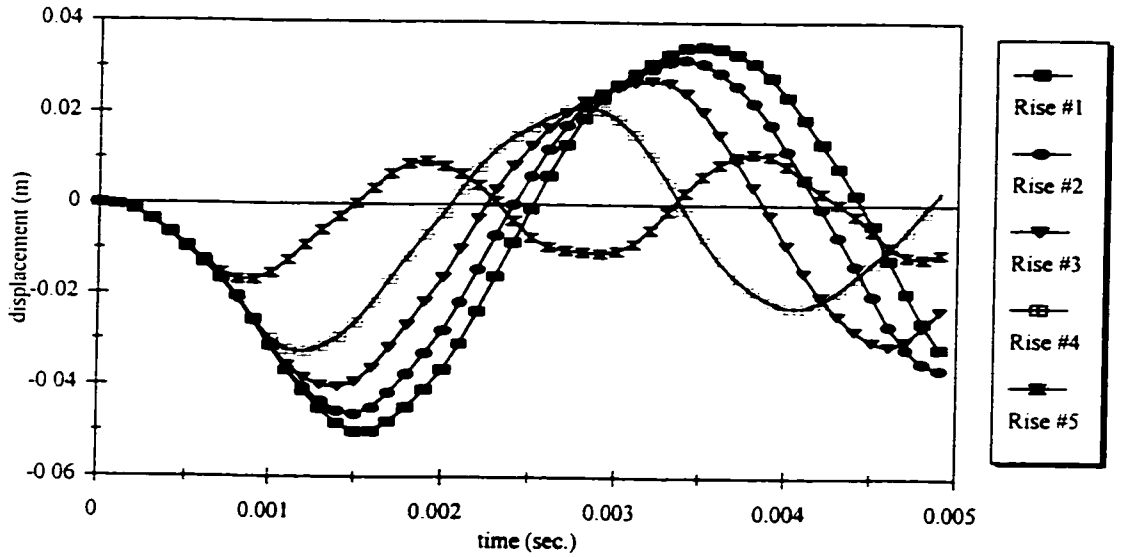

Figure 5.40 Time Response of Panel at $x=a/2$, $y=b/2$ for SSCC

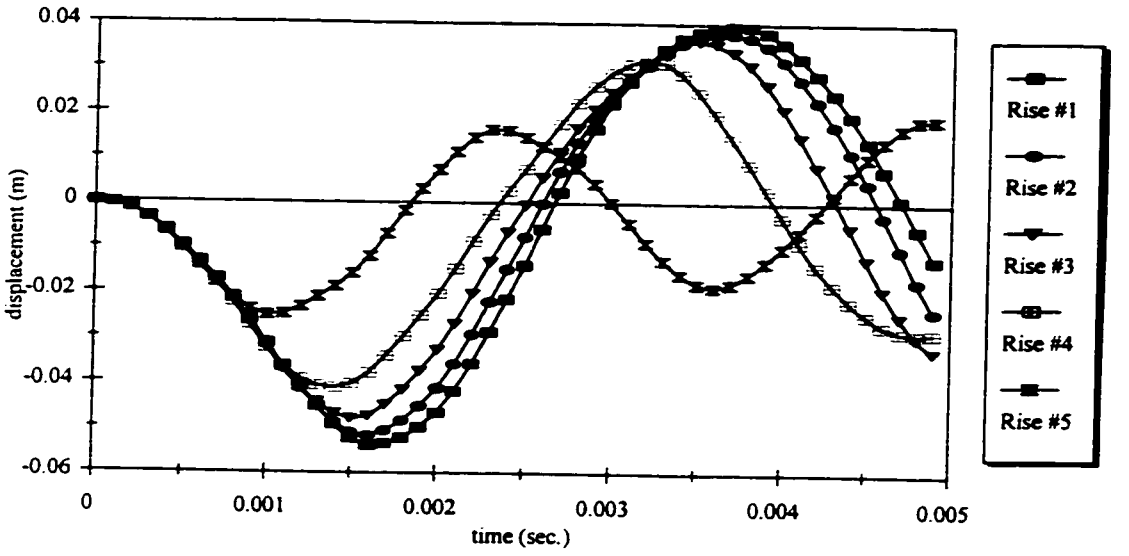

Figure 5.41 Time Response of Panel at $x=a/2$, $y=0.5817b$ for SSCS

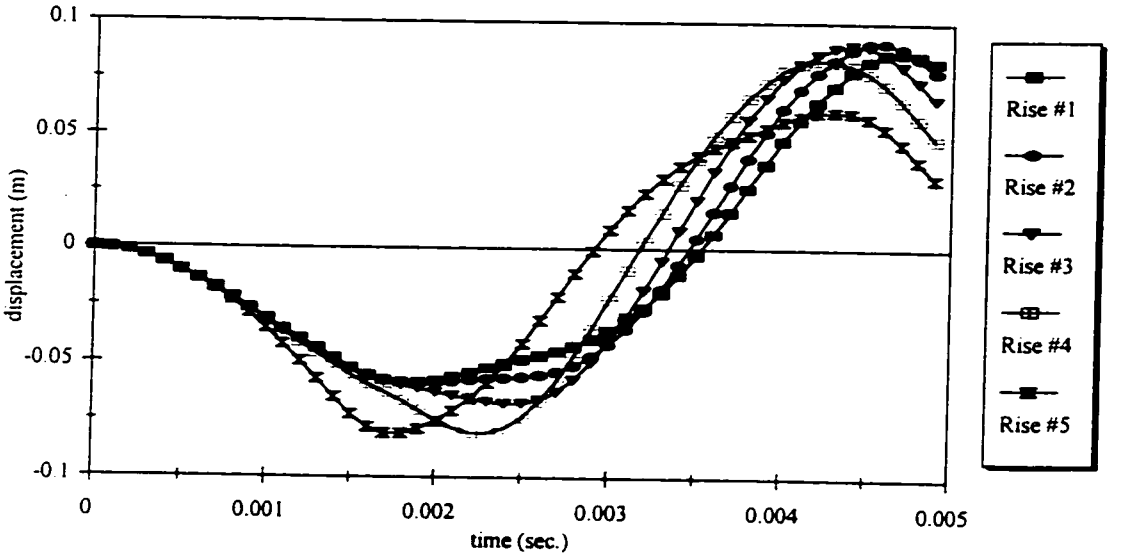

Figure 5.42 Time Response of Panel at $x=a/2$, $y=b$ for SSCF

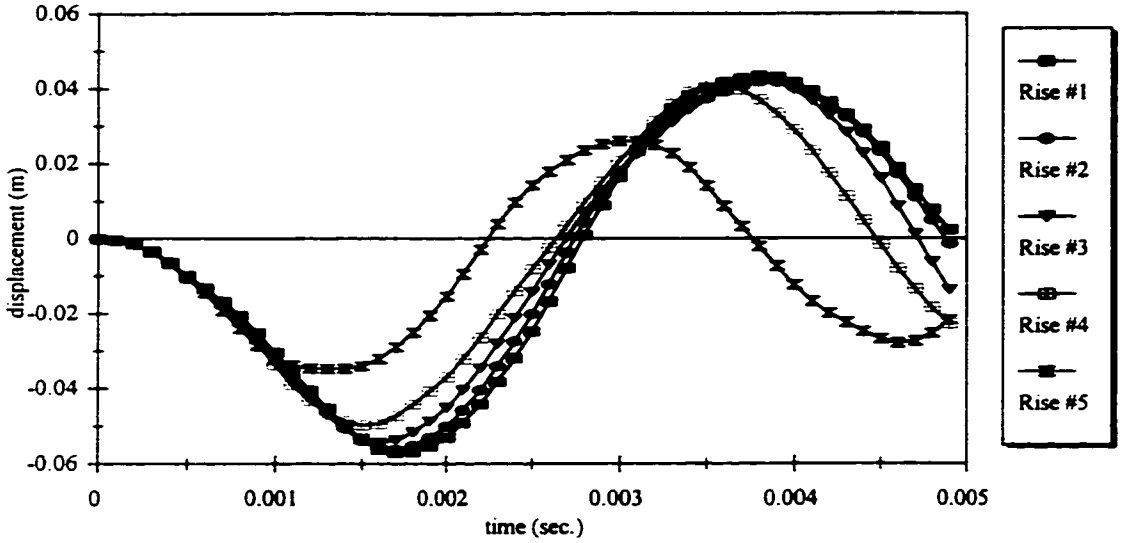

Figure 5.43 Time Response of Panel at $x=a/2$, $y=b/2$ for SSSS

LINEAR FE SOLUTION FOR SSFF

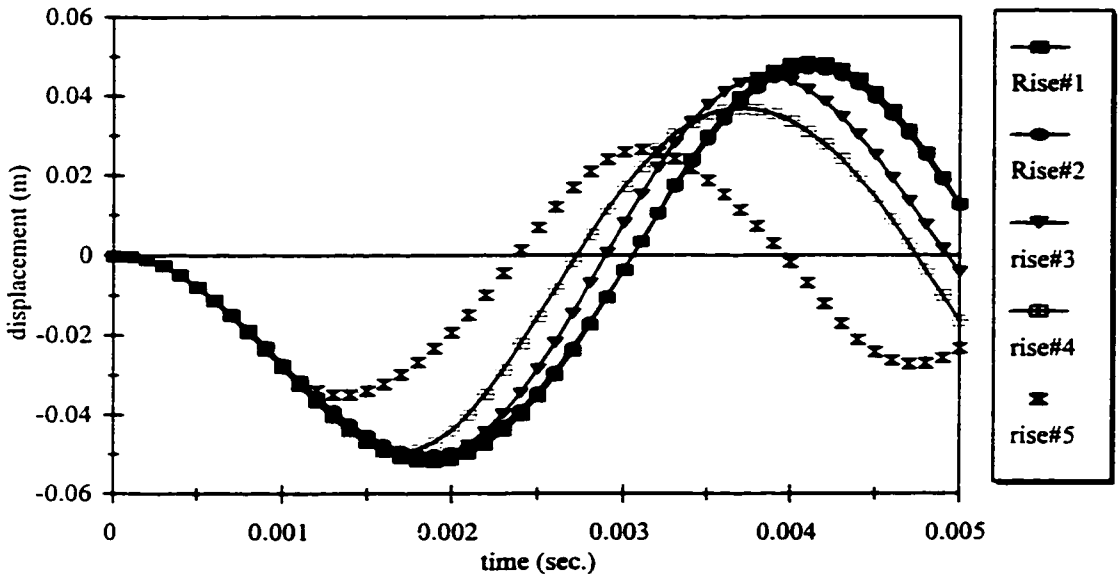

Figure 5.44 Time Response of Panel at $x=a/2$, $y=b/2$ for SSFF

NONLINEAR SOLUTION FOR SSFF

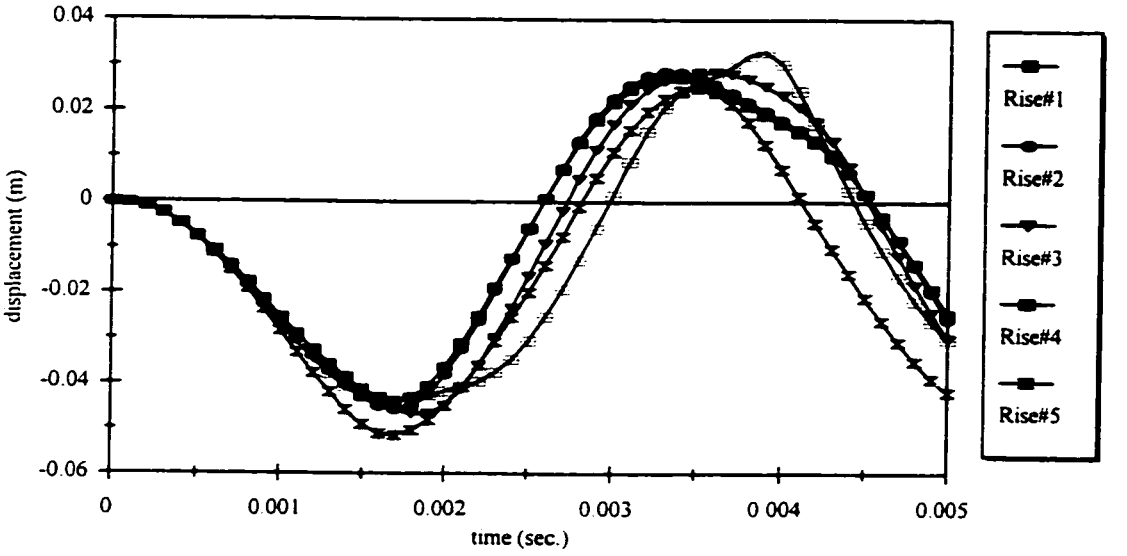

Figure 5.45 Time Response of Panel at $x=a/2$, $y=b/2$ for SSFF

NONLINEAR SOLUTION FOR SSSS

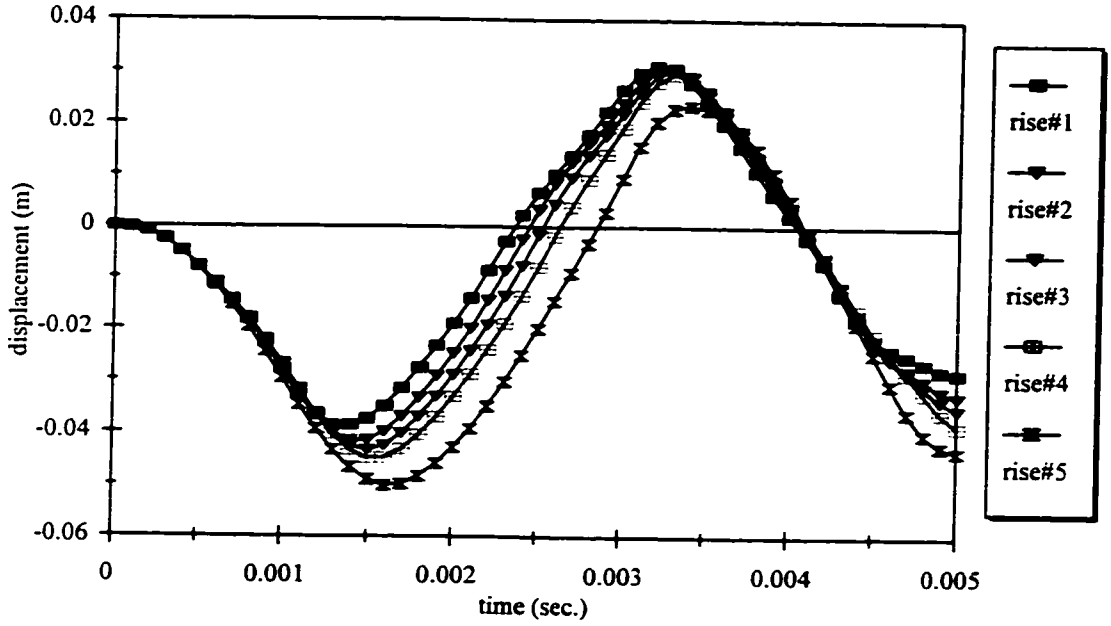

Figure 5.46 Time Response of Panel at $x=a/2$, $y=b/2$ for SSSS

LINEAR COMPARISON OF SSSS VS SSFF

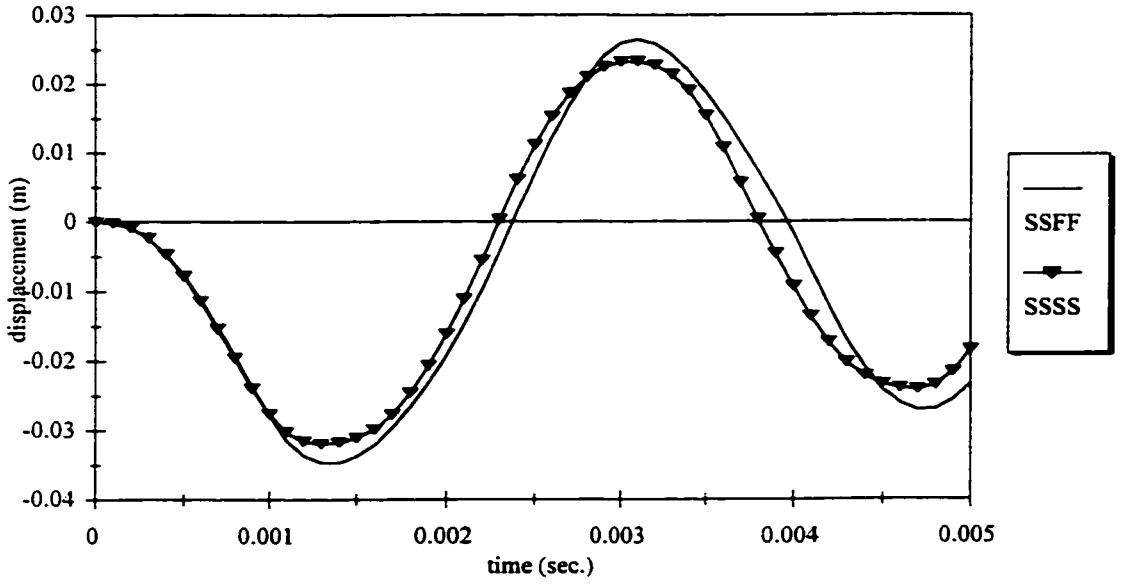

Figure 6.1 Time Response of Panel at $x=a/2$, $y=b/2$

NONLINEAR COMPARISON OF SSSS VS SSFF

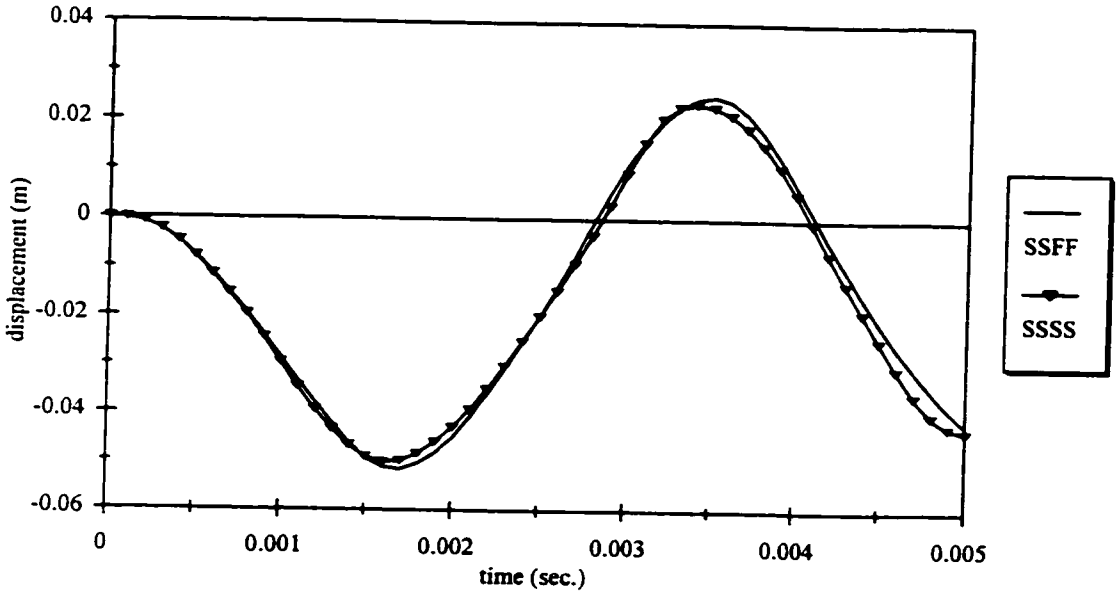

Figure 6.2 Time Response of Panel at $x=a/2$, $y=b/2$

TABLES

TYPE	Boundary Conditions	Frequency Equation	Eigenfunction $w_m(\xi)$	Roots of Frequency Equations
Clamped-clamped	w(0)=w'(0)=0 w(l)=w'(l)=0	$\cos\lambda\cosh\lambda=1$	$w_m(\xi) = J\left(\frac{\lambda_m\xi}{l}\right) - \frac{J(\lambda_m)}{H(\lambda_m)}H\left(\frac{\lambda_m\xi}{l}\right)$	λ_1= 4.7300 λ_2= 7.8532 λ_3=10.9956 λ_4=14.1372
Clamped-hinged	w(0)=w'(0)=0 w(l)=w''(l)=0	$\tan\lambda=\tanh\lambda$	$w_m(\xi) = J\left(\frac{\lambda_m\xi}{l}\right) - \frac{G(\lambda_m)}{F(\lambda_m)}H\left(\frac{\lambda_m\xi}{l}\right)$	λ_1= 3.9266 λ_2= 7.0686 λ_3=10.2102 λ_4=13.3518 $\lambda_m=(4m+1)\pi/4$
Clamped-free	w(0)=w'(0)=0 w''(l)=w'''(l)=0	$\cos\lambda\cosh\lambda=-1$	$w_m(\xi) = J\left(\frac{\lambda_m\xi}{l}\right) - \frac{J(\lambda_m)}{H(\lambda_m)}H\left(\frac{\lambda_m\xi}{l}\right)$	λ_1= 1.8751 λ_2= 4.6941 λ_3=7.8548 λ_4=10.9955
Hinged-hinged	w(0)=w''(0)=0 w(l)=w''(l)=0	$\sin\lambda=0$	$w_m(\xi) = \sin\left(\frac{m\pi\xi}{l}\right)$	$\lambda_m=m\pi$
Free-free	w(0)''=w'''(0)=0 w''(l)=w'''(l)=0	$\cos\lambda\cosh\lambda=1$	$w_1(\xi) = 1$ $w_2 = 1 - \frac{2\xi}{l}$ $w_m(\xi) = G\left(\frac{\lambda_m\xi}{l}\right) - \frac{J(\lambda_m)}{H(\lambda_m)}F\left(\frac{\lambda_m\xi}{l}\right)$	for m>3 same as cmaped-clamped beam

where

$$F(u) = \sinh u + \sin u$$
$$G(u) = \cosh u + \cos u$$
$$H(u) = \sinh u - \sin u$$
$$J(u) = \cosh u - \cos u$$
$$u = \frac{\lambda_m\zeta}{l}$$

Table 3.1 Frequencies and Eigenfunctions for Uniform Beams, ref [48]

Type of analysis	Description	Typical formulation used	Stress and strain measures
Materially nonlinear-only	Infinitesimal displacements and strains; the stress-strain relation is nonlinear	materially nonlinear-only (MNO)	Engineering stress and strain
Large displacements, large rotations, but small strains	Displacements and rotations of fibers are large, but fiber extensions and angle changes between fibers are small; the stress-strain relation may be linear or nonlinear	Total Lagrangian (TL) Updated Lagrangian (UL)	Second Piola-Kirchhoff stress, Green-Lagrange strain Cauchy stress, Alamansi strain
Large displacements, large rotations, but large strains	Fiber extensions and angle changes between fibers are large, fiber displacements and rotations may also be large; the stress-strain relation may be linear or nonlinear	Total Lagrangian (TL) Updated Lagrangian (UL)	Second Piola-Kirchhoff stress, Green-Lagrange strain Cauchy stress, logarithmic strain

Table 4.1 Classification of Nonlinear Analysis, ref. [45]

Rise Cases	1	2	3	4	5
CCCC	0.016784 (10 ms)	0.016741 (9 ms)	0.016612 (9 ms)	0.016523 (9 ms)	0.015623 (8 ms)
CCCS	0.016961 (10 ms)	0.016862 (10 ms)	0.016636 (9 ms)	0.016621 (9 ms)	0.016422 (8 ms)
CCCF	0.014871 (9 ms)	0.014865 (9 ms)	0.014855 (9 ms)	0.015166 (33 ms)	0.018483 (32 ms)
CCSS	0.017580 (10 ms)	0.016983 (10 ms)	0.016371 (10 ms)	0.016310 (10 ms)	0.01623 (9 ms)
CSCC	0.029151 (12 ms)	0.028640 (12 ms)	0.027513 (11 ms)	0.025796 (11 ms)	0.019319 (10 ms)
CSCS	0.029840 (13 ms)	0.029643 (13 ms)	0.029284 (12 ms)	0.028332 (12 ms)	0.023560 (10 ms)
CSCF	0.028579 (14 ms)	0.028604 (13 ms)	0.031406 (32 ms)	0.035135 (31 ms)	0.039305 (16 ms)
CSSS	0.030699 (13 ms)	0.030895 (13 ms)	0.030656 (13 ms)	0.030598 (12 ms)	0.027137 (11 ms)
CFCC	0.153664 (25 ms)	0.060701 (17 ms)	0.020245 (13 ms)	0.015547 (39 ms)	0.011989 (8 ms)
CFCS	0.191385 (31 ms)	0.085241 (18 ms)	0.036451 (15 ms)	0.009658 (10 ms)	0.012580 (9 ms)
CFCF	0.37610 (52 ms)	0.337219 (36 ms)	0.242979 (27 ms)	0.177454 (26 ms)	0.082962 (19 ms)
CFSS	0.256147 (35 ms)	0.125055 (21 ms)	0.070650 (17 ms)	0.035976 (41 ms)	0.016144 (29 ms)
SSCC	0.050201 (15 ms)	0.046311 (15 ms)	0.040417 (14 ms)	0.032681 (12 ms)	0.016797 (9 ms)
SSCS	0.053803 (16 ms)	0.051727 (16 ms)	0.047893 (15 ms)	0.041114 (14 ms)	0.025029 (10 ms)
SSCF	0.087009 (47 ms)	0.091437 (46 ms)	0.090406 (44 ms)	0.083637 (42 ms)	0.081083 (18 ms)
SSSS	0.057061 (17 ms)	0.056195 (17 ms)	0.054408 (16 ms)	0.049672 (15 ms)	0.034611 (13 ms)

Table 6.1 Results for Maximum Absolute Deflection

Boundary	Theoretical	Finite Element	% difference
CCCC	0.01562	0.01706	9.22
CCCS	0.01642	0.01798	9.47
CCCF	0.01848	0.02036	10.13
CCSS	0.01758	0.01912	8.74
CSCC	0.01932	0.02116	9.51
CSCS	0.02356	0.02586	9.78
CSCF	0.03931	0.04556	15.92
CSSS	0.02714	0.02951	8.74
CFCC	0.01199	0.01350	12.60
CFCS	0.01258	0.01424	13.12
CFCF	0.08296	0.09370	12.94
CFSS	0.01614	0.01813	12.28
SSCC	0.01679	0.01826	8.78
SSCS	0.02503	0.02726	8.91
SSCF	0.08083	0.09044	11.89
SSSS	0.03461	0.03192	8.42

Table 6.2 Comparison of the Analytical and FEM for the 5th Rise Case

Rise Cases	1	2	3	4	5
SSSS	0.05323 (17 ms)	0.05245 (17 ms)	0.050504 (17 ms)	0.04645 (16 ms)	0.03192 (13 ms)
SSFF	0.055430 (17 ms)	0.05389 (19 ms)	0.05099 (18 ms)	0.04940 (17 ms)	0.03466 (13 ms)

Table 6.3 Results for Maximum Absolute Deformation at Panel Center, Linear Case

Rise Cases	1	2	3	4	5
SSSS	0.03857 (14 ms)	0.04161 (14 ms)	0.04336 (15 ms)	0.04486 (15 ms)	0.05012 (16 ms)
SSFF	0.04395 (17 ms)	0.04593 (17 ms)	0.04582 (17 ms)	0.04409 (17 ms)	0.05151 (17 ms)

Table 6.4 Results for Maximum Absolute Deformation at Panel Center, Nonlinear Case

APPENDIX A

FORTRAN PROGRAM FOR THE

ANALYTICAL SOLUTION

```
C*************************************************************************
C    LAST MODIFICATION    JUNE 02 1996
C    BLAST LOADING OF CYLINDRICAL. SHELL PANEL
C    MODE SHAPES TAKEN AS PRODUCT OF BEAM FUNCTIONS
C*************************************************************************
     IMPLICIT REAL*8 (A-H,O-Z)
     COMMON/AAA/RC,HC,PA,PB,EY,POI,RHO,I,L,M,N,MHI,NHI,NT,II,JJ
     COMMON/CCC/DEEC,CONL
     COMMON/FFF/PMAX,OML,DELT
     COMMON/ZMN/XMN(21,21,16),PMN(21,21),OMMN(21,21)
     COMMON/AIM/AI1,AI2,AI3,AI4,AI5,AI6,AI7
     COMMON/AIN/AI8,AI9,AI10,AI11,AI12,AI13,AI14
     OPEN(UNIT=8,FILE='OUTPUT')
     OPEN(UNIT=9,FILE='DISPLACEMENT.TXT')

     DO 666 I=1,1
     DO 766 L=3,3
     CALL RESP
  766 CONTINUE
  666 CONTINUE

     STOP
     END
C*************************************************************************
     SUBROUTINE RESP
     IMPLICIT REAL*8 (A-H,O-Z)
     COMMON/AAA/RC,HC,PA,PB,EY,POI,RHO,I,L,M,N,MHI,NHI,NT
     COMMON/CCC/DEEC,CONL
     COMMON/FFF/PMAX,OML,DELT
     COMMON/CTS/ALM(10,4),ALN(10,4),AFM(10,4),AFN(10,4)
     COMMON/ZMN/XMN(21,21,16),PMN(21,21),OMMN(21,21)
     COMMON/FNS/RESC(101,3)
     COMMON/BLA/AP,TP
```

```
      PI=3.14159265358979D0
      RAD=PI/180.D0
C     INPUT THE PRIMARY DATA
      ALFA=2.*ASIN(0.5*PB/RC)/RAD
      RO=7770.
      POIS=.3
      EY=.2068D+12
      PMAX=.689D+07
      AP=1.98
      TP=0.004
      DELT=0.0001

C     WRITEOUT THE INPUT DATA
      WRITE(8,106) PA,PB,HC,RC,ALFA
  106 FORMAT(/' PANEL DIMENSIONS'/
     1     ' ----------------'/
     2 ' PANEL WIDTH     (M) Y-DIRECTION      PA = ',F12.5/
     3 ' PANEL LENGTH    (M) X-DIRECTION      PB = ',F12.5/
     4 ' PANEL THICKNESS (M)                  HC = ',F12.5/
     5 ' CYLD RADIUS     (M)                  RC = ',F12.5/
     6 ' SUBTENDED ANGLE (DEG)                ALFA = ',F12.5)
      ALFR=ALFA*RAD
      WRITE(8,116) RO,POIS,EY
  116 FORMAT(/' MATERIAL PARAMETERS'/
     1     ' -------------------'/
     2 ' MASS DENSITY (KG/M3)                 RO = ',D12.3/
     2 ' POISSON RATIO                        POIS = ',F12.3/
     3 ' YOUNGS MODULUS (PA)                  EY = ',D12.3)
      WRITE(8,126) PMAX,DELT
  126 FORMAT(/' LOAD PARAMETERS'/
     1     ' ------------'/
     2 ' PEAK PRESSURE              (PA)      PMAX = ',D12.5/
     3 ' TIME STEP                  (SEC)     DELT = ',F12.5)
      WRITE(8,136) MHI,NHI,NT
  136 FORMAT(/' SOLUTION PARAMETERS'/
     1     ' -------------------'/
     2 ' TERMS IN X DIRECTION (WIDTH)         MHI = ',I5/
     3 ' TERMS IN Y DIRECTION (LENGTH)        NHI = ',I5/
     4 ' NUMBER OF SAMPLING TIMES             NT  = ',I5)

      DEE=EY*HC*HC*HC/(12.*(1.-POIS*POIS))
      POI=POIS
      RHO=RO
```

```
      POI2=POI*POI
      DEEC=DEE

      WRITE(8,6)
    6 FORMAT(/,' SS SOLUTION - CHARACTERISTICS '/
     1 5X,'M',4X,'N',11X,'Q',11X,'A',11X,'B',10X,'OM')

      DO 900 J=1,NT
      DO 910 KK=2,2
  910 RESC(J,KK)=0.00
  900 CONTINUE



C     1=CC, 2=CS, 3=CF, 4=SS
      CALL CONST

C     INTEGRALS EVALUATIONS

      DO 150 M=1,MHI
      DO 160 N=1,NHI

      IF (I.EQ.4) GO TO 111

C IN X-DIRECTION FOR CC,CS,CF

      ZM=ALM(M,I)
      ELM=DEXP(ZM)
      ELM2=ELM*ELM
      ELM3=ELM*ELM2
      ELM4=ELM2*ELM2
      CM=AFM(M,I)
      CM2=AFM(M,I)*AFM(M,I)
      CELM=DCOS(ZM)*ELM
      CELM3=DCOS(ZM)*ELM3
      SELM=DSIN(ZM)*ELM
      SELM3=DSIN(ZM)*ELM3
      CSELM2=DCOS(ZM)*DSIN(ZM)*ELM2
      C2M=DCOS(ZM)*DCOS(ZM)

      AI1=.125*PB*(-1.00-4*CELM3+4*CM2*CELM3-4*SELM3-4*CM2*SELM3
     1    -2*CM*ELM4-4*CM2*CELM+CM2*ELM4-4*CM2*SELM+8*ZM*ELM2
     2    -CM2-8*CM*SELM + ELM4+8*CM*SELM3+4*CELM-4*CM2*CSELM2-4*SELM
```

```
     3   +4*CSELM2+8*CM*C2M*ELM2-2*CM)/(ZM*ELM2) -0.5*CM*PB/ZM
      AI2=-.125*(1.00+2*CM+8*CM2*ZM*ELM2-4*CM2*CSELM2+4*CSELM2+CM2
     1   +2.00*CM*ELM4+ 8*CM*C2M*ELM2-CM2*ELM4-ELM4)*ZM/(PB*ELM2)
     2   + 1.5*CM*ZM/PB
      AI3=(ZM*ZM*ZM*ZM/(PB*PB*PB*PB))*AI1
      AI4=(ZM*ZM*ZM*ZM/(PB*PB*PB*PB))*AI2
      AI5=(ZM*ZM*ZM*ZM/(PB*PB*PB*PB))*(ZM*ZM*ZM*ZM/(PB*PB*PB*PB))*AI1
      AI11=-0.5*PB*(-ELM2+1+2*SELM+CM*ELM2+CM+2*CM*CELM)/(ELM*ZM)
     1    +2*CM*PB/ZM
      AI12=AI1
      GO TO 121
C CASE FOR SS ONLY X-DIRECTION
  111 AI1=0.5*PB
      ZETA=(2*M-1)*PI/PB
      ZETA2=ZETA*ZETA
      ZETA4=ZETA2*ZETA2
      ZETA6=ZETA2*ZETA4
      ZETA8=ZETA4*ZETA4
      AI2=-ZETA2*AI1
      AI3=ZETA4*AI1
      AI4=-ZETA6*AI1
      AI5=ZETA8*AI1
      AI11=2*PB/((2*M-1)*PI)
      AI12=AI1

C Y-DIRECTION

  121  IF (L.EQ.4) GO TO 131

      ZN=ALN(N,L)
      ELN=DEXP(ZN)
      ELN2=ELN*ELN
      ELN3=ELN*ELN2
      ELN4=ELN2*ELN2
      CN=AFN(N,L)
      CN2=AFN(N,L)*AFN(N,L)
      CELN=DCOS(ZN)*ELN
      CELN3=DCOS(ZN)*ELN3
      SELN=DSIN(ZN)*ELN
      SELN3=DSIN(ZN)*ELN3
      CSELN2=DCOS(ZN)*DSIN(ZN)*ELN2
      C2N=DCOS(ZN)*DCOS(ZN)
      AI6=.125*PA*(-1.00-4*CELN3+4*CN2*CELN3-4*SELN3-4*CN2*SELN3
```

```
     1    -2*CN*ELN4-4*CN2*CELN+CN2*ELN4-4*CN2*SELN+8*ZN*ELN2
     2    -CN2-8*CN*SELN + ELN4+8*CN*SELN3+4*CELN-4*CN2*CSELN2-4*SELN
     3   +4*CSELN2+8*CN*C2N*ELN2-2*CN)/(ZN*ELN2) -0.5*CN*PA/ZN
      AI7=-.125*(1.00+2*CN+8*CN2*ZN*ELN2-4*CN2*CSELN2+4*CSELN2+CN2
     1   +2.00*CN*ELN4+ 8*CN*C2N*ELN2-CN2*ELN4-ELN4)*ZN/(PA*ELN2)
     2   + 1.5*CN*ZN/PA
      AI8=(ZN*ZN*ZN*ZN/(PA*PA*PA*PA))*AI6
      AI9=(ZN*ZN*ZN*ZN/(PA*PA*PA*PA))*AI7
      AI10=(ZN*ZN*ZN*ZN/(PA*PA*PA*PA))*(ZN*ZN*ZN*ZN/(PA*PA*PA*PA))*AI6
      AI13=-0.5*PA*(-ELN2+1+2*SELN+CN*ELN2+CN+2*CN*CELN)/(ELN*ZN)
     1     +2*CN*PA/ZN
      AI14=AI6
      GO TO 141
C FOR THE SS CASE
  131 AI6=0.5*PA
      ETA=(2*N-1)*PI/PA
      ETA2=ETA*ETA
      ETA4=ETA2*ETA2
      ETA6=ETA2*ETA4
      ETA8=ETA4*ETA4
      AI7=-ETA2*AI6
      AI8=ETA4*AI6
      AI9=-ETA6*AI6
      AI10=ETA8*AI6
      AI13=2*PA/((2*N-1)*PI)
      AI14=AI6

C FREQUENCY CALCULATION

  141 DNUM=DEEC*(AI5*AI6+AI1*AI10+6*AI3*AI8+4*(AI4*AI7+AI2*AI9))
     1   + EY*HC*AI1*AI8/(RC*RC)
      DENOM=RHO*HC*(AI3*AI6+2*AI2*AI7+AI1*AI8)
      OM2=DNUM/DENOM
      OM=DSQRT(OM2)
      OMMN(M,N)=OM
      Q=PMAX*AI11*AI13/(RHO*HC*AI12*AI14)
      PMN(M,N)=Q

C  CONSTANTS

      RR=PMN(M,N)
      SS=PMN(M,N)/TP
      GG=AP/TP
```

```
      RRR=(RR*(GG*GG+OM*OM)-2*GG*SS)/((GG*GG+OM*OM)*(GG*GG+OM*OM))
      SSS=SS/(GG*GG+OM*OM)
      B=-RRR
      A=(SSS+GG*RRR)/OM
      XMN(M,N,1)=A
      XMN(M,N,2)=B
      XMN(M,N,3)=RRR
      XMN(M,N,4)=SSS

      IF(I.EQ.1.OR.I.EQ.4) THEN
      ZX=0.5*PB
      ELSEIF (I.EQ.2.) THEN
      ZX=0.5816998E0*PB
      ELSE
      ZX=PB
      ENDIF




      IF(L.EQ.1.OR.L.EQ.4) THEN
      ZY=0.5*PA
      ELSEIF (L.EQ.2.) THEN
      ZY=0.5816998E0*PA
      ELSE
      ZY=PA
      ENDIF

C LOOP OVER TIME STEPS

      T=0.00
      DO 950 J=1,NT

      IF(T.LE.TP) THEN
      TIMEF=XMN(M,N,1)*DSIN(OM*T)+XMN(M,N,2)*DCOS(OM*T)
     1      +(XMN(M,N,3)-XMN(M,N,4)*T)*DEXP(-GG*T)
      ELSE
C CALCULATION OF 'INITIAL' DISPLACEMENT AND VELOCITY AND NEW
C       CONSTANTS

      XT=XMN(M,N,1)*DSIN(OM*TP)+XMN(M,N,2)*DCOS(OM*TP)
     1      +(XMN(M,N,3)-XMN(M,N,4)*TP)*DEXP(-GG*TP)
      VT=OM*(XMN(M,N,1)*DCOS(OM*TP)-XMN(M,N,2)*DSIN(OM*TP))
```

```
     1  -GG*XMN(M,N,3)*EXP(-GG*TP)-XMN(M,N,4)*(1-GG*TP)*EXP(-GG*TP)
      AA=VT/OM
      BB=XT
      TIMEF=AA*SIN(OM*(T-TP))+BB*COS(OM*(T-TP))
      ENDIF
      IF(I.EQ.4) THEN
      FX=SIN((2*M-1)*PI*ZX/PB)
      ELSE
      FX=DCOSH(ZM*ZX/PB)-DCOS(ZM*ZX/PB)-CM*(DSINH(ZM*ZX/PB)
     1   -DSIN(ZM*ZX/PB))
      ENDIF
      IF (L.EQ.4) THEN
      FY=SIN((2*N-1)*PI*ZY/PA)
      ELSE
      FY=DCOSH(ZN*ZY/PA)-DCOS(ZN*ZY/PA)-CN*(DSINH(ZN*ZY/PA)
     1   -DSIN(ZN*ZY/PA))
      ENDIF
      RESC(J,1)=T
      RESC(J,2)=RESC(J,2)+FX*FY*TIMEF
  950 T=T+DELT


  160 WRITE(8,16) M,N,Q,A,B,OM
   16 FORMAT(1X,2I5,4D12.4)
  150 WRITE(8,26)
   26 FORMAT(' ')
      WRITE(9,*) I,L

C WRITING RESULTS FOR ALL TIME STEPS
      DO 1000 J=1,NT
      RESC(J,1)=RESC(J,1)
      RESC(J,2)=-RESC(J,2)
 1000 WRITE(9,256) (RESC(J,KK),KK=1,2)
  256 FORMAT(1X,F9.4,F9.6)
      WRITE(9,*)
      RETURN
      END

C*******************************************************************************
      SUBROUTINE CONST
      IMPLICIT REAL*8 (A-H,O-Z)
      COMMON/AAA/RC,HC,PA,PB,EY,POI,RHO,I,M,N,MHI,NHI,NT
      COMMON/CTS/ALM(10,4),ALN(10,4),AFM(10,4),AFN(10,4)
```

```
C     BEAM FUCTIONS CONSTANTS

C     IN X-DIRECTION
C     CC
      ALM(1,1) = 0.4730041E1
      ALM(2,1) = 0.78532E1
      ALM(3,1) = 0.1099561E2
      ALM(4,1) = 0.141372E2
      ALM(5,1) = 0.17274E2
      ALM(6,1) = 0.2042E2
      ALM(7,1) = 0.23562E2
      ALM(8,1) = 0.26703E2
      ALM(9,1) = 0.29845E2
      ALM(10,1) = 0.32987E2
C     CS
      ALM(1,2) = 0.39266E1
      ALM(2,2) = 0.7069E1
      ALM(3,2) = 0.102102E2
      ALM(4,2) = 0.13352E2
      ALM(5,2) = 0.16493E2
      ALM(6,2) = 0.19635E2
      ALM(7,2) = 0.22777E2
      ALM(8,2) = 0.25918E2
      ALM(9,2) = 0.2906E2
      ALM(10,2) = 0.32201E2
C     CF
      ALM(1,3) = 0.1875E1
      ALM(2,3) = 0.4694E1
      ALM(3,3) = 0.7855E1
      ALM(4,3) = 0.10996E2
      ALM(5,3) = 0.14137E2
      ALM(6,3) = 0.17279E2
      ALM(7,3) = 0.2042E2
      ALM(8,3) = 0.23562E2
      ALM(9,3) = 0.26704E2
      ALM(10,3) = 0.29845E2

C CONSTANTS ALFAS
C     CC
      AFM(1,1) = 0.9825022E0
      AFM(2,1) = 0.1000777E1
      AFM(3,1) = 0.9999665E0
      AFM(4,1) = 0.1000001E1
```

```
      AFM(5,1) = 0.9999999E0
      AFM(6,1) = 0.1E1
      AFM(7,1) = 0.1E1
      AFM(8,1) = 0.1E1
      AFM(9,1) = 0.1E1
      AFM(10,1) = 0.1E1
C     CS
      AFM(1,2) = 0.1000777E1
      AFM(2,2) = 0.1000002E1
      AFM(3,2) = 0.1E1
      AFM(4,2) = 0.1E1
      AFM(5,2) = 0.1E1
      AFM(6,2) = 0.1E1
      AFM(7,2) = 0.1E1
      AFM(8,2) = 0.1E1
      AFM(9,2) = 0.1E1
      AFM(10,2) = 0.1E1
C     CF
      AFM(1,3) = 0.7340955E0
      AFM(2,3) = 0.1018467E1
      AFM(3,3) = 0.9992245E0
      AFM(4,3) = 0.1000034E1
      AFM(5,3) = 0.9999986E0
      AFM(6,3) = 0.1E1
      AFM(7,3) = 0.1E1
      AFM(8,3) = 0.1E1
      AFM(9,3) = 0.1E1
      AFM(10,3) = 0.1E1

C     IN Y-DIRECTION
      ALN(1,1) = 0.4730041E1
      ALN(2,1) = 0.78532E1
      ALN(3,1) = 0.1099561E2
      ALN(4,1) = 0.141372E2
      ALN(5,1) = 0.17274E2
      ALN(6,1) = 0.2042E2
      ALN(7,1) = 0.23562E2
      ALN(8,1) = 0.26703E2
      ALN(9,1) = 0.29845E2
      ALN(10,1) = 0.32987E2
C     CS
      ALN(1,2) = 0.39266E1
      ALN(2,2) = 0.7069E1
```

```
      ALN(3,2) = 0.102102E2
      ALN(4,2) = 0.13352E2
      ALN(5,2) = 0.16493E2
      ALN(6,2) = 0.19635E2
      ALN(7,2) = 0.22777E2
      ALN(8,2) = 0.25918E2
      ALN(9,2) = 0.2906E2
      ALN(10,2) = 0.32201E2
C     CF
      ALN(1,3) = 0.1875E1
      ALN(2,3) = 0.4694E1
      ALN(3,3) = 0.7855E1
      ALN(4,3) = 0.10996E2
      ALN(5,3) = 0.14137E2
      ALN(6,3) = 0.17279E2
      ALN(7,3) = 0.2042E2
      ALN(8,3) = 0.23562E2
      ALN(9,3) = 0.26704E2
      ALN(10,3) = 0.29845E2

C CONSTANTS ALFAS
C     CC
      AFN(1,1) = 0.9825022E0
      AFN(2,1) = 0.1000777E1
      AFN(3,1) = 0.9999665E0
      AFN(4,1) = 0.1000001E1
      AFN(5,1) = 0.9999999E0
      AFN(6,1) = 0.1E1
      AFN(7,1) = 0.1E1
      AFN(8,1) = 0.1E1
      AFN(9,1) = 0.1E1
      AFN(10,1) = 0.1E1
C     CS
      AFN(1,2) = 0.1000777E1
      AFN(2,2) = 0.1000002E1
      AFN(3,2) = 0.1E1
      AFN(4,2) = 0.1E1
      AFN(5,2) = 0.1E1
      AFN(6,2) = 0.1E1
      AFN(7,2) = 0.1E1
      AFN(8,2) = 0.1E1
      AFN(9,2) = 0.1E1
      AFN(10,2) = 0.1E1
```

```
C     CF
      AFN(1,3) = 0.7340955E0
      AFN(2,3) = 0.1018467E1
      AFN(3,3) = 0.9992245E0
      AFN(4,3) = 0.1000034E1
      AFN(5,3) = 0.9999986E0
      AFN(6,3) = 0.1E1
      AFN(7,3) = 0.1E1
      AFN(8,3) = 0.1E1
      AFN(9,3) = 0.1E1
      AFN(10,3) = 0.1E1

      RETURN
      END
C*****************************************************
      BLOCK DATA
      IMPLICIT REAL*8 (A-H,O-Z)
      COMMON/AAA/RC,HC,PA,PB,EY,POI,RHO,I,L,M,N,MHI,NHI,NT,II,JJ
      COMMON/COO/ZX,ZY
      DATA RC/0.4953/,HC/0.0125/,PA/1.016/,PB/0.381/
      DATA MHI/7/,NHI/7/,NT/50/,II/1/,JJ/1/
      END
```

SAMPLE ADINA-IN INPUT FILE FOR LINEAR CASE FOR CCCC SUPPORT CONDITIONS

```
* DYNAMIC LOADING OF A SHALLOW CYLINDRICAL SHELL
*
HEADING '----------CCCC----------'
*
FILEUNITS LIST=8 LOG=7 ECHO=7
FCONTROL HEADING=UPPER ORIGIN=UPPERLEFT
CONTRTOL PLOTUNIT=PERCENT HEIGHT=1.25
*
DATABASE CREATE
*
MASTER IDOF=000001 MODEX=1 NSTEP=50 DT=.0001 TSTART=0
*
ANALYSIS TYPE=DYNAMIC MA=CONSISTENT IMODS=0 METHOD=2 DELTA=0.5
ALPHA=0.25
*
KINEMATICS DISPLACEMENTS=SMALL STRAINS=SMALL
*
SYSTEM 1 CYLINDRICAL
COORDINATES
ENTRIES NODE R THETA XL
1 0.4953 67.38 0
2 0.4953 112.62 0
3 0.4953 112.62 1.016
4 0.4953 67.38 1.016
500 0 0 0
600 0 0 1.016
*
MATERIAL 1 ELASTIC E=.2068E12 NU=0.3 DENSITY=7770
*
EGROUP 1 SHELL  DISPLACEMENTS=SMALL M=1 RINT=3 SINT=3 TINT=3
*
```

```
THICKNESS 1 0.0125
*
LINE ARC 1 2 500 EL=4 MIDNODES=1
LINE ARC 3 4 600 EL=4 MIDNODES=1
*
GSURFACE 2 3 4 1 EL1=10 EL2=4  NODES=9 NCOINCIDE=ALL
*
BOUNDARIES 111111 / 1 2 3 4
BOUNDARIES 111111
5 TO 18
BOUNDARIES 111111
19 TO 37
BOUNDARIES 111111
171 TO 189

TIMEFUNCTION 1
0.000  6.89E6
1E-4   6.393E6
2E-4  5.93E6
3E-4  5.494E6
4E-4  5.087E6
5E-4  4.707E6
6E-4  4.352E6
7E-4  4.02E6
8E-4  3.71E6
9E-4  3.43E6
10E-4 3.15E6
11E-4 2.898E6
12E-4 2.663E6
13E-4 2.444E6
14E-4 2.240E6
15E-4 2.049E6
16E-4 1.872E6
17E-4 1.708E6
18E-4 1.555E6
19E-4 1.412E6
20E-4 1.280E6
21E-4 1.157E6
22E-4 1.043E6
23E-4 9.379E5
24E-4 8.401E5
25E-4 7.496E5
26E-4 6.658E5
```

27E-4 5.884E5
28E-4 5.169E5
29E-4 4.509E5
30E-4 3.902E5
31E-4 3.342E5
32E-4 2.827E5
33E-4 2.354E5
34E-4 1.920E5
35E-4 1.523E5
36E-4 1.160E5
37E-4 8.277E4
38E-4 5.251E4
39E-4 2.499E4
40E-4 0.000
41E-4 0.000
42E-4 0.000
43E-4 0.000
44E-4 0.000
45E-4 0.000
46E-4 0.000
47E-4 0.000
48E-4 0.000
49E-4 0.000
50E-4 0.000
*
LOADS ELEMENT
1 3 1 1 1 1 1 0 3 TO
40 3 1 1 1 1 1 0 3
*
COORDINATES
DELETE 500 600
*
PRINTOUT VOLUME=MINIMUM IVC=0 IAC=0
PRINTNODES 104 104 1
LIST PRINTNODES
*
ADINA
*
FRAME
MESH NODES=11 ELEMENT=1 SUBF=2111
*
END

SAMPLE ADINA-IN INPUT FILE FOR NONLINEAR CASE FOR SSFF SUPPORT CONDITIONS

```
* DYNAMIC LOADING OF A SHALLOW CYLINDRICAL SHELL
*
HEADING '----------SSFF----------'
*
FILEUNITS LIST=8 LOG=7 ECHO=7
FCONTROL HEADING=UPPER ORIGIN=UPPERLEFT
CONTRTOL PLOTUNIT=PERCENT HEIGHT=1.25
*
DATABASE CREATE
*
MASTER IDOF=000001 MODEX=1 NSTEP=50 DT=.0001 TSTART=0
*
ANALYSIS TYPE=DYNAMIC MA=CONSISTENT IMODS=0 METHOD=2 DELTA=0.5
ALPHA=0.25
*
KINEMATICS DISPLACEMENTS=LARGE STRAINS=SMALL
*
ITERATION METHOD=FULL-NEWTON LINE-SEACH=YES
AUTOMATIC-ATS
*
SYSTEM 1 CYLINDRICAL
COORDINATES
ENTRIES NODE R THETA XL
1 0.4953 85.42 0.00
2 0.4953 94.58 0.00
3 0.4953 94.58 1.016
4 0.4953 85.42 1.016
500 0 0 0
600 0 0 1.016
*
MATERIAL 1 ELASTIC E=.2068E12 NU=0.3 DENSITY=7770
```

```
*
EGROUP 1 SHELL  DISPLACEMENTS=SMALL M=1 RINT=3 SINT=3 TINT=3
*
THICKNESS 1 0.0125
*
LINE ARC 1 2 500 EL=4 MIDNODES=1
LINE ARC 3 4 600 EL=4 MIDNODES=1
*
GSURFACE 2 3 4 1 EL1=10 EL2=4  NODES=9 NCOINCIDE=ALL
*
BOUNDARIES 111011 / 1 2 3 4
BOUNDARIES 000001
5 to 18
BOUNDARIES 101011
19 to 37
BOUNDARIES 101011
171 to 189

TIMEFUNCTION 1
0.000  6.89E6
1E-4   6.393E6
2E-4  5.93E6
3E-4  5.494E6
4E-4  5.087E6
5E-4  4.707E6
6E-4  4.352E6
7E-4  4.02E6
8E-4  3.71E6
9E-4  3.43E6
10E-4 3.15E6
11E-4 2.898E6
12E-4 2.663E6
13E-4 2.444E6
14E-4 2.240E6
15E-4 2.049E6
16E-4 1.872E6
17E-4 1.708E6
18E-4 1.555E6
19E-4 1.412E6
20E-4 1.280E6
21E-4 1.157E6
22E-4 1.043E6
23E-4 9.379E5
```

24E-4 8.401E5
25E-4 7.496E5
26E-4 6.658E5
27E-4 5.884E5
28E-4 5.169E5
29E-4 4.509E5
30E-4 3.902E5
31E-4 3.342E5
32E-4 2.827E5
33E-4 2.354E5
34E-4 1.920E5
35E-4 1.523E5
36E-4 1.160E5
37E-4 8.277E4
38E-4 5.251E4
39E-4 2.499E4
40E-4 0.000
41E-4 0.000
42E-4 0.000
43E-4 0.000
44E-4 0.000
45E-4 0.000
46E-4 0.000
47E-4 0.000
48E-4 0.000
49E-4 0.000
50E-4 0.000
*
LOADS ELEMENT
1 3 1 1 1 1 1 0 3 TO
40 3 1 1 1 1 1 0 3
*
COORDINATES
DELETE 500 600
*
PRINTOUT VOLUME=MINIMUM IVC=0 IAC=0
PRINTNODES 104 104 1
LIST PRINTNODES
*
ADINA
FRAME
MESH NODES=11 ELEMENT=1 SUBF=2111
END